Technical Report HL-93-5
May 1993



US Army Corps
of Engineers
Waterways Experiment
Station

# Numerical Model Investigation of Saugus River and Tributaries, Massachusetts, Flood Damage Reduction Project

by *Hsin-Chi J. Lin, David R. Richards*
*Hydraulics Laboratory*



Prepared for U.S. Army Engineer Division, New England

Technical Report HL-93-5
May 1993

# Numerical Model Investigation of Saugus River and Tributaries, Massachusetts, Flood Damage Reduction Project

by Hsin-Chi J. Lin, David R. Richards
Hydraulics Laboratory

U.S. Army Corps of Engineers
Waterways Experiment Station
3909 Halls Ferry Road
Vicksburg, MS 39180-6199

Final report

Approved for public release; distribution is unlimited

Prepared for U.S. Army Engineer Division, New England
424 Trapelo Road, Waltham, MA 02254-9149

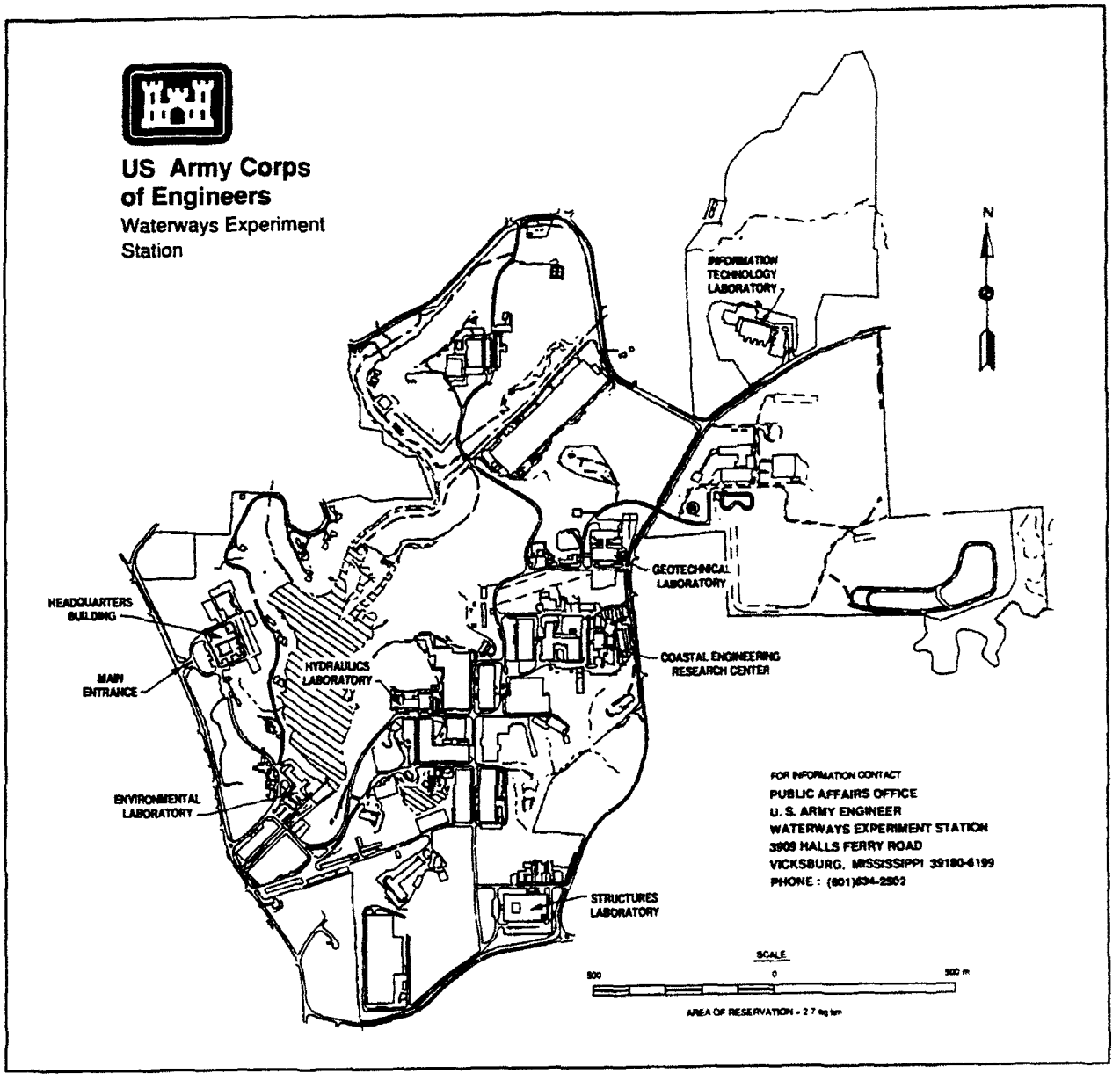


**Waterways Experiment Station Cataloging-in-Publication Data**

Lin, Hsin-Chi J.

Numerical model investigation of Saugus River and tributaries, Massachusetts, flood damage reduction project / by Hsin-Chi J. Lin, David R. Richards ; prepared for U.S. Army Engineer Division, New England.

103 p. : ill. ; 28 cm. — (Technical report ; HL-93-5)

Includes bibliographical references.

1. Flood control — Massachusetts — Mathematical models. 2. Diversion structures (Hydraulic engineering) — Massachusetts — Pines River. 3. Saugus River Watershed (Mass.) — Mathematical models. 4. Sluice gates. I. Richards, David R., P. Eng. II. United States. Army. Corps of Engineers. New England Division. III. U.S. Army Engineer Waterways Experiment Station. IV. Title. V. Series: Technical report (U.S. Army Engineer Waterways Experiment Station) ; HL-93-5.

TA7 W34 no.HL-93-5

# Contents

# Preface

The Saugus River Floodgate numerical modeling study, as documented in this report, was performed for the U.S. Army Engineer Division, New England (NED). Mr. C. J. Wener, Chief of NED's Hydraulics and Water Quality Branch, was point of contact.

The study was conducted in the Hydraulics Laboratory (HL) of the U.S. Army Engineer Waterways Experiment Station (WES) during the period September 1990 to June 1992 under the direction of Messrs. F. A. Herrmann, Jr., Director, HL; R. A. Sager, Assistant Director, HL; W. H. McAnally, Jr., Chief, Estuaries Division (ED), HL; and W. D. Martin, Chief, Estuarine Engineering Branch (EEB), ED.

This study was conducted by Dr. Hsin-Chi J. Lin, EEB, and the report was prepared by Dr. Lin and Mr. David R. Richards, Chief, Estuarine Simulation Branch (ESB), ED.

Dr. Robert W. Whalin was Director of WES during the publication of this report. COL Leonard G. Hassell, EN, was Commander.

# Conversion Factors, Non-SI to SI Units of Measurement

Non-SI units of measurement used in this report can be converted to SI units as follows:

| Multiply | By | To Obtain |
|---|---|---|
| acres | 4046.85642 | square meters |
| cubic feet | 0.02831685 | cubic meters |
| feet | 0.3048 | meters |
| miles (US statute) | 1.609344 | kilometers |
| pounds (force)-second per square foot | 47.88026 | pascals-second |
| square miles | 2.589988 | square kilometers |
| square feet | 0.0929030 | square meters |

# 1 Introduction

## Background

The Saugus and Pines River estuary is located along the Atlantic coast approximately 10 miles[1] north of Boston, MA, near the cities of Lynn, Malden, and Revere, and the town of Saugus (Figure 1). The Saugus and Pines Rivers and their tributaries compose a 47-square-mile watershed area that drains into a tidal estuary at the mouths of the rivers. These estuaries and the adjacent saltwater marshes total approximately 1,660 acres. Freshwater flows from the Saugus and Pines Rivers are relatively small. Storm water drainage is temporarily stored in many areas in the form of surface ponding when the tide is high followed by drainage when the tide is falling.

Because of the topography and hydraulics of the Saugus and Pines river basins, storm events that increase tide levels create a significant potential for flooding. In 1978, the eastern New England coastline was struck by a storm that created a 100-year tidal flood event. The storm caused widespread and record-setting flooding in residential, commercial, and transportation areas along the Saugus and Pines Rivers.

A plan was developed by the U.S. Army Engineer Division, New England, to provide flood damage reduction against the Standard Project Northeaster (SPN) event for nearly the entire project's protected area. The principal component of this plan is construction of tidal floodgates at the mouth of the Saugus River. These floodgates will prevent tidal surges from entering the river, thereby reducing flooding within the study area. The floodgates will be constructed to maintain both safe navigation and natural tide levels and flushing patterns in the estuary under normal conditions. The gates will be closed only when the projected tide levels are expected to cause significant damage.

A field investigation by the New England Division showed that the *phragmites* reed, which indicates deterioration in saltwater wetlands, appears to be expanding in the northwest corner of the marsh. Due to Federal, State, and

[1] A table of factors for converting non-SI units of measurement to SI units is found on page v.

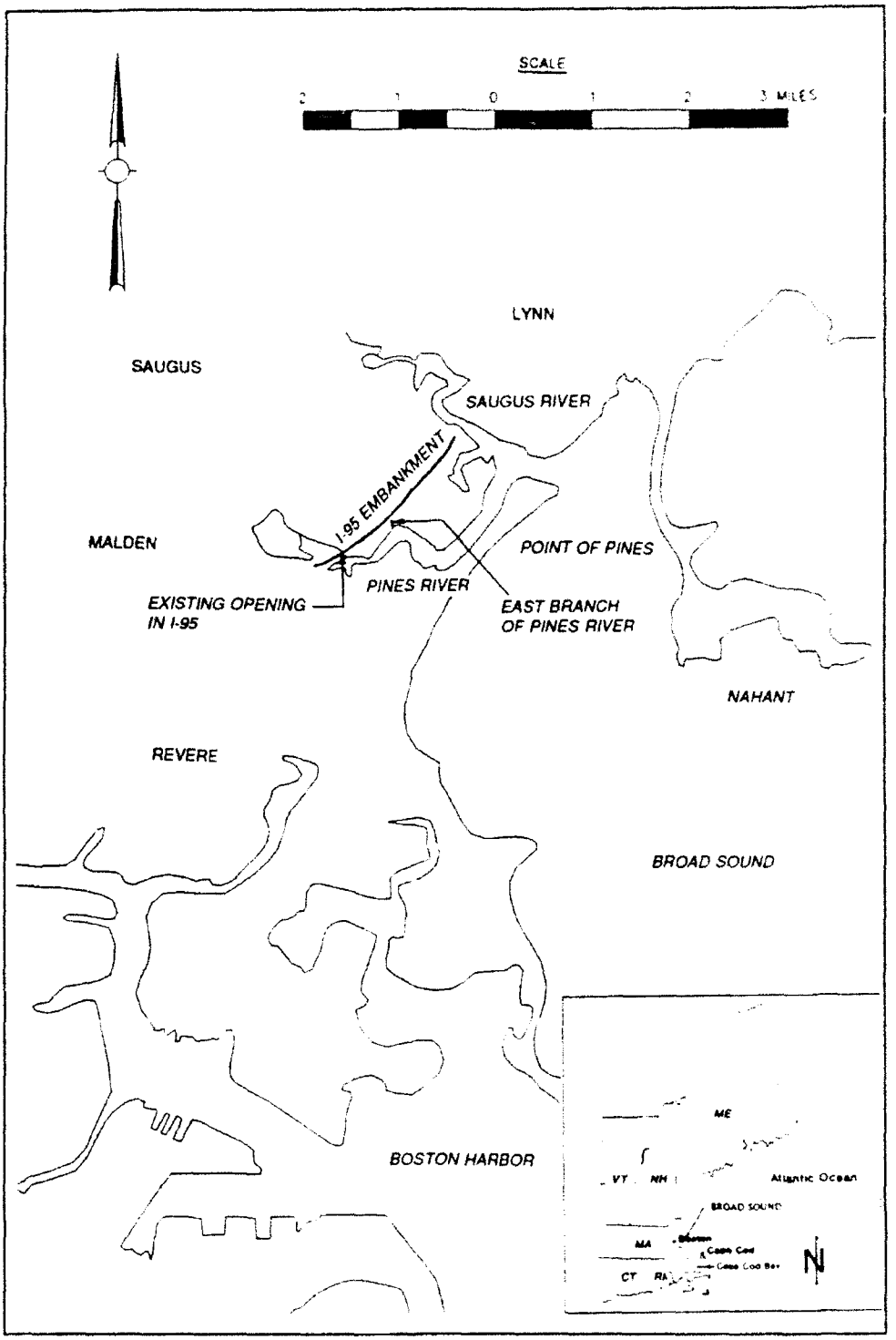


Figure 1. Vicinity and location maps

local interest in preserving and restoring this wetland by breaching the abandoned I-95 embankment (Figure 1), a breaching plan was developed by the New England Division to restore degraded wetlands and increase tide

levels, resulting in increased flushing of nearly 500 acres. The I-95 embankment is an abandoned highway fill remaining from roadway construction activity that was never completed. The plan includes breaching the I-95 embankment at the east branch of the Pines River and widening the existing Pines River opening in the I-95 embankment.

## Objectives

The objectives of the numerical model study were to

*a.* Describe the existing hydrodynamics of the Saugus and Pines Rivers.

*b.* Provide upstream and downstream boundary conditions for testing the proposed floodgate plan in a physical model study.

*c.* Determine the impacts caused by breaching of the I-95 embankment at the east branch of Pines River and widened Pines River openings in the I-95 embankment.

*d.* Evaluate the impacts of the floodgate structure on basin tide levels, circulation patterns, storm surges, and sedimentation and the effect of sea level rise on these responses.

## Approach

A hybrid modeling study approach (a combination of physical and numerical models) was chosen to address the numerous and complex concerns raised by the construction and operation of the proposed floodgates. An undistorted, 1:50-scale physical model representing a section of the estuary was constructed. It provided detailed three-dimensional information needed for the design of the gate structure. The results of the physical model provided input to the navigation study.

Results from the physical model and navigation studies are documented by Brogdon (in preparation) and Park (in preparation), respectively.

The approach chosen for the numerical modeling portion of the overall study was to use the TABS-MD numerical modeling system (Thomas and McAnally 1991) to evaluate the hydrodynamics and sediment transport of the proposed plans and compare these to existing conditions. A finite element mesh that covered the Saugus and Pines estuary and Lynn Harbor was constructed to include marshy areas in the upper Pines River. The designed mesh was sufficiently refined to allow the model to handle the wetting and drying process properly in the marshy areas and to allow the observation of circulation patterns in the floodgate area. The numerical model was also used to

provide boundary condition information with which to control the physical model.

Historically, the Saugus River near the proposed floodgate has not experienced shoaling problems and it is not likely that the project will cause new sedimentation problems. However, to quantify this assessment, a sensitivity study using a sediment transport model was performed to evaluate shoaling potential.

# 2 Description of the Model

## TABS-MD

TABS-MD (Thomas and McAnally 1991) is the name of a family of computer programs used in the multidimensional modeling of hydrodynamics (RMA-2V), sedimentation (STUDH), and constituent transport (RMA-4) in rivers, reservoirs, bays, and estuaries. In this study only two-dimensional models were used. The system contains all of the necessary preprocessing and postprocessing utilities to allow relatively user-friendly applications. A more detailed description of the models in the TABS-MD system appears in Appendix A.

## Mesh Design

A numerical model mesh was designed to allow replication of tidal circulation throughout the Saugus and Pines estuary, Lynn Harbor, and the marshy areas in the upper Pines River (Figure 2). The mesh was sufficiently refined to model the wetting and drying response in the marshy areas. The mesh was generated with high resolution in the channel to represent the flow patterns in sufficient detail to allow accurate representation of currents near the floodgate areas. The mesh consists of more than 8,000 elements and 19,000 nodes, which were necessary to accurately represent the bathymetry of the study area.

A total of four meshes were developed over the course of the study. The first mesh (existing condition) was developed for the existing condition of the Saugus and Pines estuary that extended from Broad Sound to the marshy areas in the upper Pines River (Figure 2). The second mesh (base condition) was developed from the first mesh by adding elements to account for a breach section at the east branch of the Pines River (where creeks were previously cut off by the I-95 fill) and widening the Pines River opening in I-95 (Figure 3). The third mesh (Plan 2C+7) was developed from the second mesh by adding more elements to the floodgate area and including the layout of the structure (Figure 4). The fourth mesh (Plan 3) was developed from the third mesh by deleting the mesh upstream of the floodgate to simulate the floodgate closed condition (Figure 5).

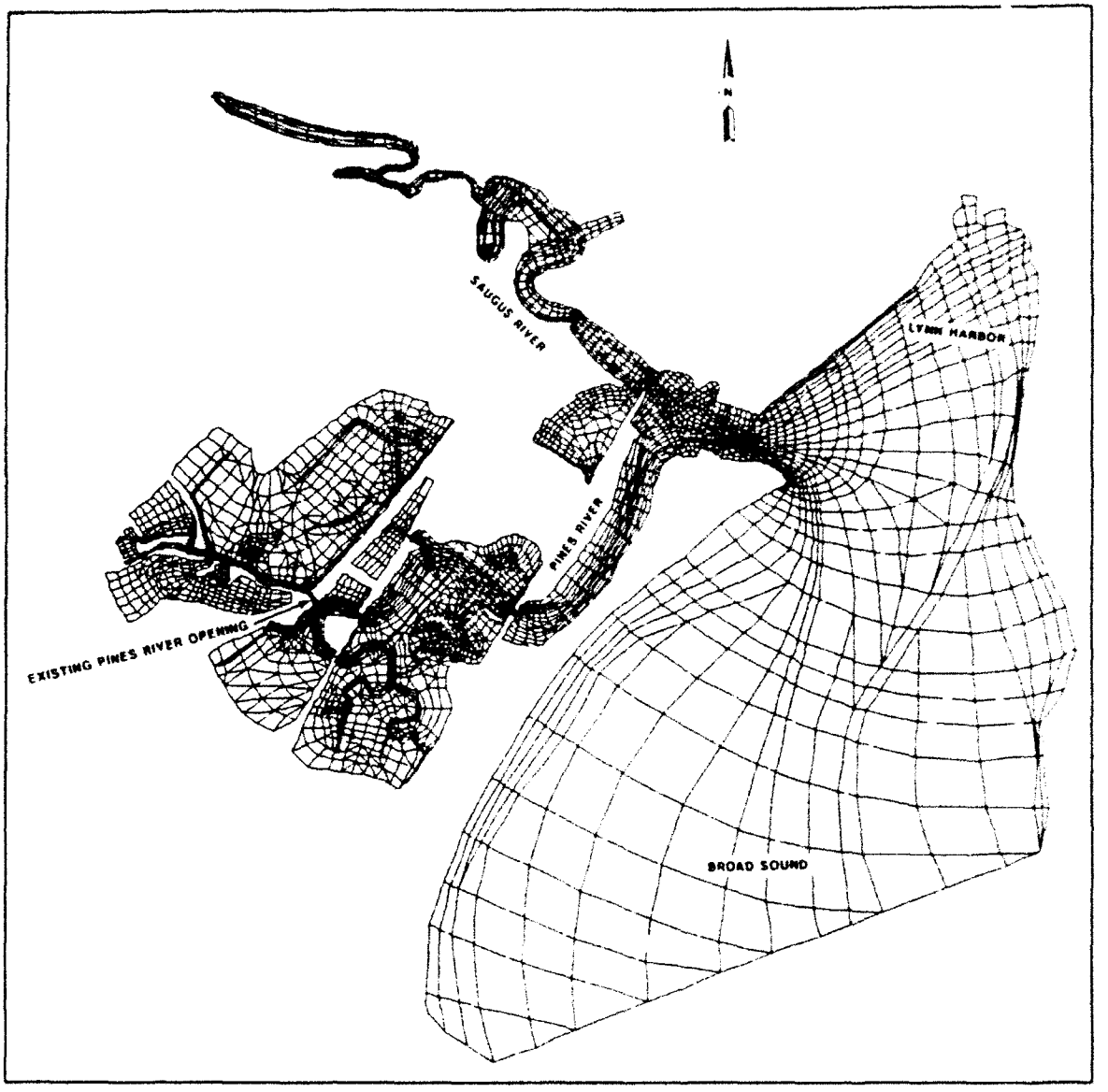


Figure 2. Saugus River estuary numerical model mesh, existing condition (mesh 1)

Model geometry for the existing conditions was defined by the U.S. Geological Survey (USGS) 1:25,000-scale metric topographical map, Lynn, Massachusetts, dated 1985, and Boston North, Massachusetts, dated 1979. Additional bathymetry was provided by the New England Division in the areas of poor coverage. These include the marshy areas of Diamond Creek and the upper Pines and Saugus Rivers, and the deeper waters of Broad Sound, Lynn Harbor, and the proposed floodgate area.

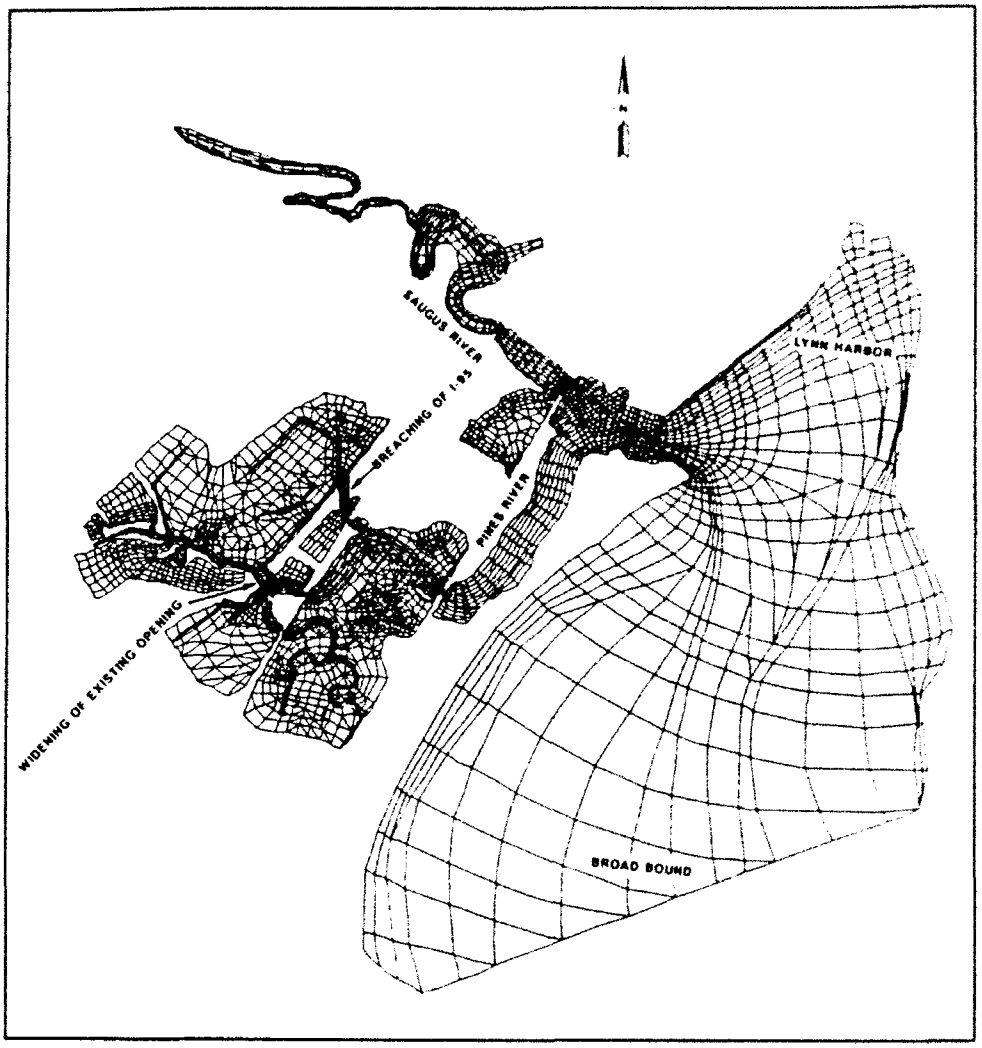


Figure 3. Saugus River estuary numerical model mesh, base condition (mesh 2)

# Numerical Hydrodynamic Model

## Boundary conditions

Boundary conditions for the study were obtained from a field survey conducted by the U.S. Army Engineer Waterways Experiment Station between 30 October and 8 December 1990. Tide and velocity data were collected to provide boundary conditions for the model as well as to use as a verification data set. The 14-hr intensive velocity data collection period on 3 November 1990 encompassed an entire tide cycle during a spring tide. The tidal range during the survey was 13.13 ft. Mostly clear skies existed at the time of the survey, and wind conditions ranged from a slight breeze to light winds of 4 to 5 mph. A detailed report on the field survey is given by Fagerburg et al. (1991). The tide gauge S0.6, located in Broad Sound, was used as a

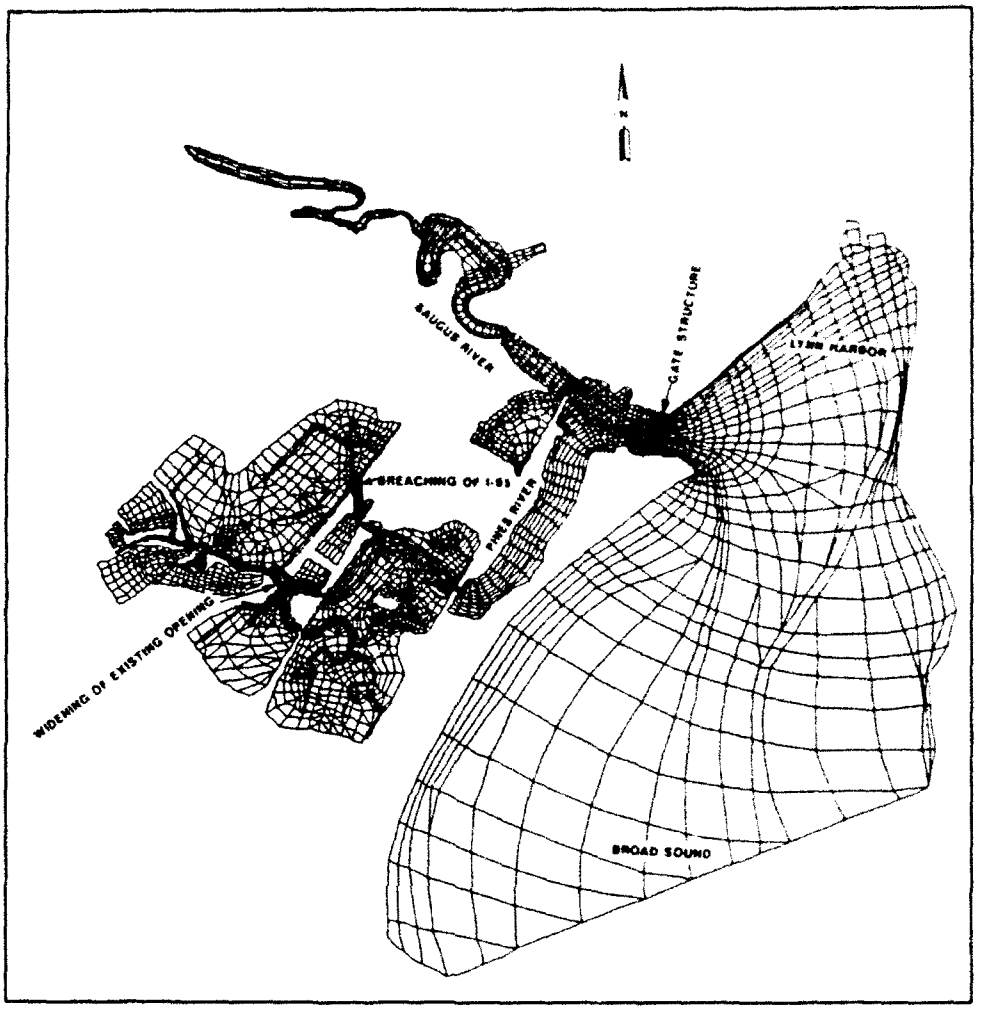


Figure 4. Saugus River estuary numerical model mesh, Plan 2C+7 (mesh 3)

water-surface elevation boundary condition. The drainage areas of both Saugus and Pines Rivers are very small, and less than 1.0 cfs of inflow was observed in the field trip. Therefore, no freshwater inflow boundary was specified in the Saugus and Pines Rivers.

## Model parameters

Model verification resulted in one final set of model parameters representing Manning's n values and eddy viscosities. The parameter values were selected by adjustment within a range of realistic values until an optimum comparison of the model's computed water levels and currents to field measurements was obtained. The following tabulation lists eddy viscosity coefficients and Manning's values used in this study:

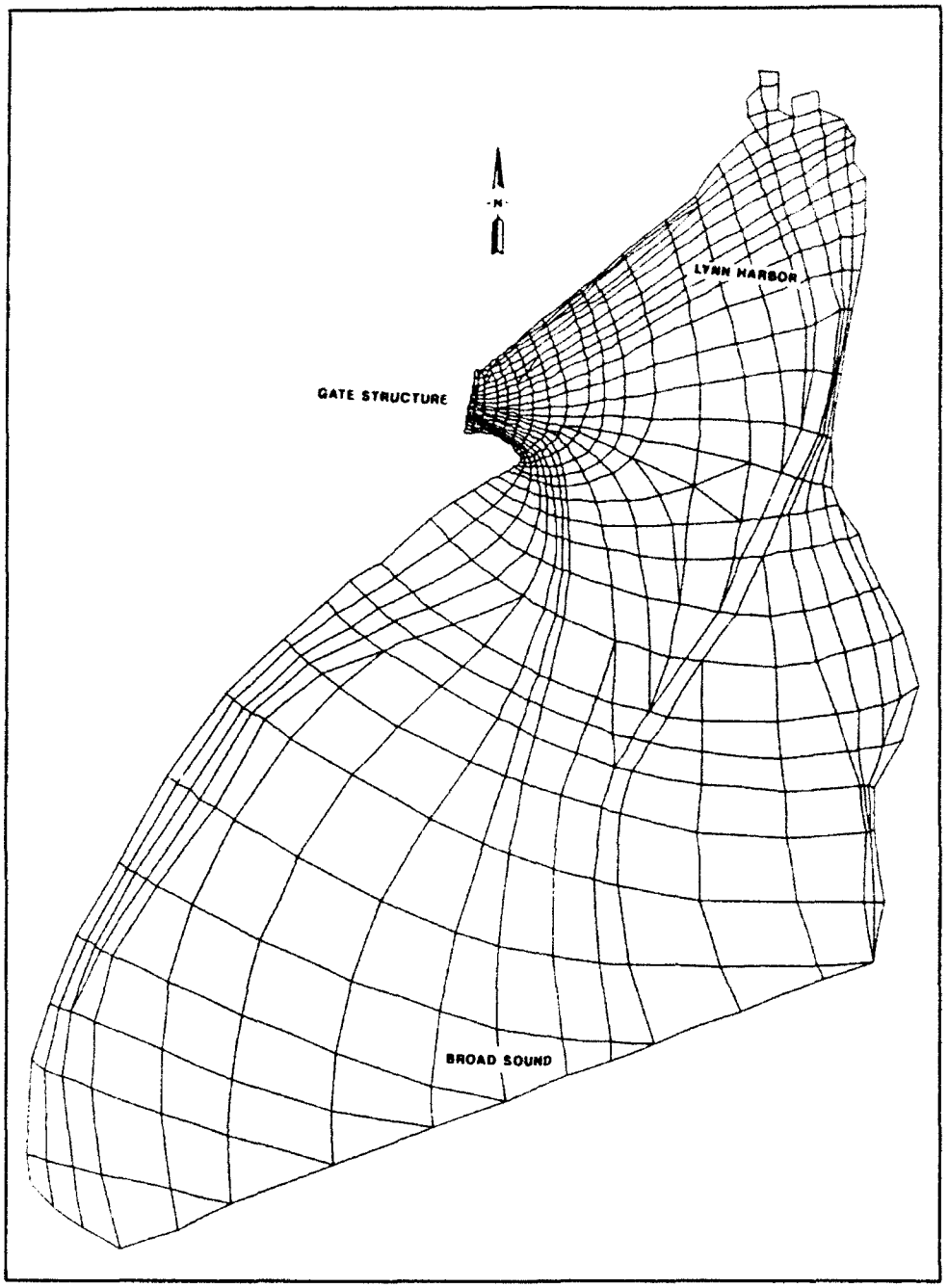


Figure 5. Saugus River estuary numerical model mesh, floodgate closed condition (mesh 4)

| Location | Eddy Viscosity, lb-sec/ft$^2$ | Manning's n |
|---|---|---|
| Broad Sound | 50 | 0.020 |
| Saugus River | 50-100 | 0.020-0.040 |
| Pines River | 50 | 0.040-0.080 |
| Marshy area | 100 | 0.070 |

## Verification

The field verification data were obtained from 9 water level stations (Figure 6) and 11 current stations (Figure 7) located in Saugus and Pines Rivers. Water level elevation measurements at each station were recorded using Microtide water level recorders. Velocities at each station were measured with the deployment of recording instruments. A Gurley Model 665 vertical-axis, cup-type impeller velocity meter with direct velocity readout capabilities was used to measure current speeds. At each station the velocity data were measured at three depths—surface, middepth, and bottom—for each hour of the survey period. The bottom measurement was made 2 ft from the actual bottom. The middepth data were obtained at the calculated middepth. The surface measurement was obtained 2 ft below the water surface.

Because of high tidal amplitudes, RMA-2V was operated with a variable time-step ranging from 5 to 15 min. The simulation started when the tide was at its peak in Broad Sound. A 6-hr initial period allowed the transients induced by initialization (spin-up) of RMA-2V to dissipate and the model solution to respond correctly to imposed boundary conditions. A 1-day data set (two tidal cycles) was used for tide verification. A 14-hr period of velocity data was used for velocity verification.

## Tide verification results

Water levels from the model and field measurements are compared in Plates 1-8. The water level comparisons indicated good agreement between model results and field measurements. The entire estuary is nearly in phase in both model and field data except at tide Gages S4.4, S9.1, and S9.3. All three stations are located in marshy areas. At Gage S4.4, located in Diamond Creek, comparisons of rising and falling tide calculated by the model with the field measurements showed good agreement; however, the computed peak water level was slightly high (about 0.3 ft at peak tide) and the phasing of peak tide was off by about 15 min. At Gages S9.1 and S9.3, located in the upper Pines River, the phasing of flood tide was good; however, the computed water levels were slightly high (about 0.2 to 0.3 ft) at the peak tide and the ebb tide fell faster than the field data by about 1.0 hr. The marshes are full of dense grasses (about 1 ft high) and many interconnected mosquito ditches (1 to 2 ft wide and 2 to 4 ft deep). Water was stored in the marshes and ditches during

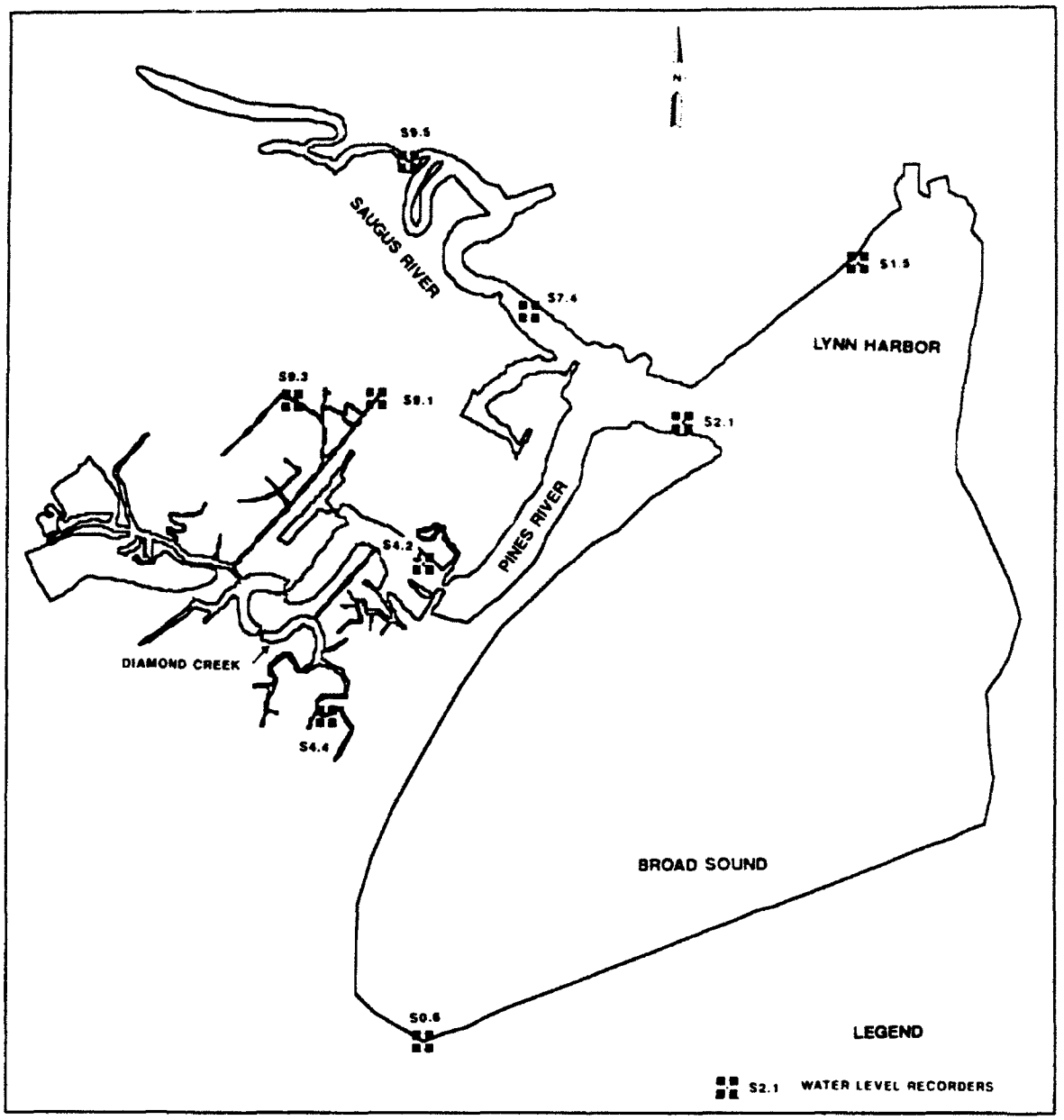


Figure 6. Water level field stations

the high tide and was drained slowly to the channel during the low tide. At Gage S9.5, located in upper Saugus River, the computed water levels were slightly high (about 0.2 ft) at the peak ebb tide and the phasing was off by about 1 hr. In general, the computed water levels showed good agreement, except in the marshy areas. The computed water level in the marshy area was slightly high by about 0.3 ft. This level of verification is the best possible given the present state of technology. A more highly refined mesh that included each ditch would have provided better verification, but it was not possible to include all ditches. The tidal verification is acceptable for the purpose of this study.

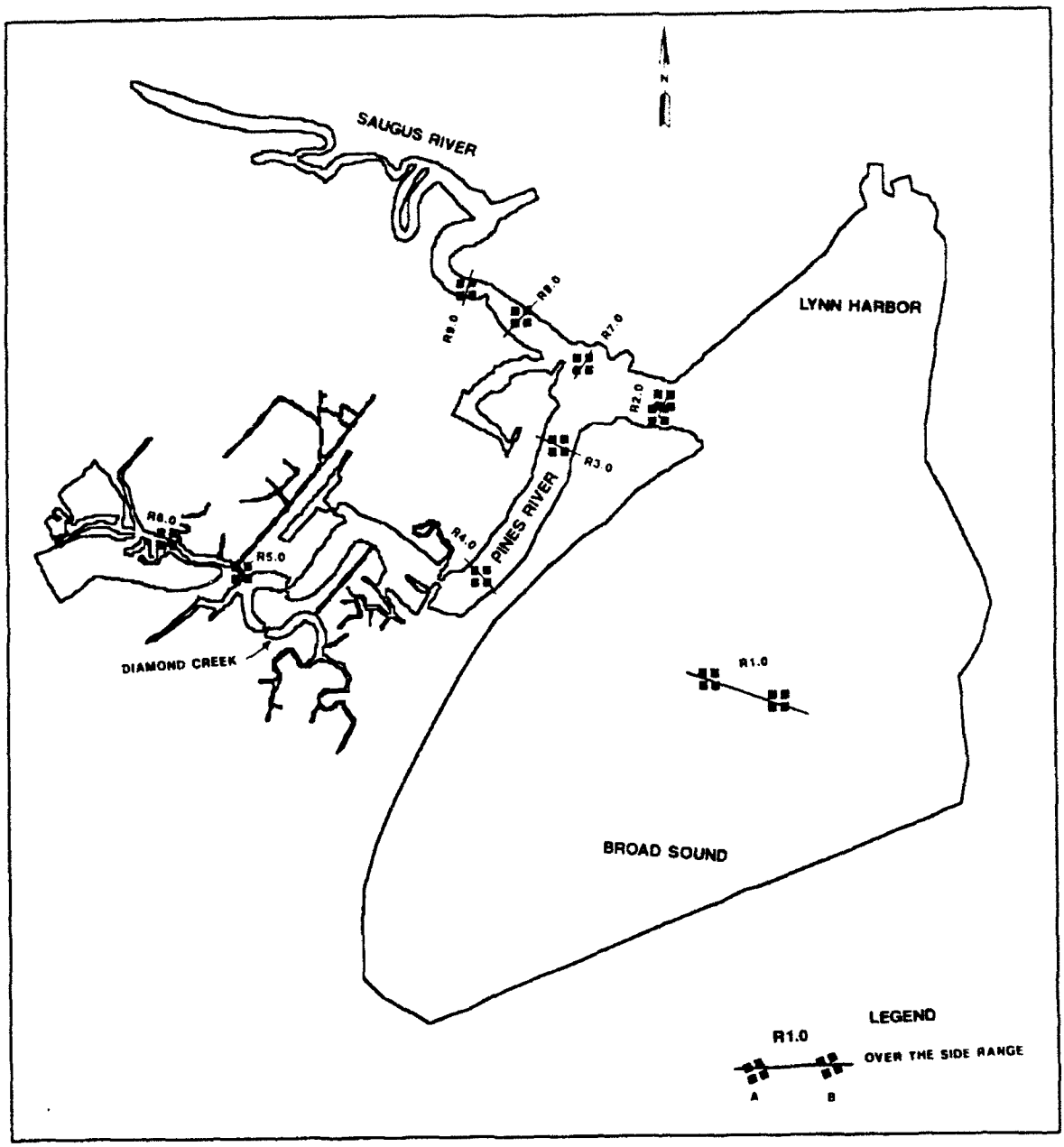


Figure 7. Ranges and locations for 14-hr velocity data collection

## Velocity verification results

Velocities predicted by the model are compared with field-measured values in Plates 9-19. At all survey stations, the vertical depth profile from the field survey was averaged to obtained a single value for comparison with the depth-averaged model. The model-predicted velocities compared quite favorably with the vertically averaged field measurements. Small variations of model results compared to field measurements occurred at sta 1.0A and 1.0B in Broad Sound. Good comparisons occurred at sta 2.0A and 2.0B, located

near the proposed floodgates area. At sta 3.0B, 4.0B, 5.0B, and 6.0B, located in the Pines River, peak flood velocities were underpredicted by about 0.4 fps and peak ebb velocities were overpredicted by about 1.0 fps. Good comparisons occurred at all stations in the Saugus River, except 7.0B, where peak flood velocities were underpredicted by about 0.4 fps and peak ebb velocities were overpredicted by about 0.4 fps. All of the underprediction in peak flood velocities and overprediction in peak ebb velocities can be explained by model elements being removed or added when an element became dry or wet. When the water level falls and the element becomes dry or when the water level rises and the element becomes wet again, this condition causes numerical instability and shocks the system. The numerical shocks caused by wetting and drying are one of the most difficult problems in numerical modeling. It can be improved by adding more resolution in the areas when the wetting and drying occur, but the penalty is more computer time. The level of accuracy in the velocity verification was as good as could be obtained within time and cost constraints and is considered adequate for the purposes of the study.

Plates 20 and 21 provide model velocity vector plots for maximum flood and maximum ebb, respectively, for the existing conditions. These plots show the general flow pattern in the Saugus and Pines Rivers.

## Numerical Sediment Transport Model

Boundary conditions for the STUDH sediment transport model consisted of suspended sediment concentrations. The nodal velocities from the hydrodynamic model were saved and used to update the velocity field in the model at the beginning of each time-step.

Since the floodgate area has not experienced sediment problems, the sediment study focused on a sensitivity analysis of model parameters. The STUDH code uses the Ackers-White sediment transport function for computing noncohesive sediment transport (Ackers and White 1973).

Sediment data were insufficient to verify the sediment model. However, some suspended sediment concentration data samples were collected at the individual sampling stations during the 14-hr survey (Fagerburg et al. 1991). The suspended sediment concentrations were found to be low during the survey period. The suspended sediment concentrations at sta R1.0A were less than 5 mg/ℓ during the flood tide and about 30.0 mg/ℓ during the ebb tide. It appears that the sediment concentration in the study areas is very low during normal tide conditions. A constant suspended sediment concentration of 30 mg/ℓ was specified at the boundary in order to produce some shoaling for an evaluation of parameter sensitivity. The various input variables included diffusion coefficients, Manning's n to compute bed shear stress, and effective particle size for transport. Each was adjusted until the model produced reasonable shoaling and scour patterns. The model parameter values are listed in the following tabulation.

| Parameter | Value |
|---|---|
| Effective particle size for transport, mm | 0.10 |
| Effective settling velocity, m/sec | 0.007 |
| Diffusion coefficient, $m^2$/sec | 10 |
| Manning's n for bed shear stress | 0.045 |
| Computation time-step, min | 15 |

Plate 22 shows the deposition and erosion pattern after a 24-hr simulation near the proposed floodgate area. The simulation indicated that there is little deposition or erosion near the proposed floodgate area. The deposition occurred at the boundary in Broad Sound and was caused by the excessive sediment load (30 mg/ℓ) at the boundary.

The sensitivity analysis of sediment movement was conducted for the normal tide conditions. It did not address the sediment movement associated with runoff, storm surge, and wave-producing storm events. The analysis was focused on any change of the sediment deposition and scour pattern under the proposed floodgate as compared to the existing condition. A 24-hr simulation (about two tidal cycles) was used to indicate any significant change in sediment deposition and scour pattern in the estuary.

# 3 Model Results

## Hydrodynamics

The verified hydrodynamic model was used to provide water levels and discharges as the boundary conditions for use in the physical model. It was also used to evaluate the impacts of breaching the I-95 embankment and to determine the effects of the proposed floodgate, rising sea levels, and storm surges on the area.

### Physical model boundary conditions

The computed water levels and discharges from the numerical model at cross sections 1, 2, 3, 4, and 5 (Figure 8) were provided for use in the physical model study. Two sets of water levels and discharges for existing and base conditions were based on the maximum discharges (both flood and ebb tide) at the proposed floodgate site during spring and neap tide cycles.

Table 1 shows the boundary conditions for the physical model under the existing spring tide conditions. The flows were 29,000 and 22,000 cfs for the flood and ebb tides, respectively. The water levels were 3.48 ft[1] and 4.81 ft for the flood and ebb tides, respectively.

Table 2 shows the boundary conditions for the physical model under the existing neap tide conditions. The flows were 12,300 and 11,300 cfs for the flood and ebb tides, respectively. The water levels were 1.46 ft and -0.30 ft for the flood and ebb tides, respectively.

Table 3 shows the boundary conditions for the physical model under the base spring tide conditions. The flows were 27,100 and 28,200 cfs for the flood and ebb tides, respectively. The water levels were 6.24 ft and 2.70 ft for the flood and ebb tides, respectively.

[1] All elevations (el) cited herein are in feet referred to the National Geodetic Vertical Datum (NGVD).

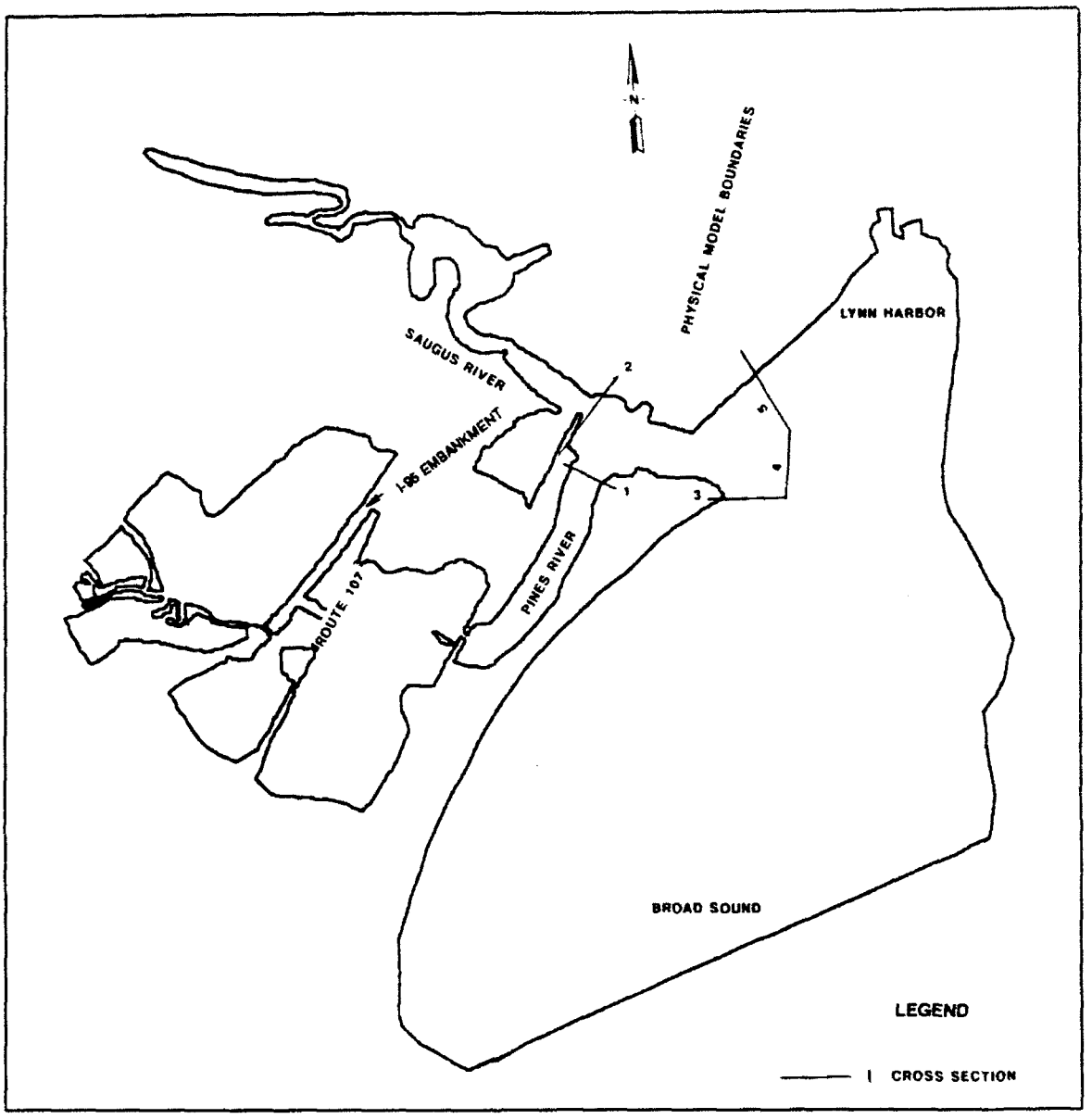


Figure 8. Locations of boundary conditions for physical model study

Table 4 shows the boundary conditions for the physical model under the base neap tide conditions. The flows were 11,900 and 10,900 cfs for the flood and ebb tides, respectively. The water levels were 1.46 ft and -0.31 ft for the flood and ebb tides, respectively.

## Breaching of I-95 embankment

The purpose of considering breaching the abandoned I-95 embankment and widening the Pines River opening through the embankment was to restore deteriorated wetlands in the Pines River. If the breaching was implemented, it

was important to determine the increase in tide level in the upper Pines River due to the cut of I-95. The layout and dimensions of the breach site (700 sq ft) in I-95 and the enlarged opening (4,200 sq ft) in Pines River (Figure 9) were provided by the New England Division.

After the abandoned I-95 embankment was breached, the Route 107 bridge opening became a control section. The existing opening is very small and the computed velocity was more than 6.0 fps (Plate 23). A 2-fps target velocity was suggested by New England Division. Two flow areas (40 ft wide and 90 ft wide) at the Route 107 bridge were studied based on the 2-fps criteria. Plates 24 and 25 show that the velocity at the bridge will be about 3.0 fps for a 40-ft-wide opening and 1.5 fps for a 90-ft-wide opening, respectively. Plates 26-28 show that the water levels in the marshes will not change significantly (less than 0.05 ft).

Plates 29-36 compare the computed water levels for the existing and base conditions. The breaching of the I-95 embankment will increase the water level in marshy areas of the upper Pines River by about 0.5 ft at the peak tide during the spring tide condition and will not affect the water level in the marshy area of Diamond Creek. The time lag between the peak water levels at sta S0.6 and at sta S9.3 is about 2 hr in the existing condition. The time lag was reduced to 1.0 hr due to breaching of the abandoned I-95 embankment.

## Floodgate

The layout and dimensions of the proposed floodgate (Plan 2C+7) and approach channel were provided by the physical model study (Figure 10). The third mesh (Figure 4) with the same boundary conditions as specified for existing conditions was the input to the model. Plates 37-44 compare the computed water levels for the existing condition and the proposed floodgate. The results indicated no measurable change in water levels in the estuary except in the marshy area of the upper Pines River. Water levels at sta S9.1 and S9.3 will increase about 0.5 ft at the peak tide during the spring tide condition, and the time to peak water level will decrease about 1.0 hr compared to the existing condition. Plates 45-52 compare the computed water levels for the base condition and the proposed floodgate. The results show no measurable change in estuary water levels due to the floodgate compared to the base condition. Based on these results, it is concluded that floodgates will not cause significant change of water levels in the Pines and Saugus Rivers. Plates 53-55 compare the computed velocity for the base condition and the Plan 2C+7 condition at the enlarged opening in the Pines River, at the breach cross section, and at the upstream side of the General Edwards bridge in Saugus River. The results show no significant change of velocity. Plates 56 and 57 show the model velocity vector plots for maximum flood and ebb, respectively. Plates 58 and 59 show the model velocity vector plots for maximum flood and ebb, respectively, near the floodgate area.

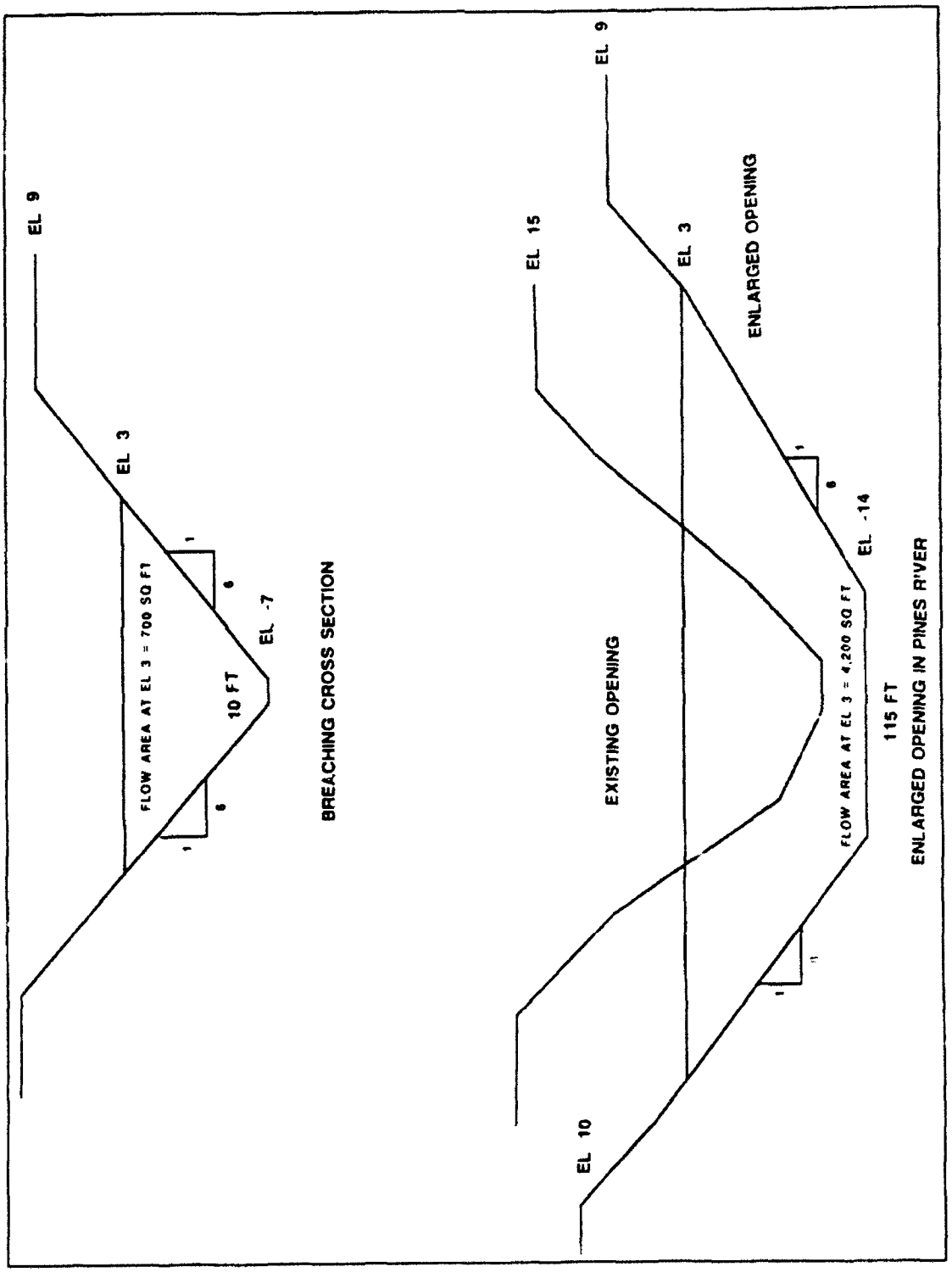


Figure 9. Dimensions of breaching cross section and enlarged opening in Pines River

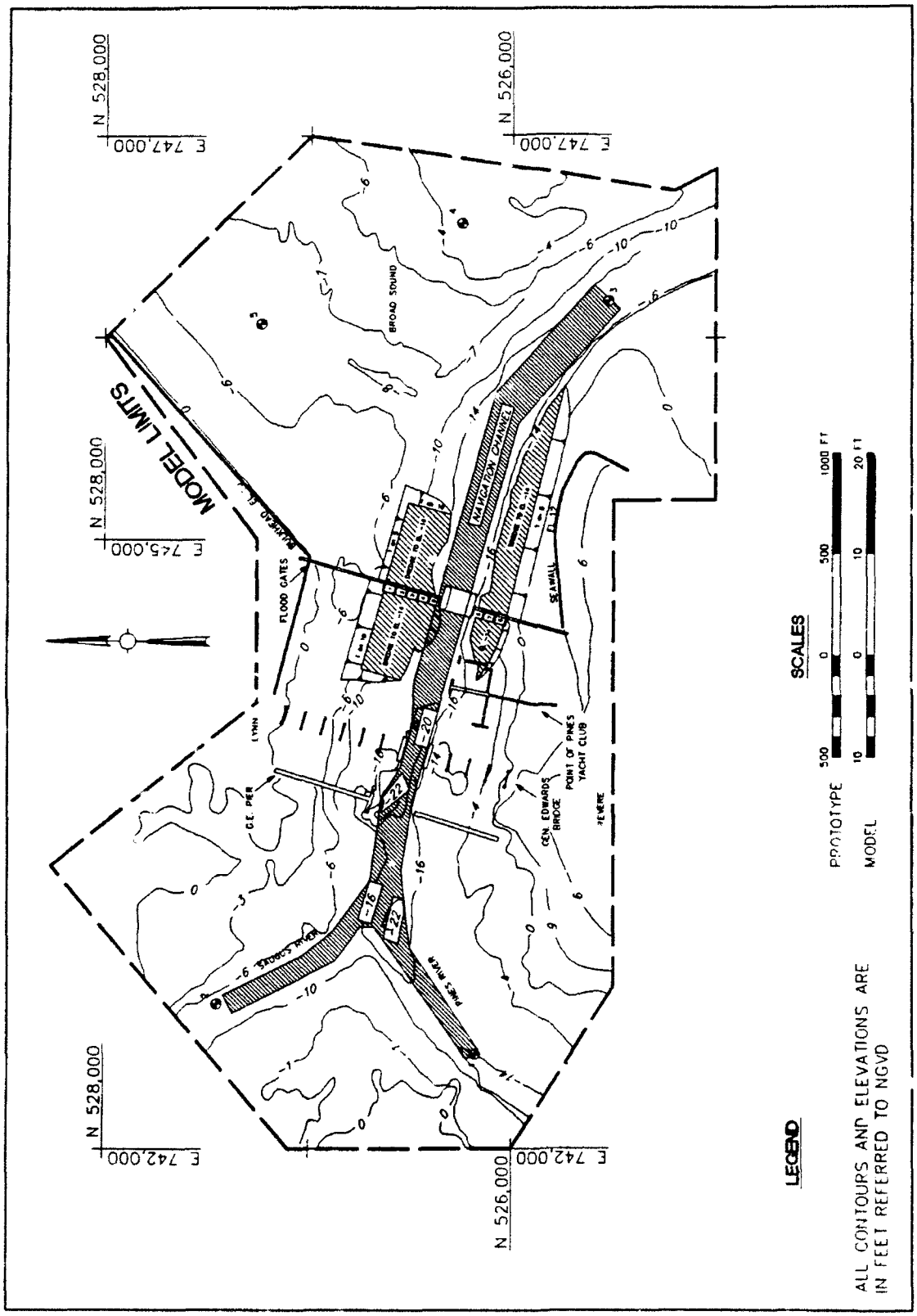


Figure 10. Layout and dimensions of Plan 2C+7 and the approach channel

### Sea level rise

The third mesh was used for this task with 1.0-ft elevated tide boundary conditions. Plates 60-67 compare the computed water levels between the spring tide and elevated spring tide under Plan 2C+7. The water levels at the peak flood tide and the peak ebb tide will increase 1.0 ft in the study area. The effects of water level changes due to the 1-ft rise in sea level for the existing and the base condition were not included in the study. Based on the results discussed in the sections "Breaching of I-95 embankment" and "Floodgate," the floodgate will not significantly affect the water levels in the estuary for the 1-ft rise in sea level.

### Storm surges

The floodgate will be closed when the projected tide levels are expected to cause significant damage. The fourth mesh with the same boundary conditions as specified in existing conditions was the input to the model. Comparisons of the computed water levels in the proposed floodgate area between the existing and the floodgate closed condition show no measurable differences (Plate 68). The results indicated that the closure of the floodgate will not cause significant change of water level in Broad Sound. This comparison is based on hydrodynamics and does not include effects of wind and wave setup. This analysis was just a sensitivity test to see if closure of the floodgate would cause any change in tide level in Broad Sound.

## Sedimentation

Plate 69 shows the shoaling and scour pattern near the proposed floodgate area under Plan 2C+7. The plot was generated based on the same input data as specified in the existing condition (Plate 22). The results indicated little difference in deposition and erosion pattern compared to the existing condition. The proposed floodgate will not alter the shoaling and scour pattern in the study area, but local shoaling and scour may occur near the proposed floodgate pier.

# 4 Conclusions

The RMA-2V model was successfully verified to limited field measurements including a 14-hr field survey of water levels and velocity measurements. The comparisons of the computed water levels and velocities to field measurements were good. At the stations in marshy areas, the computed water levels were slightly high by about 0.2 ft and the ebb tide fell about 1 hr faster than the field data. The model error was suspected to be the result of difficulties in properly representing the storage of water in marshes and interconnected mosquito ditches. In the Pines River, the velocities were underpredicted by about 0.3 fps for peak flood and overpredicted about 1.0 fps for peak ebb. These variations were caused by the elements that are removed when they are dry and added when they are wet again. These differences were small and not expected to significantly impact the use of model results for the intended purposes.

The study provided boundary conditions for the physical model study under the existing and base conditions for both spring and neap tides. For the existing spring tide conditions, the flows were 29,000 and 22,000 cfs for the flood and ebb tides, respectively. The corresponding water levels were 3.48 ft and 4.81 ft for the flood and ebb tides, respectively. For the existing neap tide conditions, the flows were 12,300 and 11,300 cfs for the flood and ebb tides, respectively. The corresponding water levels were 1.46 ft and -0.30 ft for the flood and ebb tides, respectively. For the base spring tide conditions, the flows were 27,100 and 28,200 cfs for the flood and ebb tides, respectively. The corresponding water levels were 6.24 ft and 2.70 ft for the flood and ebb tides, respectively. For the base neap tide conditions, the flows were 11,900 and 10,900 cfs for the flood and ebb tides, respectively. The corresponding water levels were 1.46 ft and -0.31 ft for the flood and ebb tides, respectively.

Breaching of the abandoned I-95 embankment and widening the Pines River opening on I-95 will increase tidal flow in marshy areas. The water levels in marshy areas will increase about 0.5 ft at the peak tide under a spring tide condition. The time lag of the peak water levels between the Broad Sound and upper marshy areas was reduced from 2 hr to 1 hr.

Plan 2C+7 will not cause significant change of water levels in the Pines and Saugus Rivers under the normal tide conditions. It will protect the study areas from flooding during the storm events.

The water levels in the marshy areas under Plan 2C+7 will increase about 1.0 ft at the peak flood tide and ebb tide for the 1-ft rise in sea level.

The proposed floodgate will not alter the sediment deposition or scour pattern in the estuary under the normal tide condition, but local scour near the piers may occur.

# References


Ackers, P., and White, W. R. (1973). "Sediment transport: New approach and analysis," *Journal, Hydraulics Division, American Society of Civil Engineers*, 99 (HY11), 2041-2060.

Brogdon, N. J. "Saugus River floodgate report; physical model study" (in preparation), U.S. Army Engineer Waterways Experiment Station, Vicksburg, MS.

Fagerburg, T. L., Coleman, C. J., Parman, J. W., and Fisackerly, G. M. (1991). "Field data collection report, Saugus River and tributaries flood damage reduction project, Lynn, Malden, Revere, and Saugus, Massachusetts," Technical Report HL-91-22, U.S. Army Engineer Waterways Experiment Station, Vicksburg, MS.

Park, H. E. "Navigation conditions at Saugus River flood control project, Saugus River; hydraulic model investigation" (in preparation), U.S. Army Engineer Waterways Experiment Station, Vicksburg, MS.

Thomas, W. A., and McAnally, W. H., Jr. (1991). "User's manual for the generalized computer program system; open-channel flow and sedimentation, TABS-2; Main text and appendices A through O," Instruction Report HL-85-1, U.S. Army Engineer Waterways Experiment Station, Vicksburg, MS.

**Table 1**
**Boundary Conditions for Physical Model Under the Existing Spring Tide**

| Boundary Section | Water Surface Elevation | Discharge, cfs |
|---|---|---|
| **Flood Direction** | | |
| Inflow | | |
| 3 | 3.471 | 13,770 |
| 4 | 3.484 | 9,690 |
| 5 | 3.485 | 5,600 |
| | Total | 29,060 |
| Outflow | | |
| 1 | 3.279 | 14,760 |
| 2 | 3.297 | 6,480 |
| | Total | 21,240 |
| **Ebb Direction** | | |
| Inflow | | |
| 1 | 4.952 | 15,890 |
| 2 | 4.949 | 6,090 |
| | Total | 21,980 |
| Outflow | | |
| 3 | 4.799 | 13,850 |
| 4 | 4.813 | 11,340 |
| 5 | 4.820 | 3,050 |
| | Total | 28,240 |

**Table 2**
**Boundary Conditions for Physical Model Under Existing Neap Tide**

| Boundary Section | Water Surface Elevation | Discharge, cfs |
|---|---|---|
| **Flood Direction** | | |
| Inflow | | |
| 3 | 1.462 | 5,770 |
| 4 | 1.466 | 4,200 |
| 5 | 1.467 | 2,350 |
| | Total | 12,320 |
| Outflow | | |
| 1 | 1.412 | 5,976 |
| 2 | 1.418 | 2,995 |
| | Total | 8,991 |
| **Ebb Direction** | | |
| Inflow | | |
| 1 | -0.252 | 5,275 |
| 2 | -0.248 | 2,730 |
| | Total | 8,005 |
| Outflow | | |
| 3 | -0.313 | 5,880 |
| 4 | -0.309 | 4,160 |
| 5 | -0.306 | 1,270 |
| | Total | 11,310 |

**Table 3**
**Boundary Conditions for Physical Model Under the Base Spring Tide**

| Boundary Section | Water Surface Elevation | Discharge, cfs |
|---|---|---|
| **Flood Direction** | | |
| Inflow | | |
| 3 | 6.23 | 12,000 |
| 4 | 6.24 | 9,200 |
| 5 | 6.24 | 5,900 |
| | Total | 27,100 |
| Outflow | | |
| 1 | 6.16 | 14,500 |
| 2 | 6.18 | 7,600 |
| | Total | 22,100 |
| **Ebb Direction** | | |
| Inflow | | |
| 1 | 2.92 | 17,400 |
| 2 | 2.92 | 5,100 |
| | Total | 22,500 |
| Outflow | | |
| 3 | 2.68 | 13,700 |
| 4 | 2.71 | 11,500 |
| 5 | 2.72 | 3,000 |
| | Total | 28,200 |

**Table 4**
**Boundary Conditions for Physical Model Under Base Neap Tide**

| Boundary Section | Water Surface Elevation | Discharge, cfs |
|---|---|---|
| **Flood Direction** | | |
| Inflow | | |
| 3 | 1.462 | 5,660 |
| 4 | 1.466 | 3,990 |
| 5 | 1.467 | 2,220 |
| | Total | 11,870 |
| Outflow | | |
| 1 | 1.419 | 5,350 |
| 2 | 1.423 | 2,980 |
| | Total | 8,330 |
| **Ebb Direction** | | |
| Inflow | | |
| 1 | -0.253 | 4,940 |
| 2 | -0.251 | 2,690 |
| | Total | 7,630 |
| Outflow | | |
| 3 | -0.313 | 5,740 |
| 4 | -0.309 | 3,990 |
| 5 | -0.306 | 1,210 |
| | Total | 10,940 |

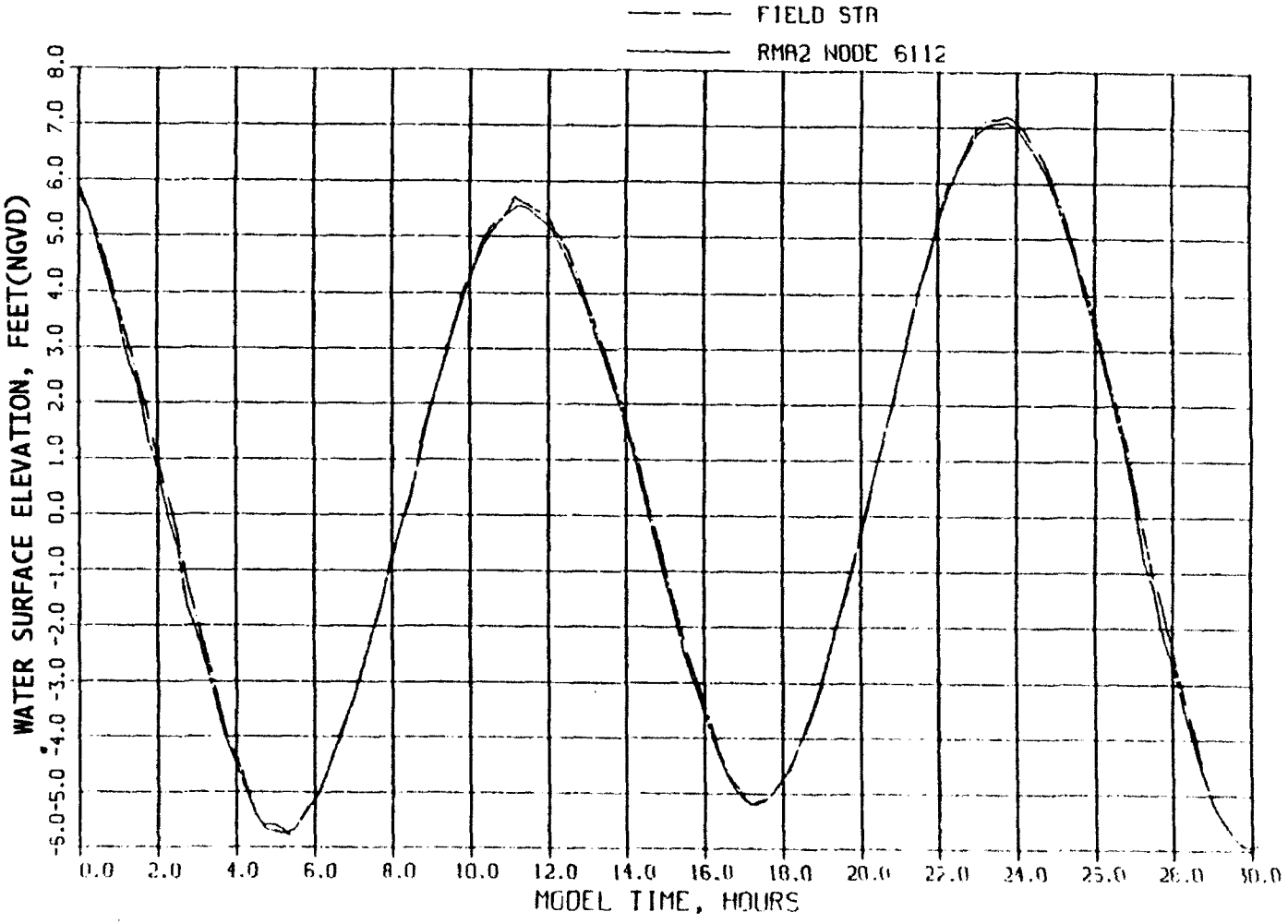


COMPUTED VERSUS MEASURED
WATER LEVEL
STA S1.5

PLATE 1

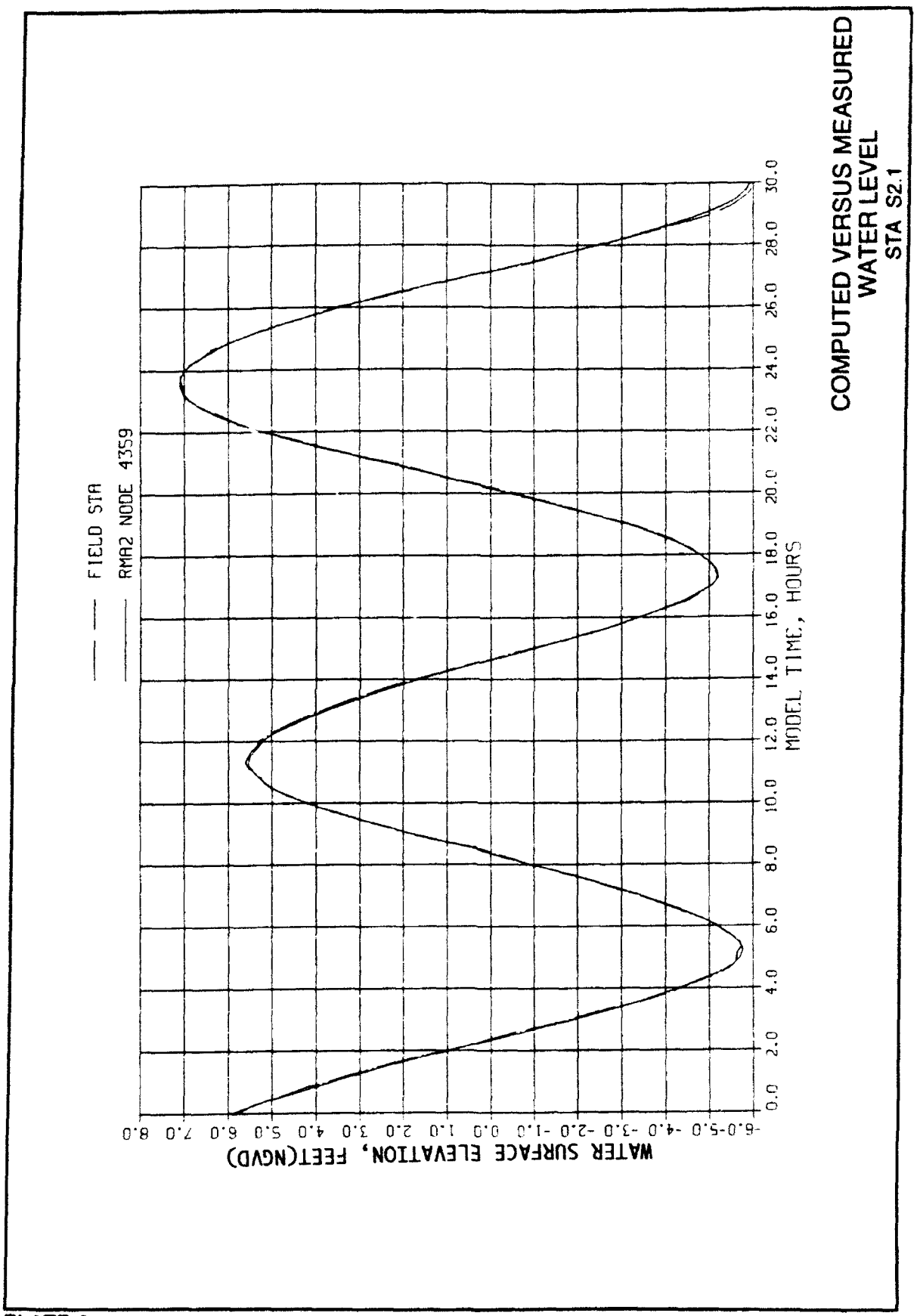
COMPUTED VERSUS MEASURED
WATER LEVEL
STA S2.1
FIELD STA
RMA2 NODE 4359
WATER SURFACE ELEVATION, FEET(NGVD)
MODEL TIME, HOURS
-6.0 -5.0 -4.0 -3.0 -2.0 -1.0 0.0 1.0 2.0 3.0 4.0 5.0 6.0 7.0 8.0
0.0 2.0 4.0 6.0 8.0 10.0 12.0 14.0 16.0 18.0 20.0 22.0 24.0 26.0 28.0 30.0

PLATE 2

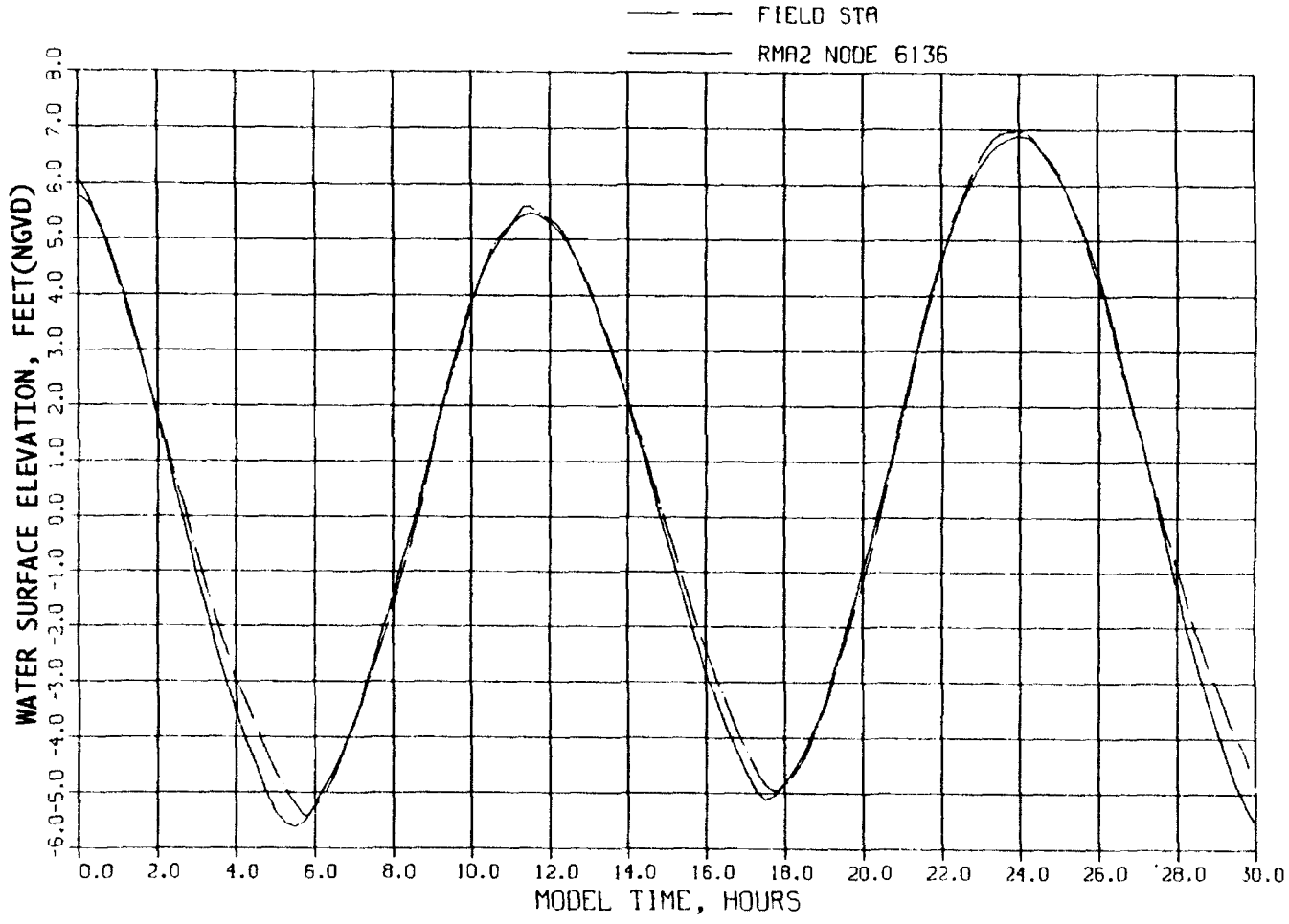


**COMPUTED VERSUS MEASURED WATER LEVEL**
**STA S4.2**

PLATE 3

PLATE 4

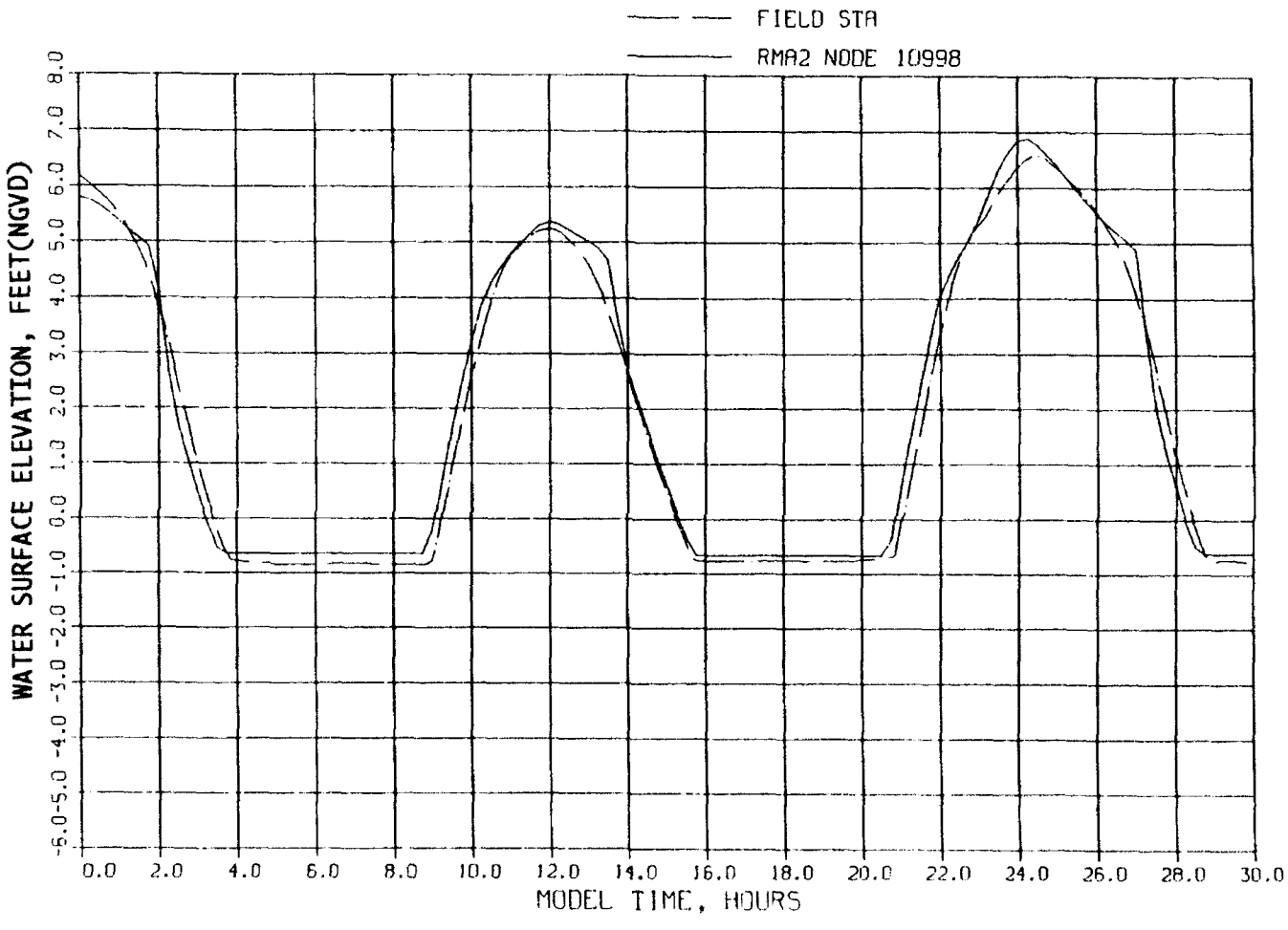


**COMPUTED VERSUS MEASURED WATER LEVEL**
**STA S4.4**

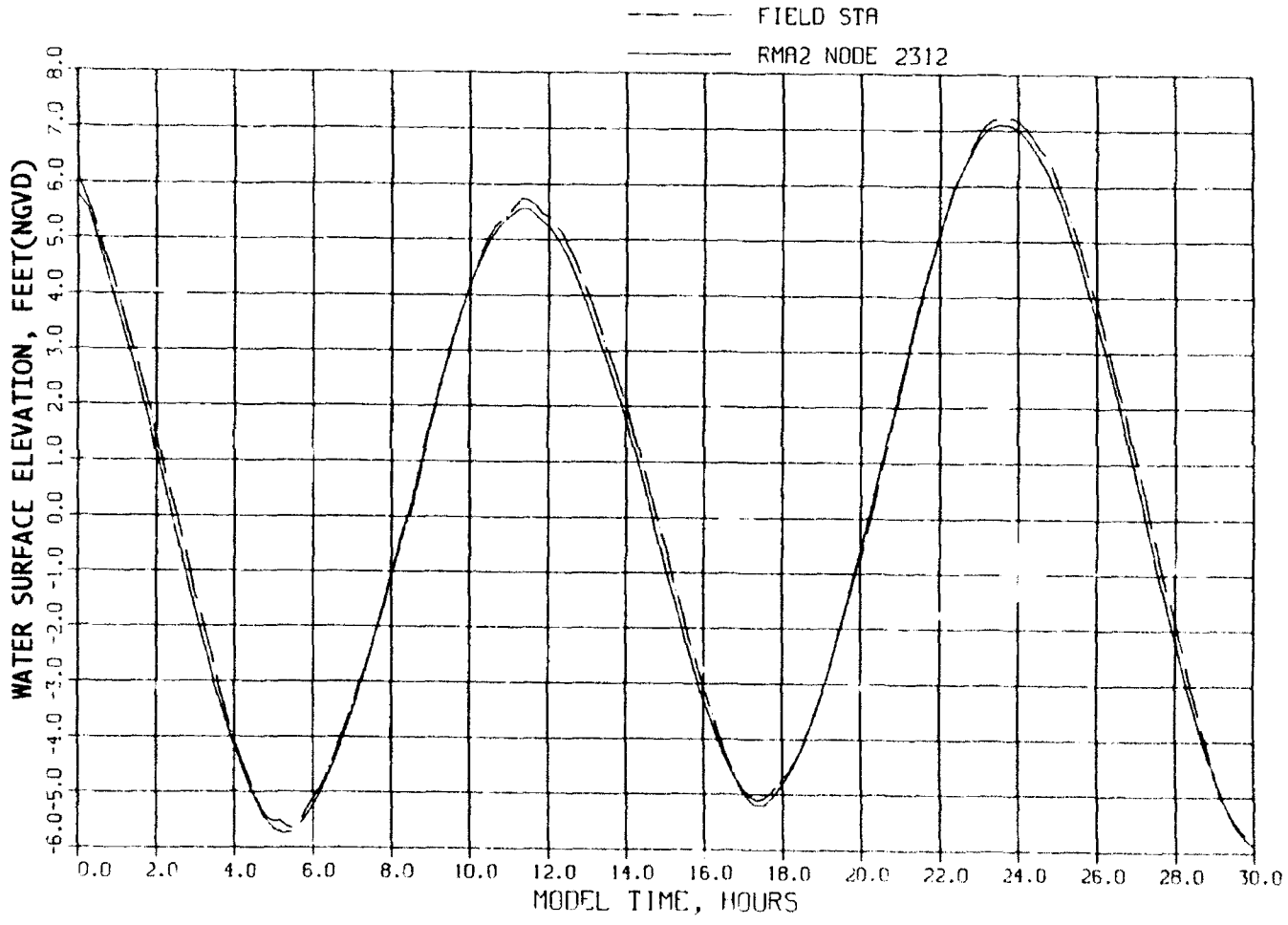


COMPUTED VERSUS MEASURED
WATER LEVEL
STA S7.4

PLATE 5

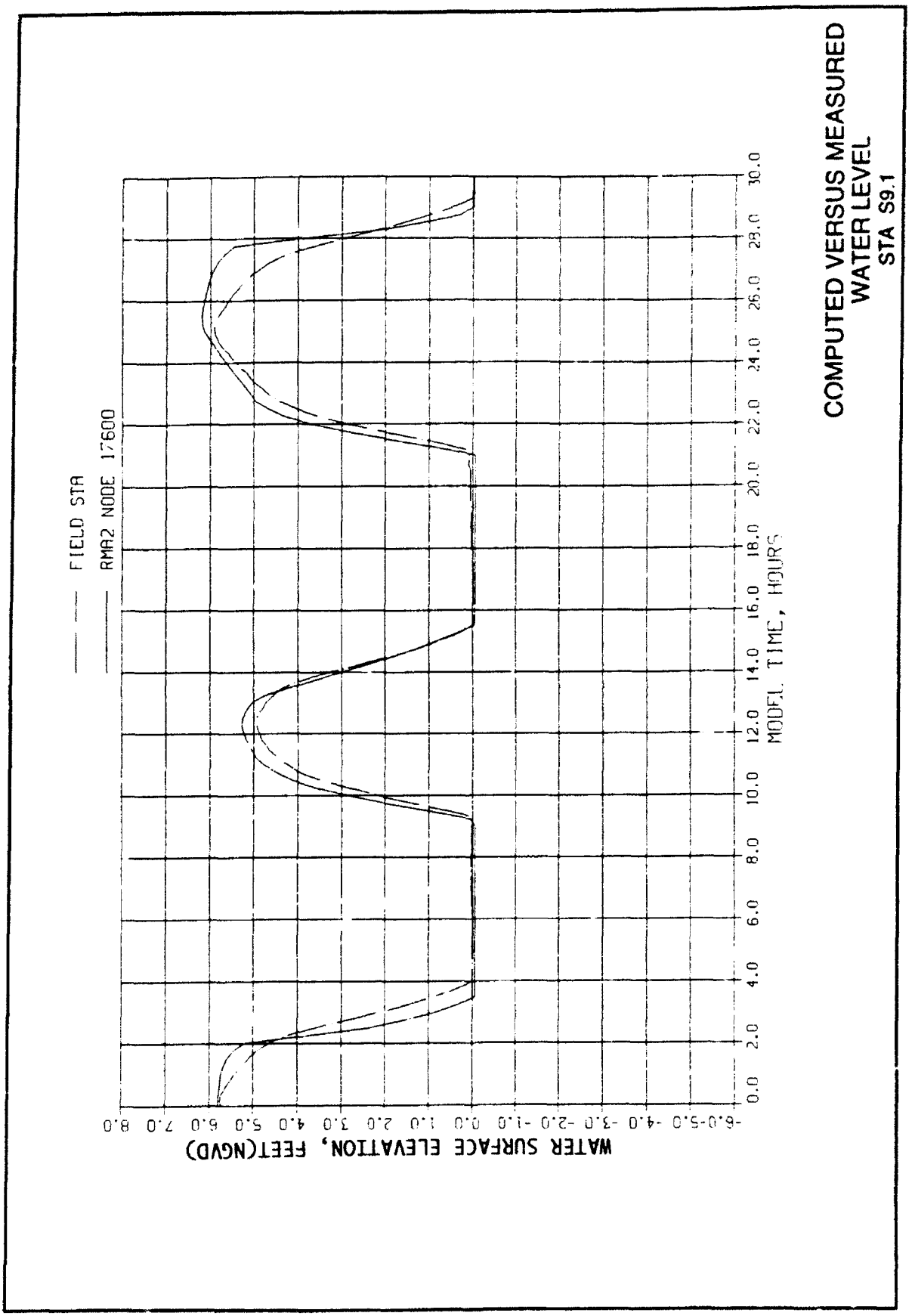
COMPUTED VERSUS MEASURED
WATER LEVEL
STA S9.1
FIELD STA
RMA2 NODE 17600
WATER SURFACE ELEVATION, FEET(NGVD)
MODEL TIME, HOURS
8.0
7.0
6.0
5.0
4.0
3.0
2.0
1.0
0.0
-1.0
-2.0
-3.0
-4.0
-5.0
-6.0
0.0
2.0
4.0
6.0
8.0
10.0
12.0
14.0
16.0
18.0
20.0
22.0
24.0
26.0
28.0
30.0

PLATE 6

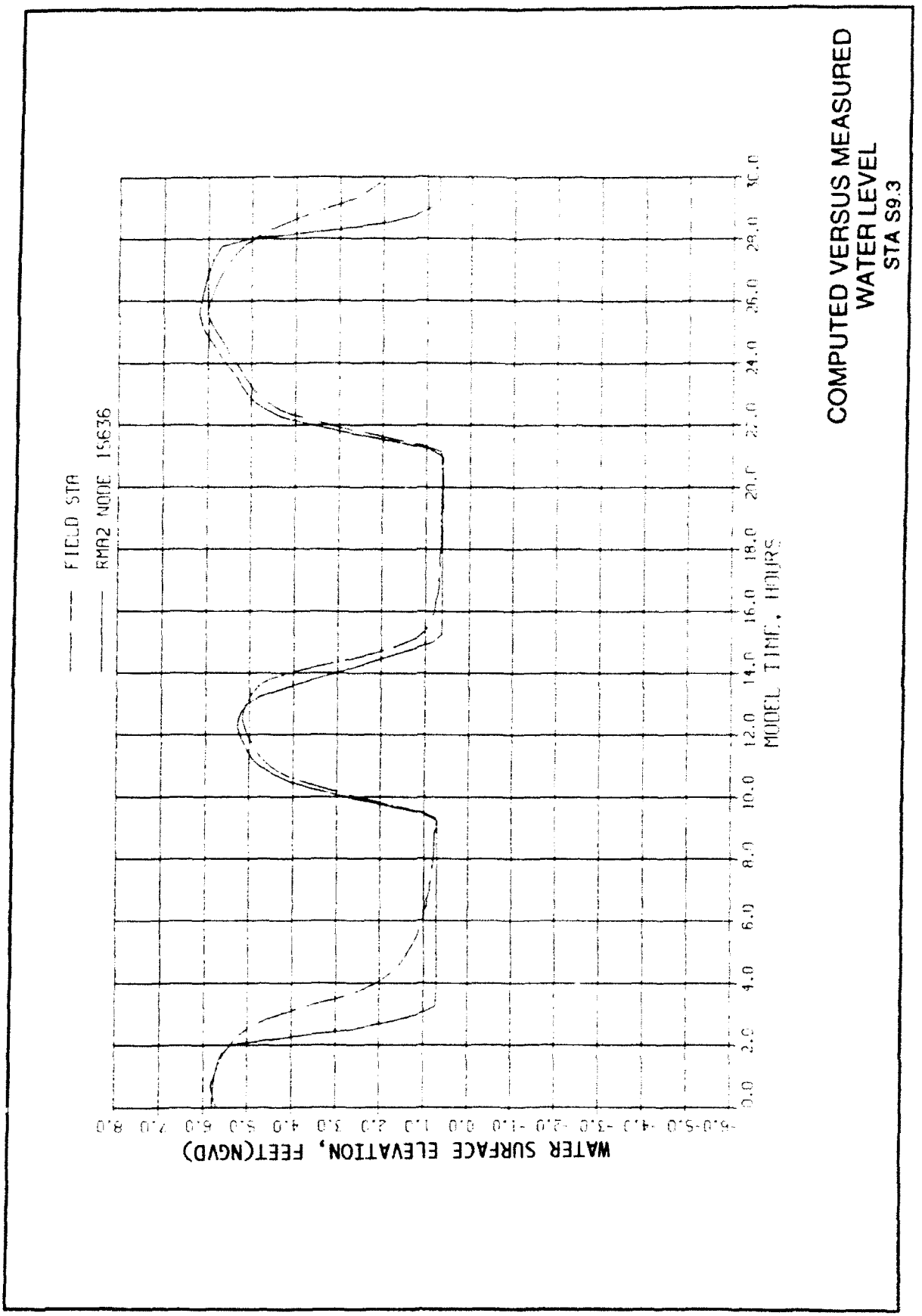
COMPUTED VERSUS MEASURED
WATER LEVEL
STA S9.3
FIELD STA
RMA2 NODE 15636
WATER SURFACE ELEVATION, FEET(NGVD)
MODEL TIME, HOURS
0.0
2.0
4.0
6.0
8.0
10.0
12.0
14.0
16.0
18.0
20.0
24.0
26.0
28.0
-5.0
-4.0
-3.0
-2.0
-1.0
0.0
1.0
2.0
3.0
4.0
5.0
6.0
7.0
8.0

PLATE 7

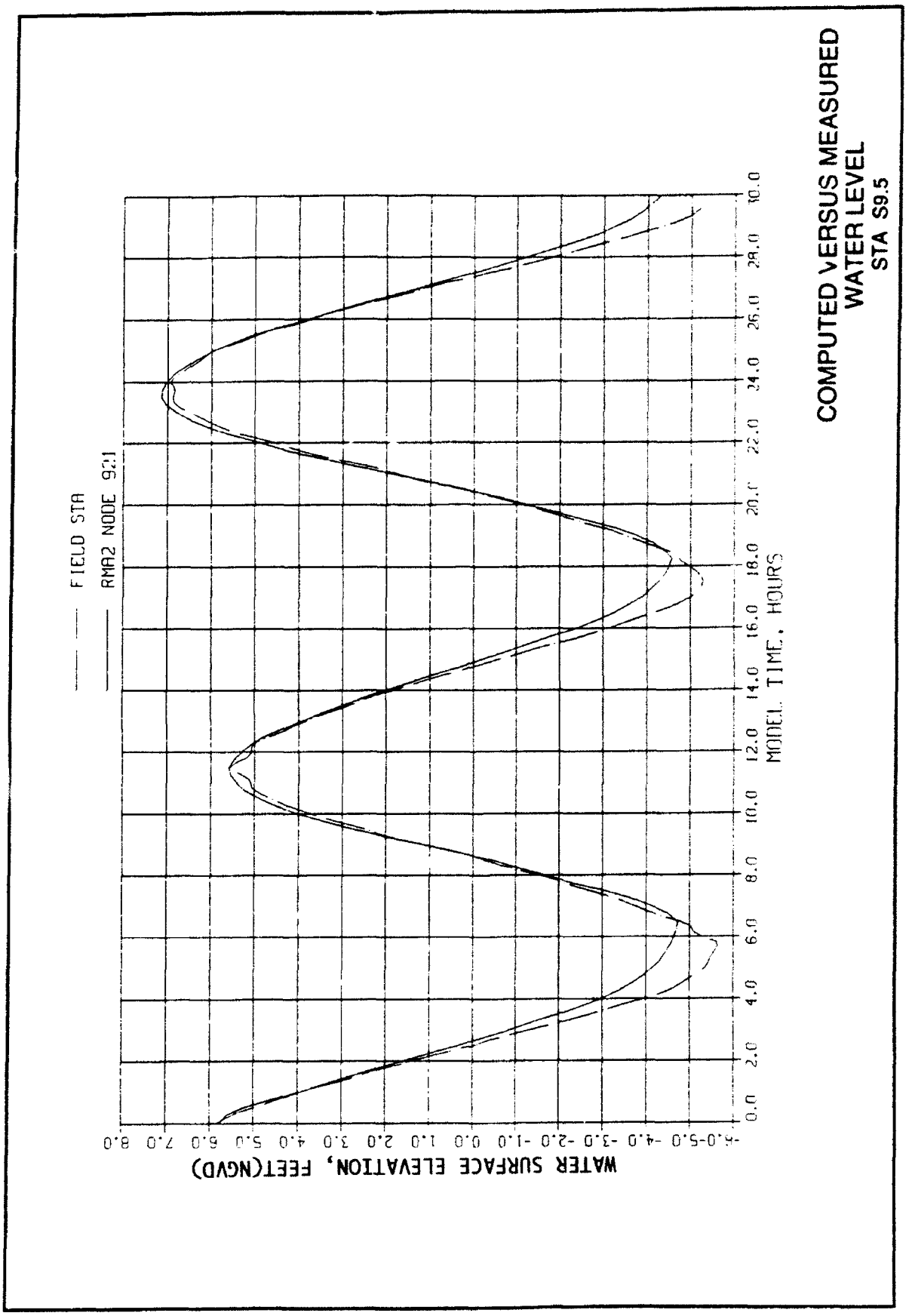
COMPUTED VERSUS MEASURED
WATER LEVEL
STA S9.5
FIELD STA
RMA2 NODE 921
WATER SURFACE ELEVATION, FEET(NGVD)
MODEL TIME, HOURS
8.0
7.0
6.0
5.0
4.0
3.0
2.0
1.0
0.0
-1.0
-2.0
-3.0
-4.0
-5.0
0.0
2.0
4.0
6.0
8.0
10.0
12.0
14.0
16.0
18.0
20.0
22.0
24.0
26.0
28.0
30.0

PLATE 8

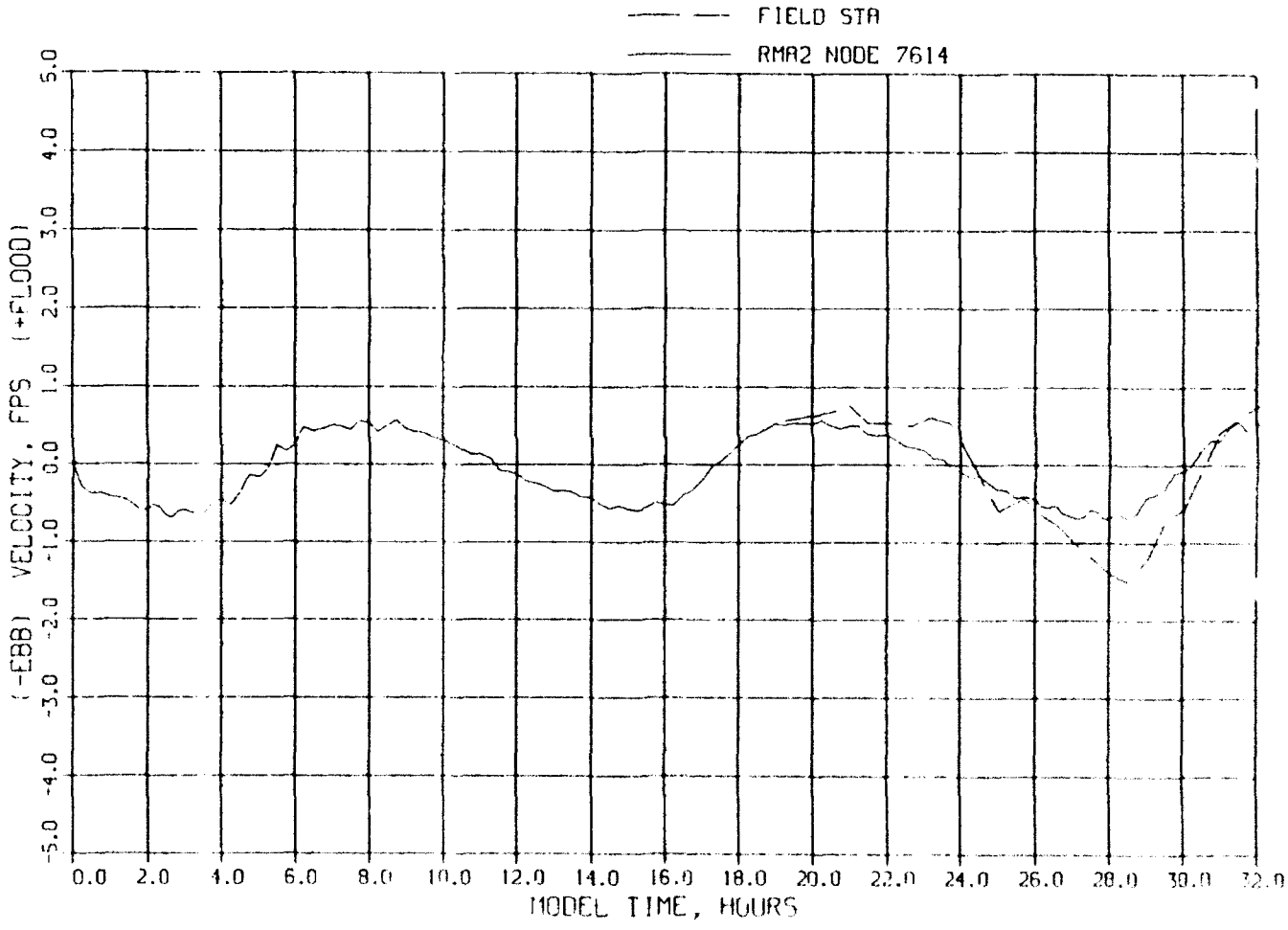


**COMPUTED VERSUS MEASURED VELOCITY**
**STA R1.0A**

PLATE 9

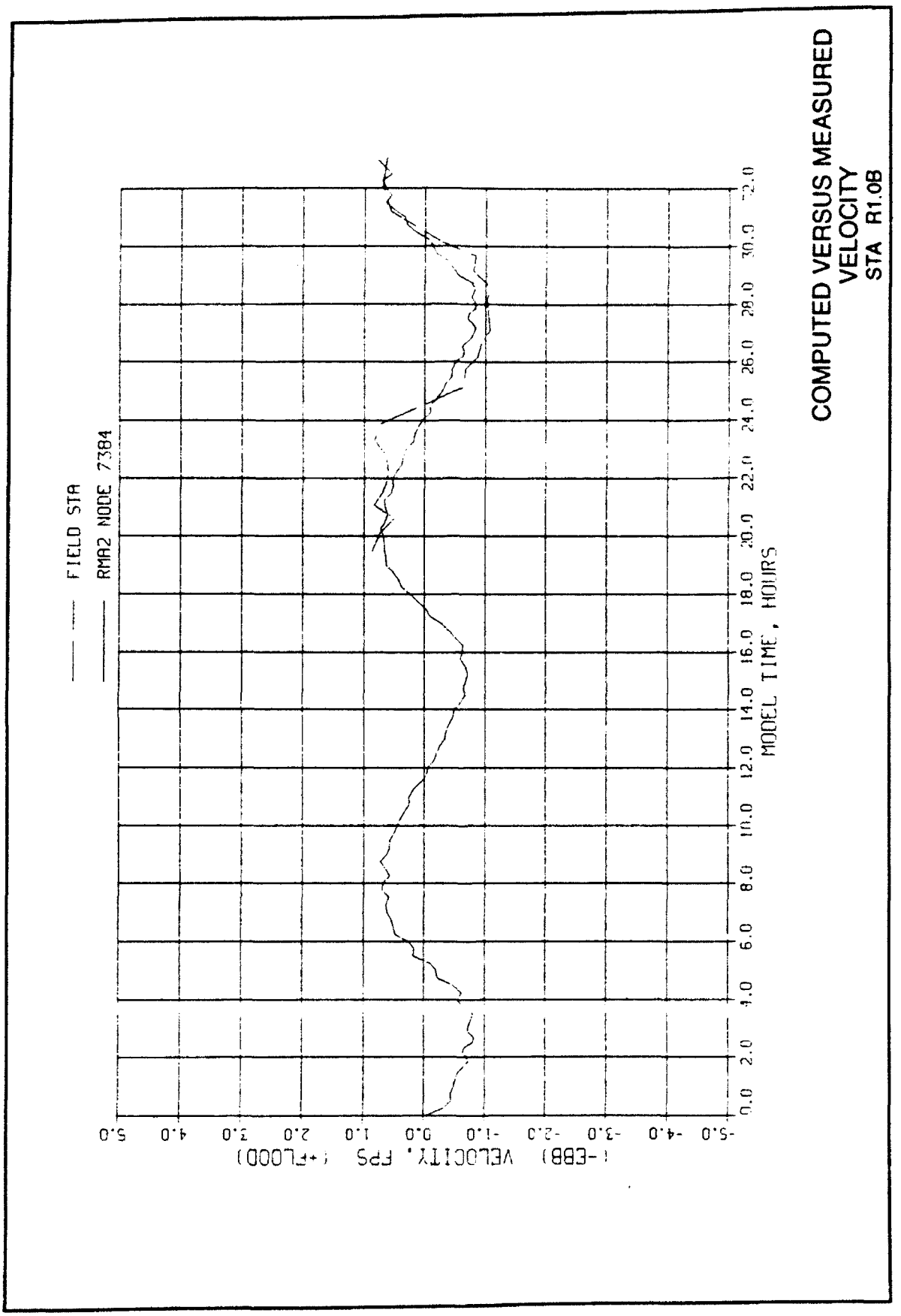
COMPUTED VERSUS MEASURED
VELOCITY
STA R1.0B
FIELD STA
RMA2 NODE 7384
MODEL TIME, HOURS
VELOCITY, FPS (+FLOOD) (-EBB)
0.0
2.0
4.0
6.0
8.0
10.0
12.0
14.0
16.0
18.0
20.0
22.0
24.0
26.0
28.0
30.0
5.0
4.0
3.0
2.0
1.0
0.0
-1.0
-2.0
-3.0
-4.0
-5.0

PLATE 10

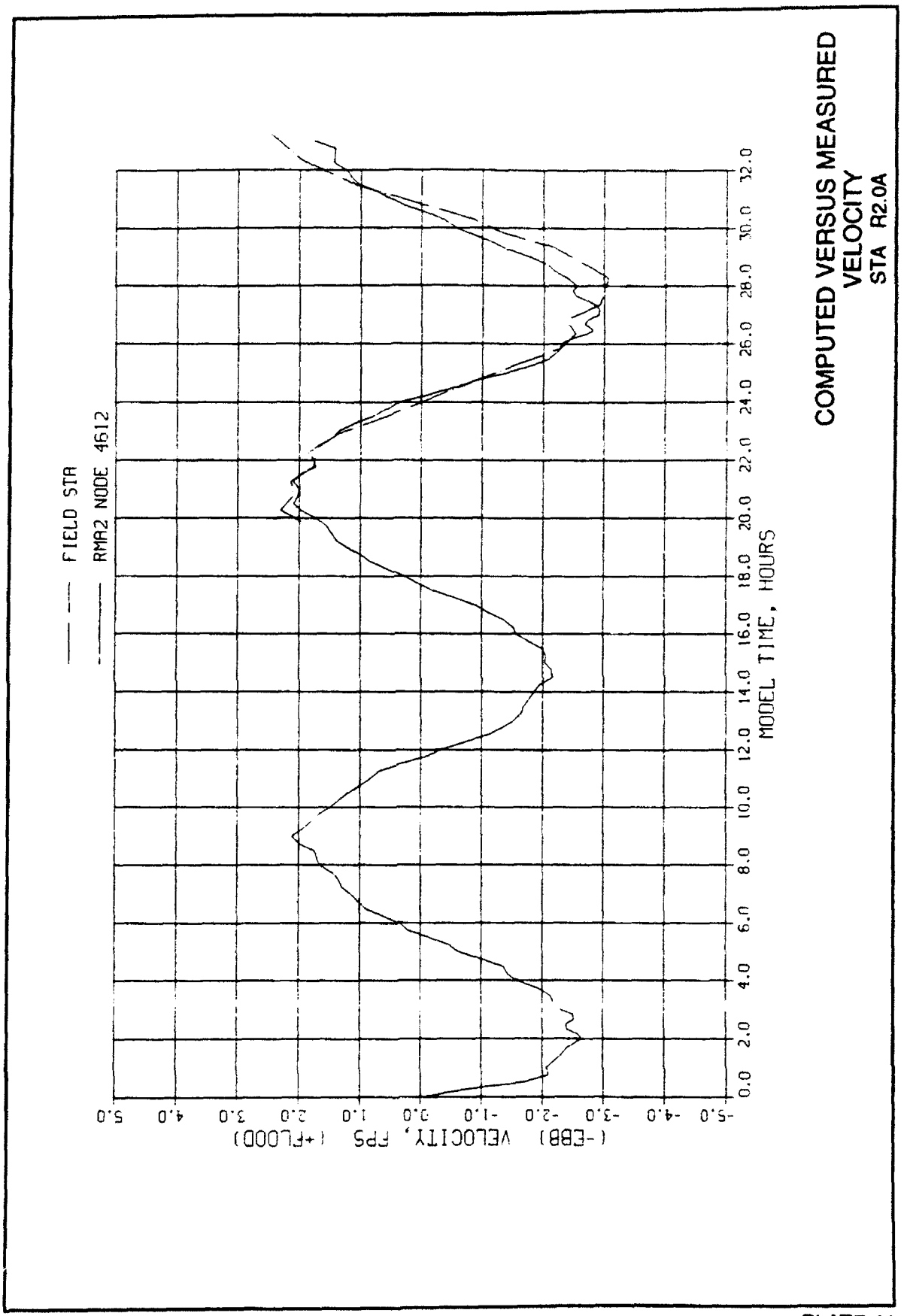
COMPUTED VERSUS MEASURED
VELOCITY
STA R2.0A
FIELD STA
RMA2 NODE 4612
MODEL TIME, HOURS
0.0
2.0
4.0
6.0
8.0
10.0
12.0
14.0
16.0
18.0
20.0
22.0
24.0
26.0
28.0
30.0
32.0
VELOCITY, FPS (+FLOOD) (-EBB)
5.0
4.0
3.0
2.0
1.0
0.0
-1.0
-2.0
-3.0
-4.0
-5.0

PLATE 11

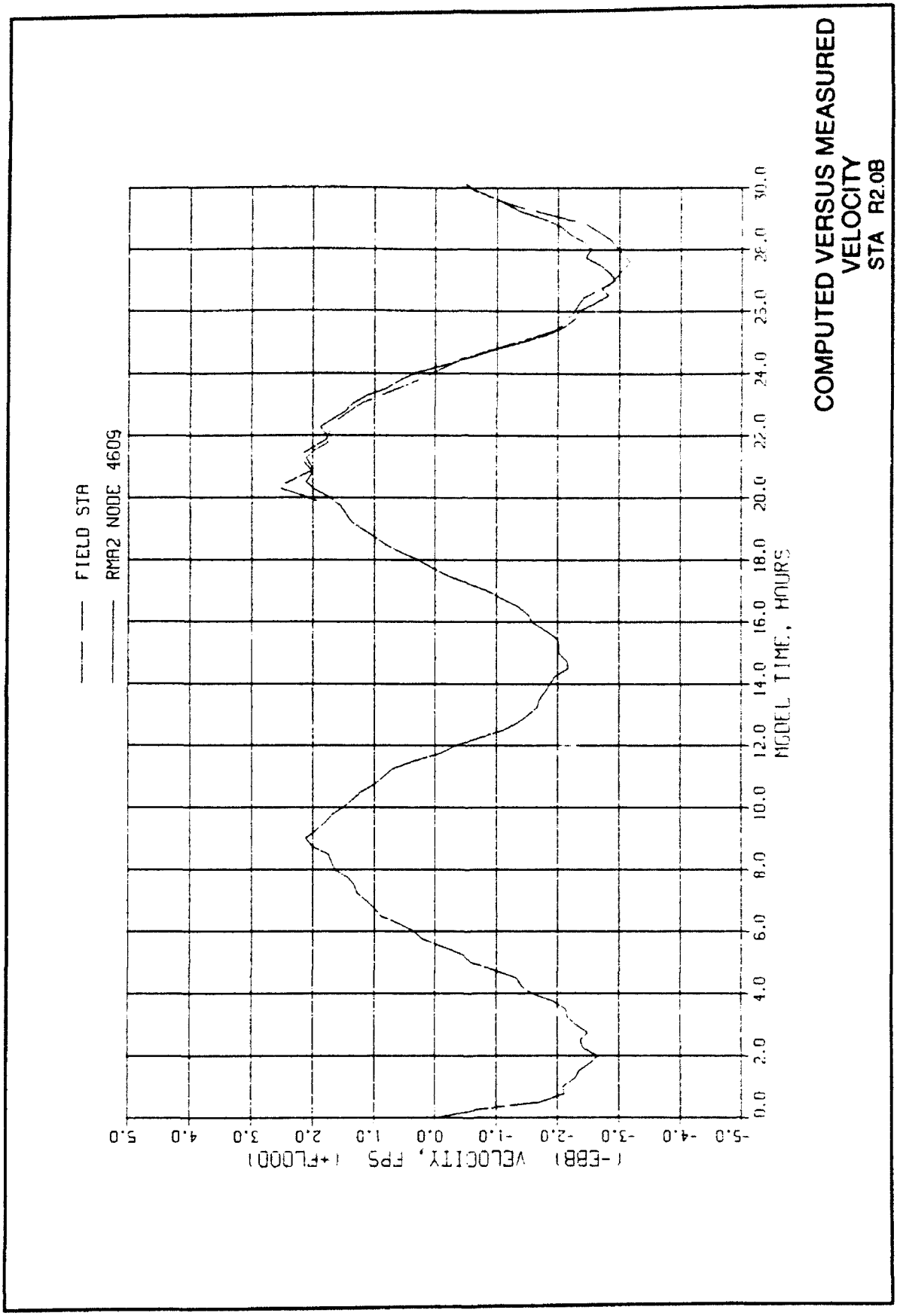
COMPUTED VERSUS MEASURED
VELOCITY
STA R2.0B
FIELD STA
RMA2 NODE 4609
MODEL TIME, HOURS
0.0
2.0
4.0
6.0
8.0
10.0
12.0
14.0
16.0
18.0
20.0
22.0
24.0
25.0
30.0
VELOCITY, FPS (-EBB) (+FLOOD)
5.0
4.0
3.0
2.0
1.0
0.0
-1.0
-2.0
-3.0
-4.0
-5.0

PLATE 12

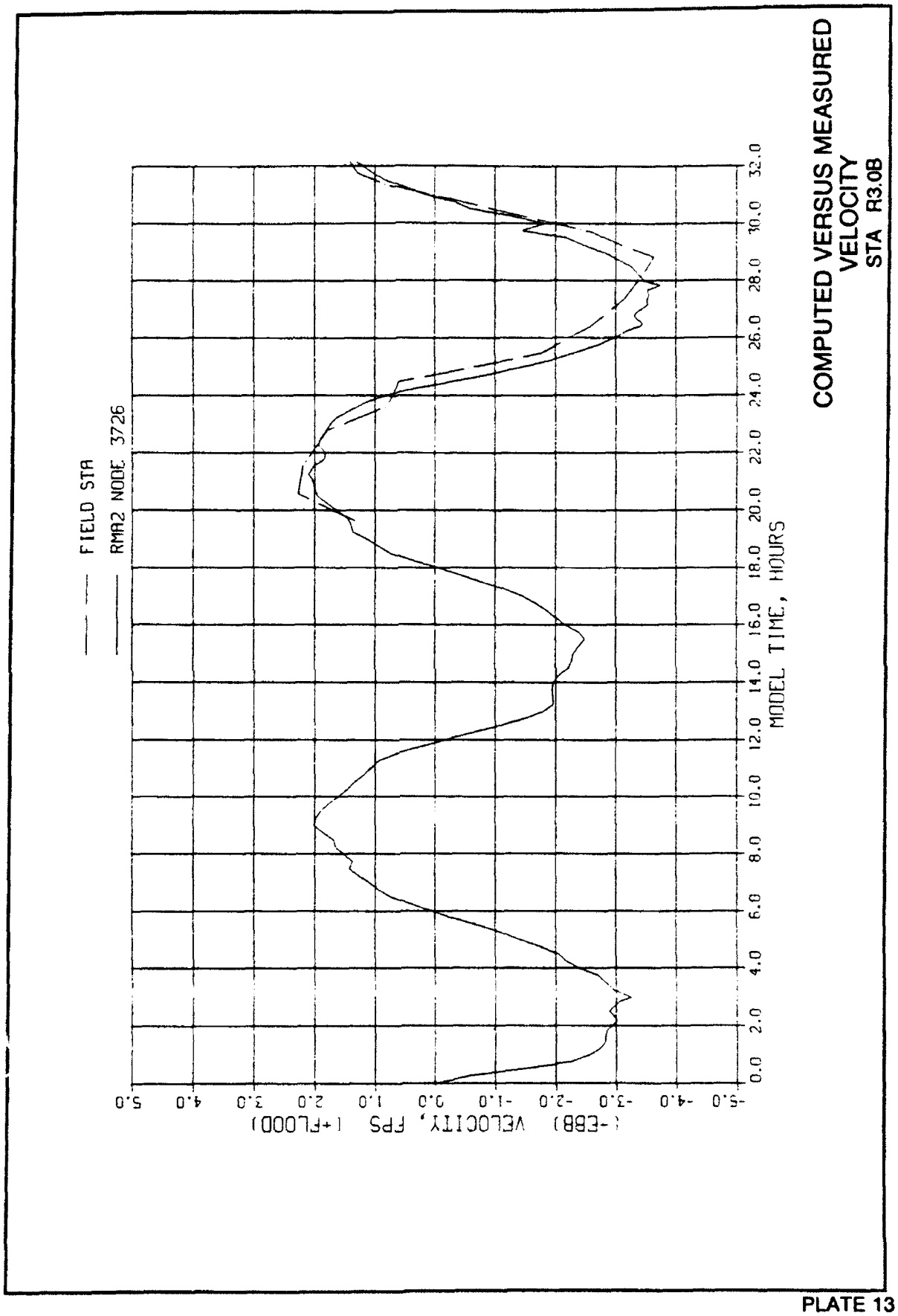
COMPUTED VERSUS MEASURED
VELOCITY
STA R3.0B
FIELD STA
RMA2 NODE 3726
MODEL TIME, HOURS
0.0
2.0
4.0
6.0
8.0
10.0
12.0
14.0
16.0
18.0
20.0
22.0
24.0
26.0
28.0
30.0
32.0
VELOCITY, FPS (+FLOOD)
(-EBB)
5.0
4.0
3.0
2.0
1.0
0.0
-1.0
-2.0
-3.0
-4.0
-5.0

PLATE 13

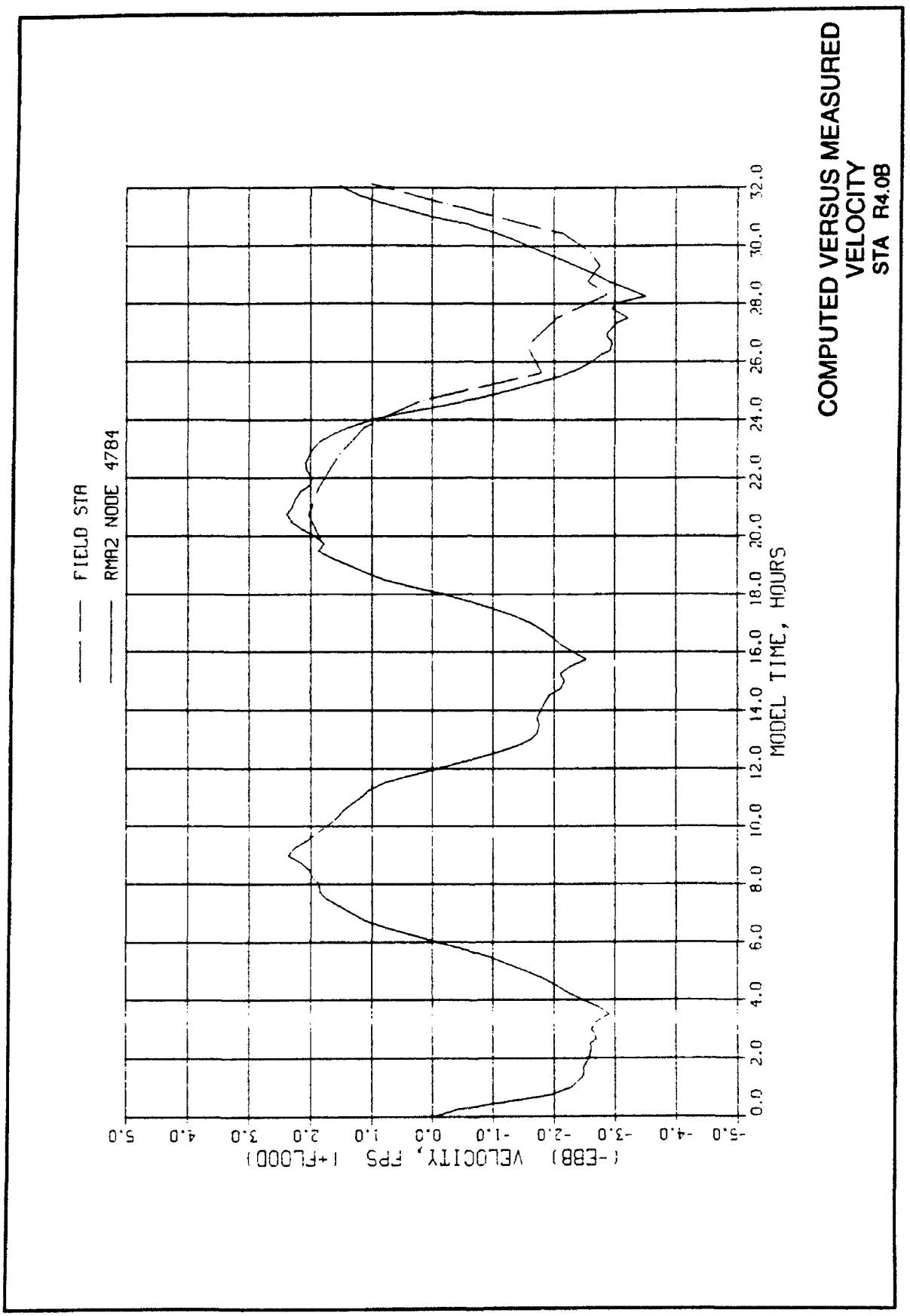
COMPUTED VERSUS MEASURED
VELOCITY
STA R4.0B
FIELD STA
RMA2 NODE 4784
MODEL TIME, HOURS
0.0
2.0
4.0
6.0
8.0
10.0
12.0
14.0
16.0
18.0
20.0
22.0
24.0
26.0
28.0
30.0
32.0
VELOCITY, FPS
(-EBB)
(+FLOOD)
5.0
4.0
3.0
2.0
1.0
0.0
-1.0
-2.0
-3.0
-4.0
-5.0

PLATE 14

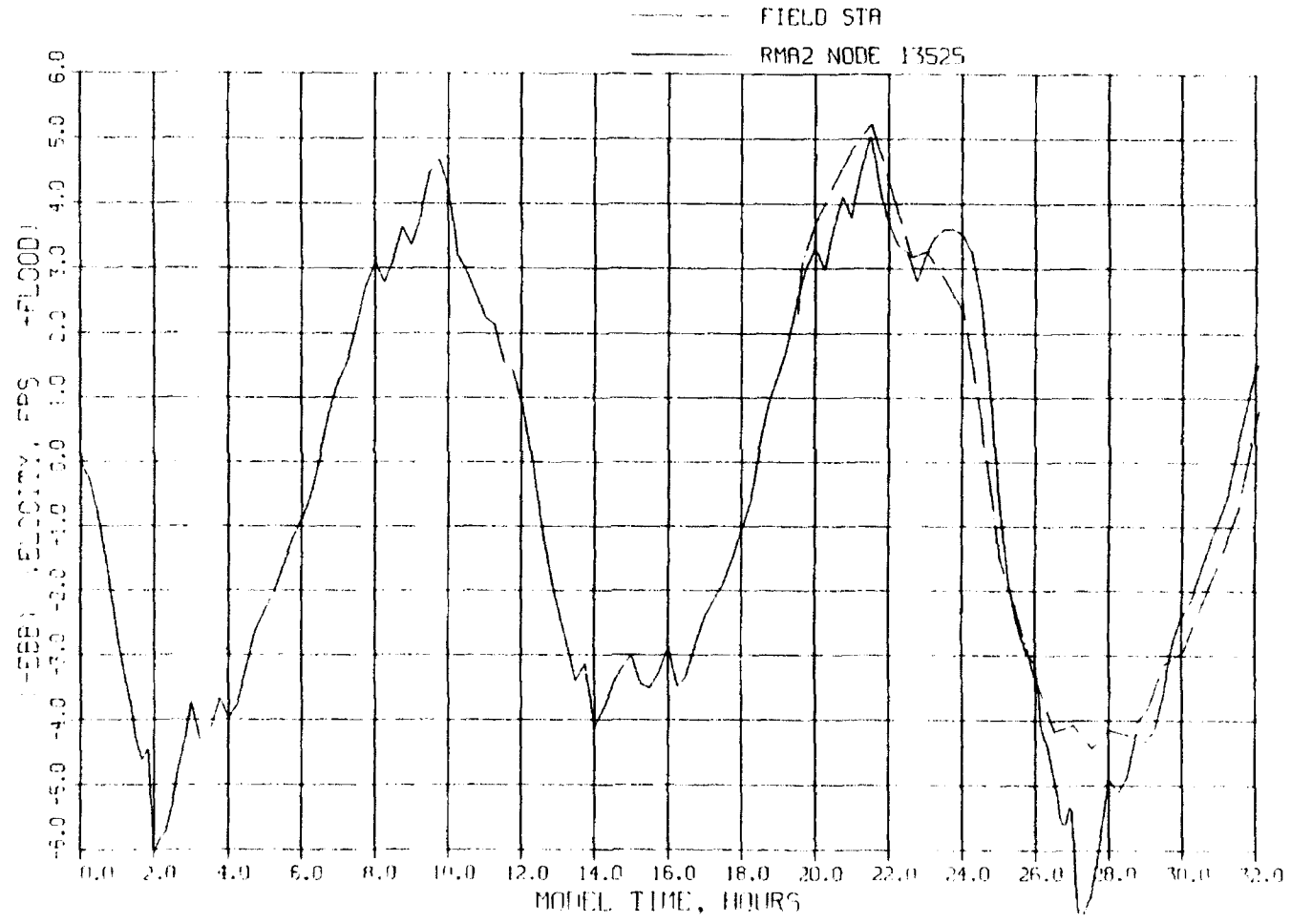


**COMPUTED VERSUS MEASURED VELOCITY**
**STA R5.0B**

PLATE 15

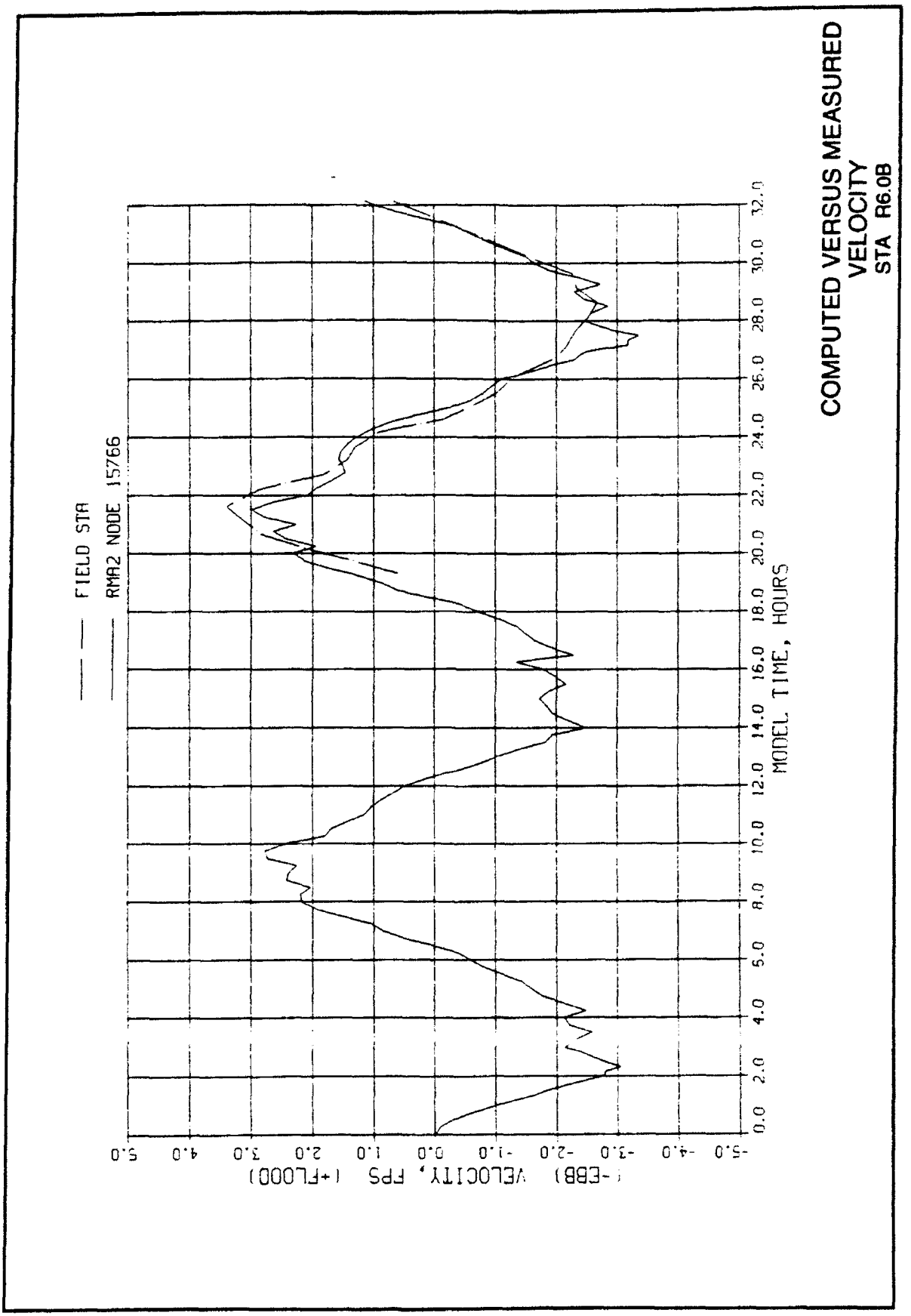
COMPUTED VERSUS MEASURED
VELOCITY
STA R6.0B
FIELD STA
RMA2 NODE 15766
MODEL TIME, HOURS
VELOCITY, FPS (+FLOOD)
(-EBB)
0.0
2.0
4.0
5.0
8.0
10.0
12.0
14.0
16.0
18.0
20.0
22.0
24.0
26.0
28.0
30.0
32.0
5.0
4.0
3.0
2.0
1.0
0.0
-1.0
-2.0
-3.0
-4.0
-5.0

PLATE 16

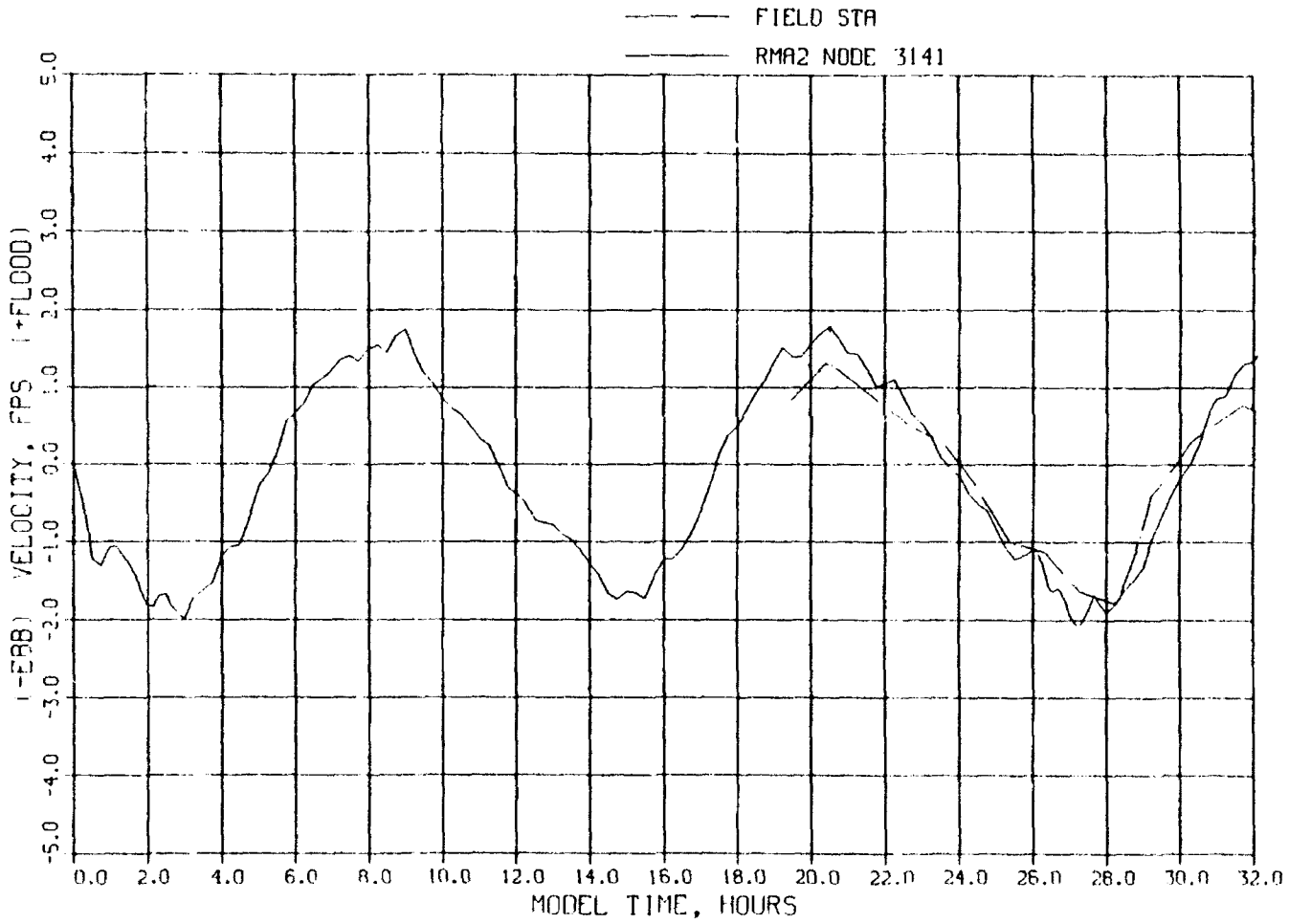


**COMPUTED VERSUS MEASURED VELOCITY**
**STA R7.0B**

PLATE 17

PLATE 18

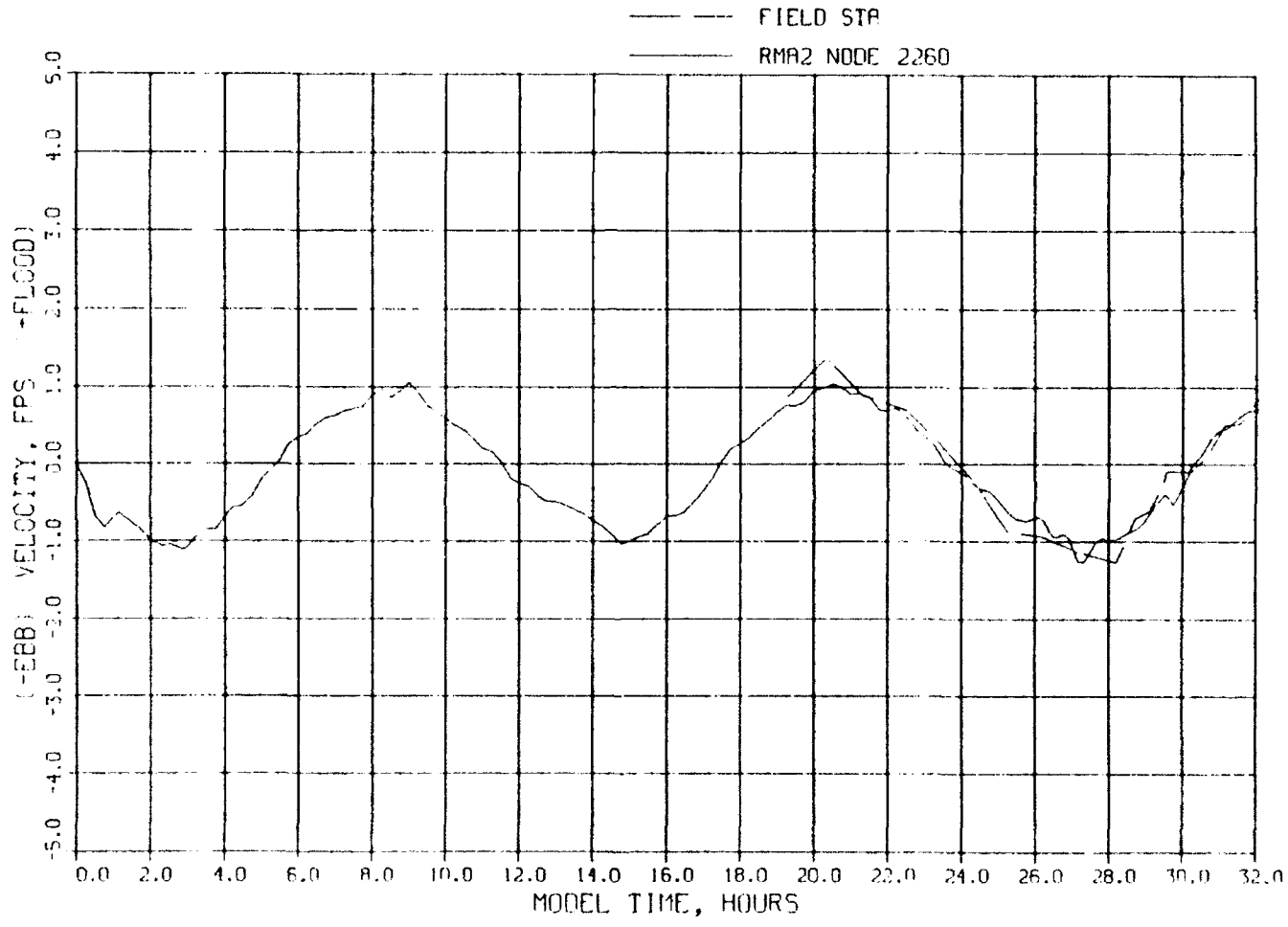


**COMPUTED VERSUS MEASURED VELOCITY**
**STA R8.0B**

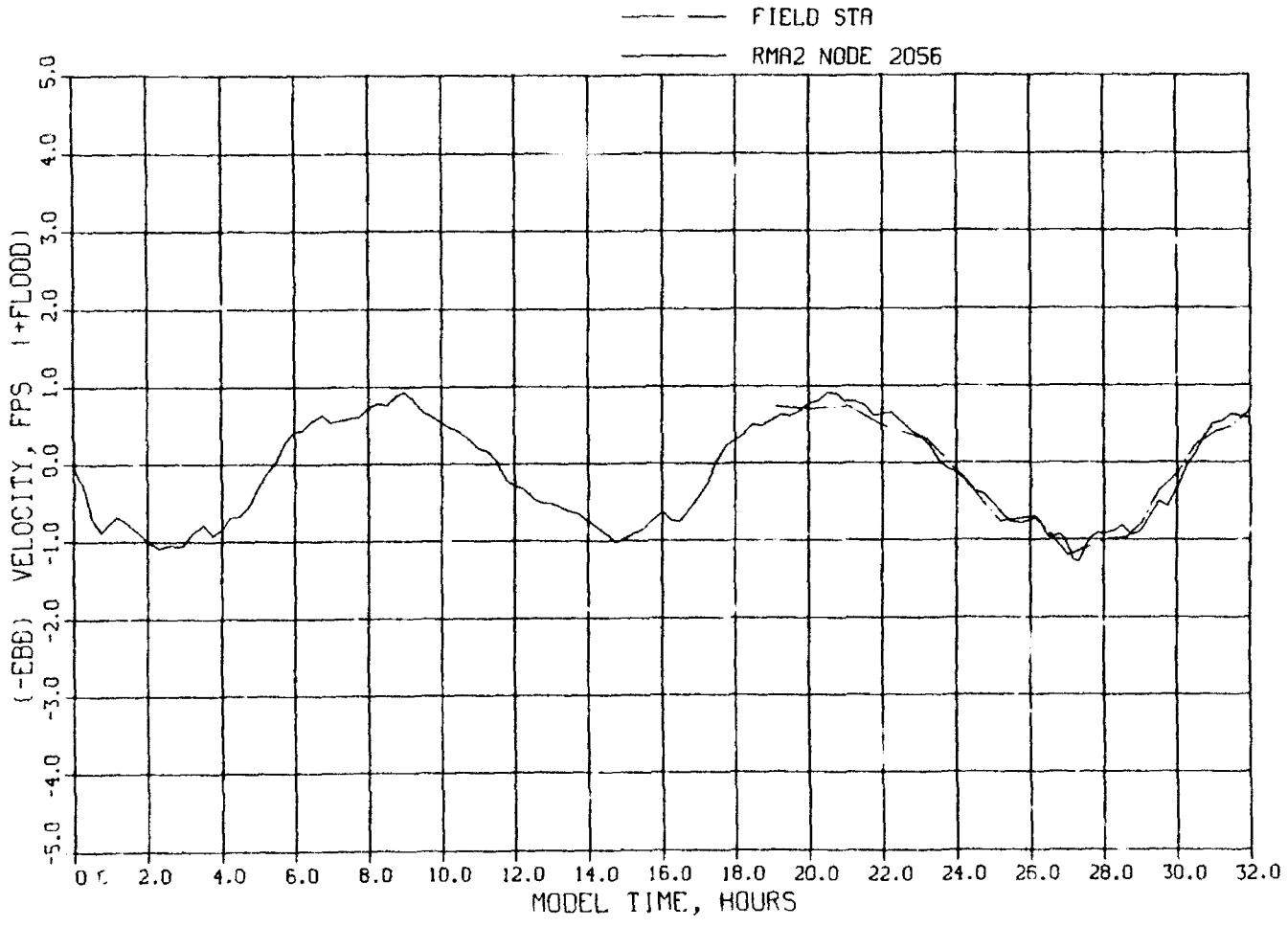


**COMPUTED VERSUS MEASURED VELOCITY**
**STA R9.0B**

PLATE 19

PLATE 20

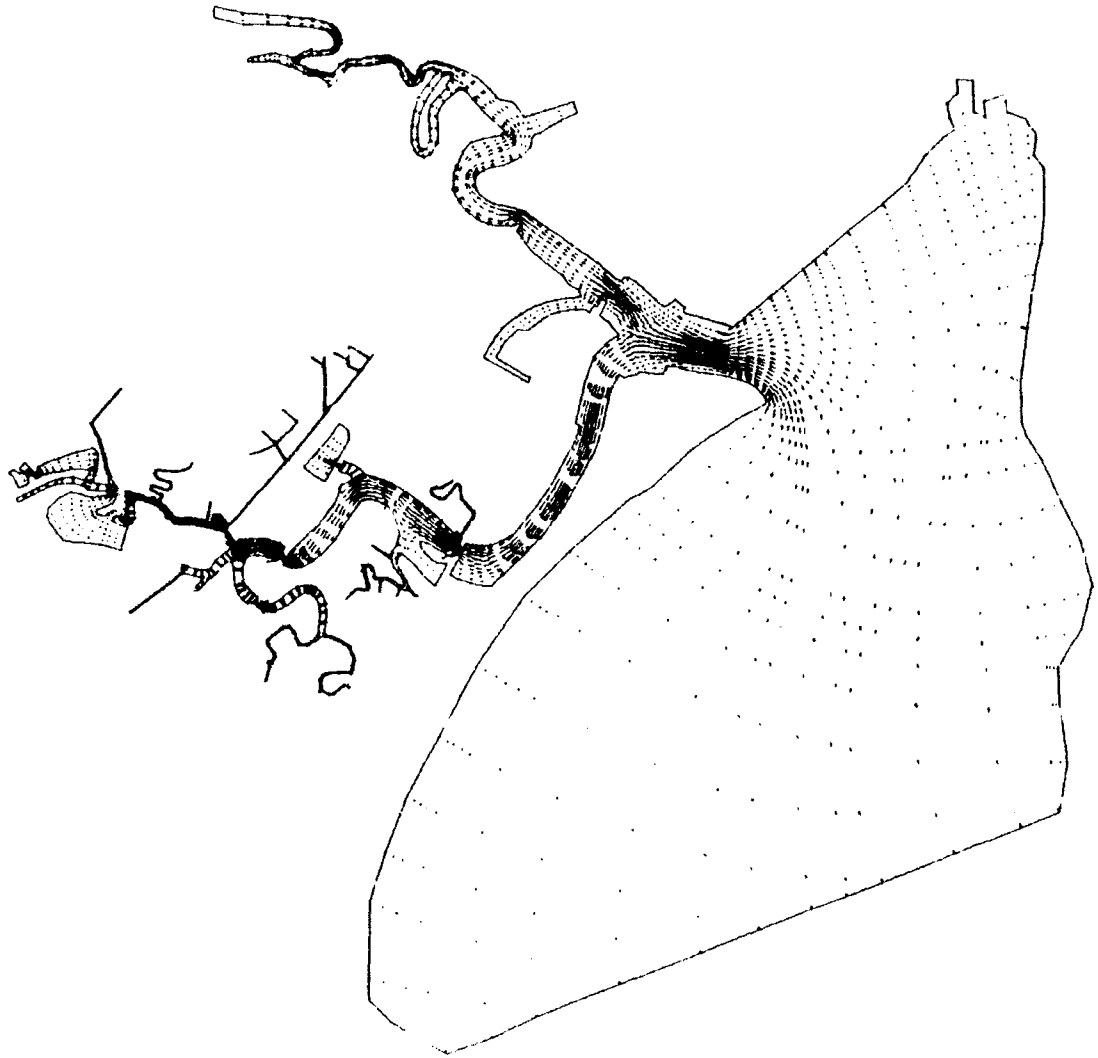

5.0 VELOCITY VECTOR SCALE, FPS

5.0

← EXCEEDS 5.0 FPS SCALE LIMIT

XS = 671.79 FT/IN.

YS = 671.79 FT/IN.

(.) RESULTANT VELOCITY =0.010 FPS

# VELOCITY VECTORS PEAK FLOOD EXISTING CONDITION

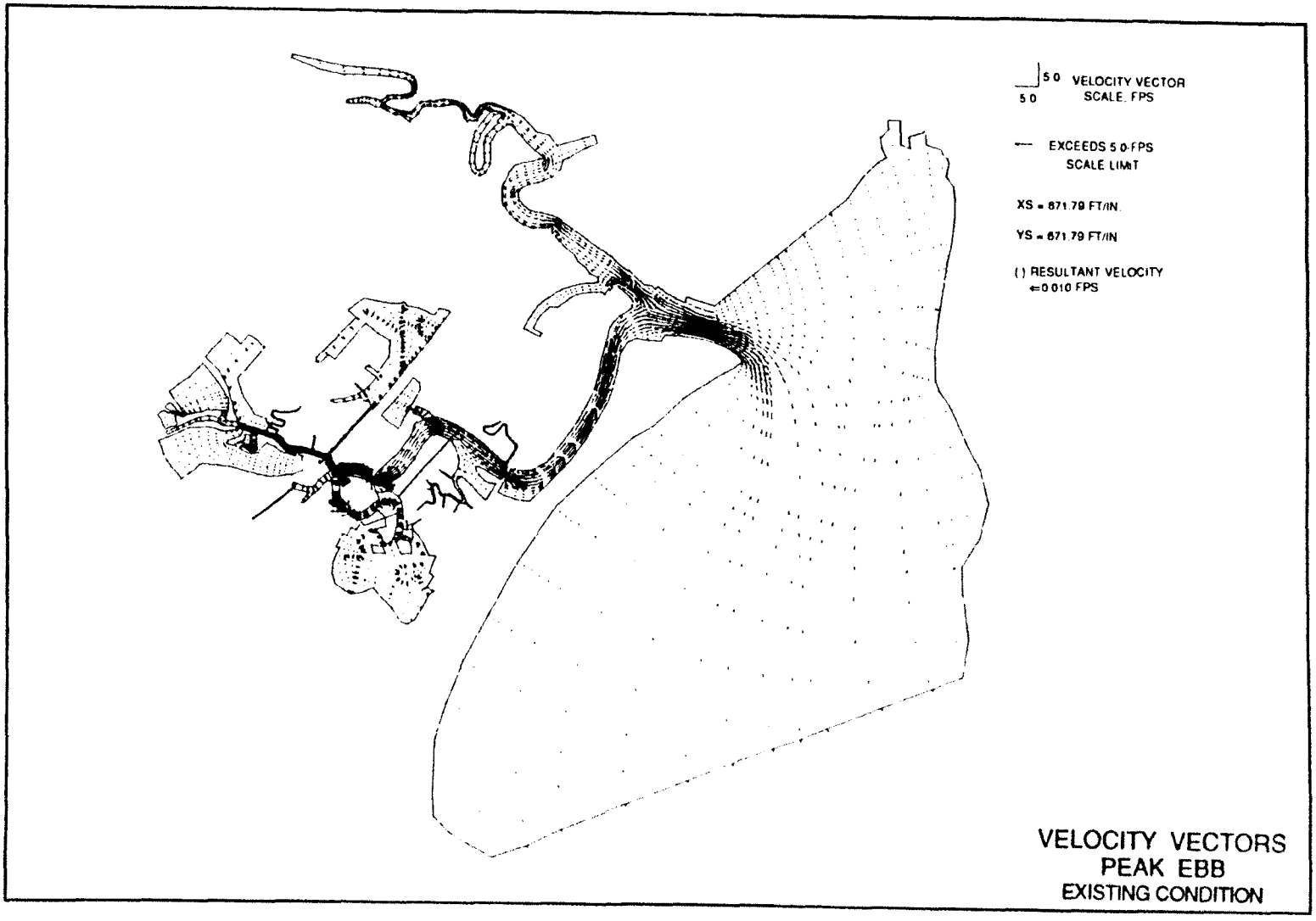


PLATE 21

VELOCITY VECTORS
PEAK EBB
EXISTING CONDITION

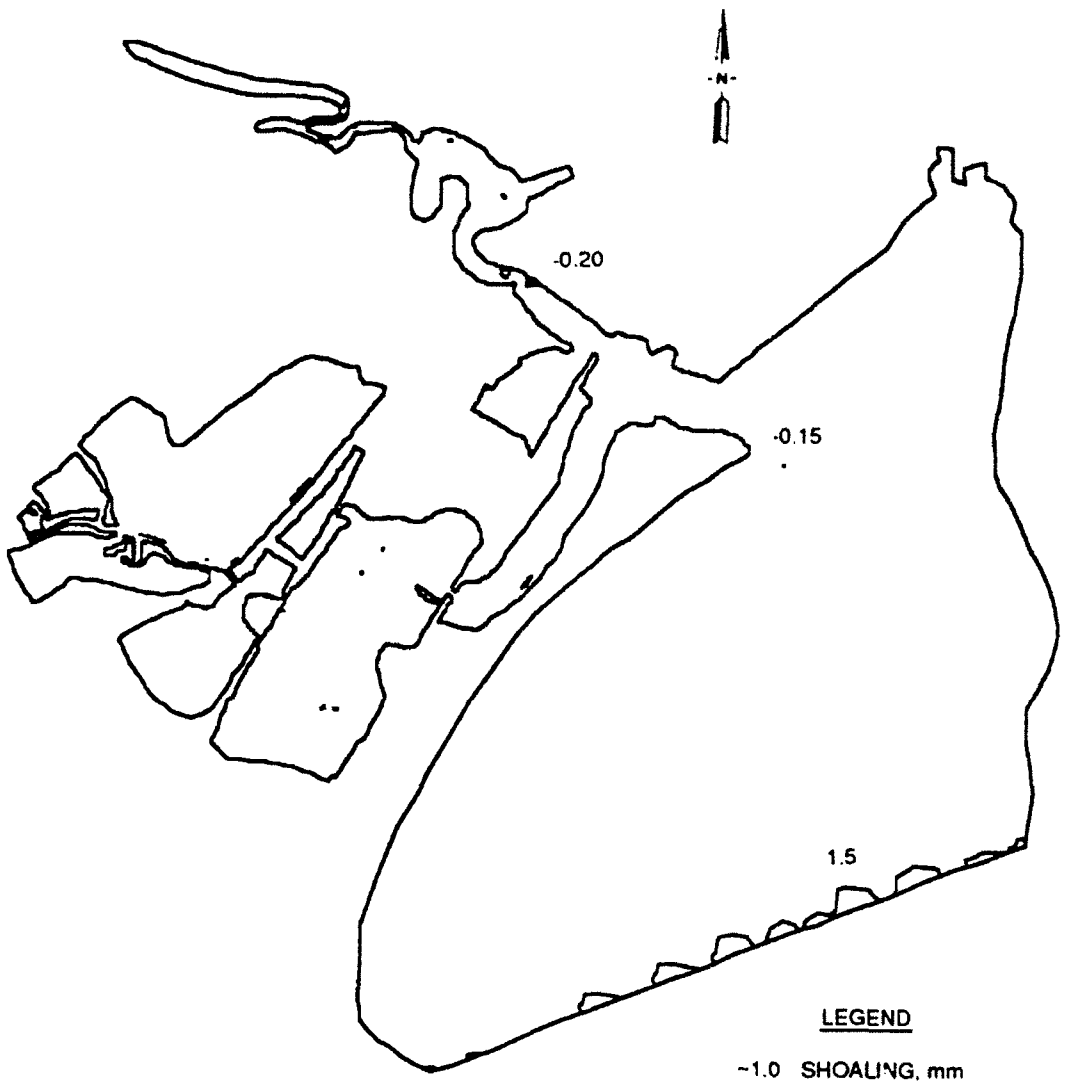


SHOALING AND SCOUR PATTERN
AFTER 1-DAY SIMULATION
EXISTING CONDITION

PLATE 22

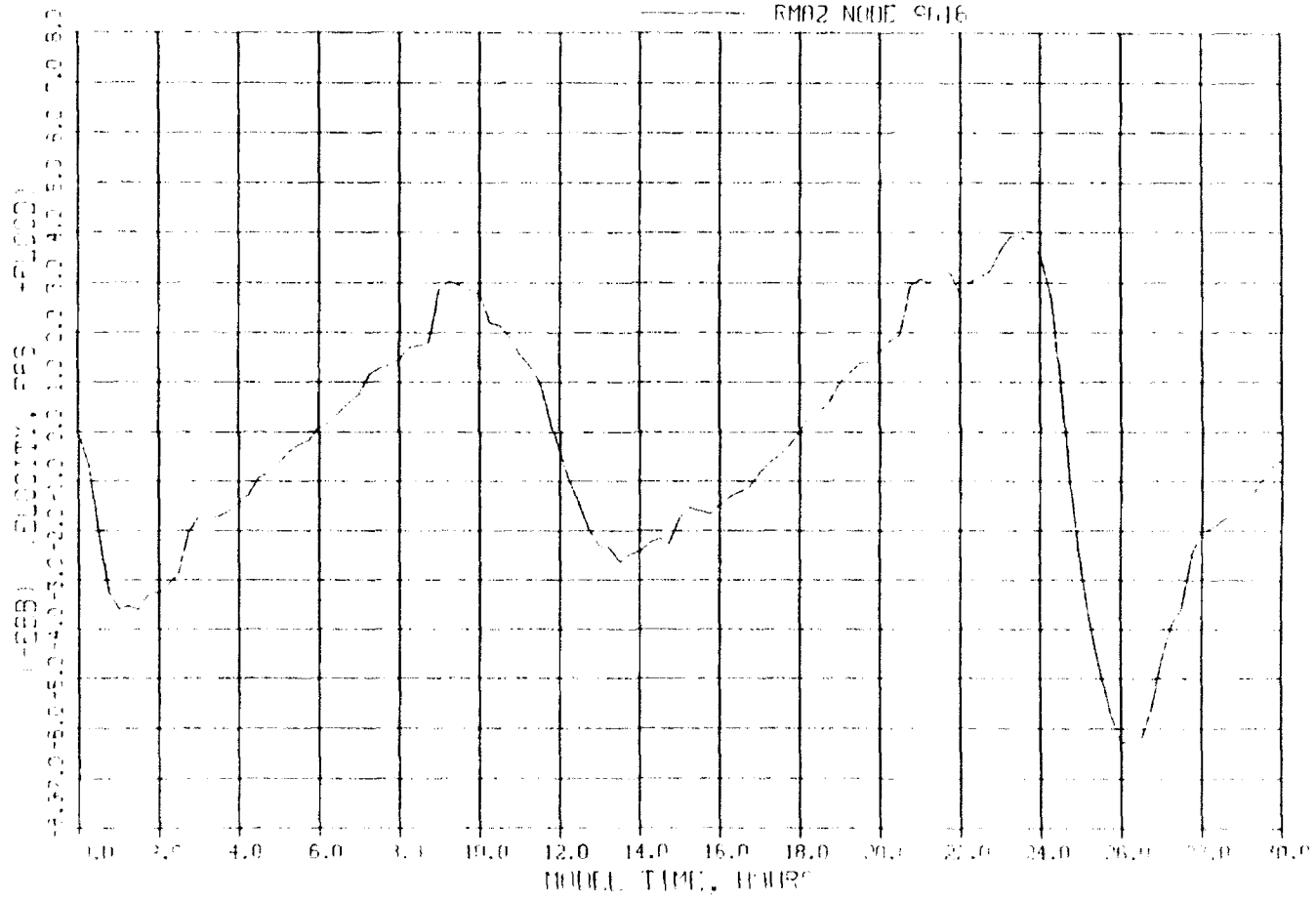


**VELOCITY TIME-HISTORY**
**BASE**
**EAST BRANCH OF PINES RIVER**
**EXISING BRIDGE WIDTH**

PLATE 23

PLATE 24

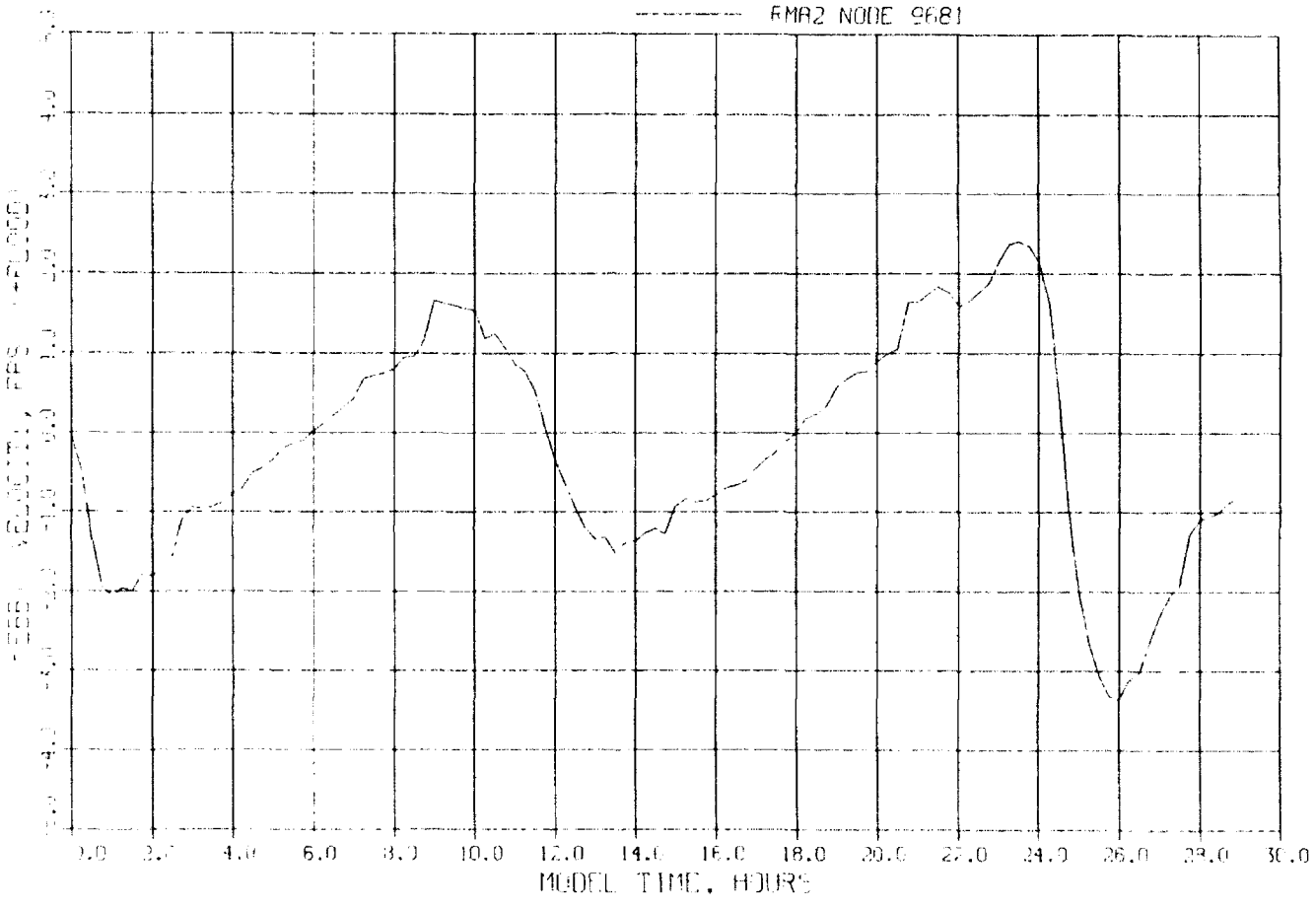


**VELOCITY TIME-HISTORY**
**BASE**
**EAST BRANCH OF PINES RIVER**
**BRIDGE OPENING = 40 FT**

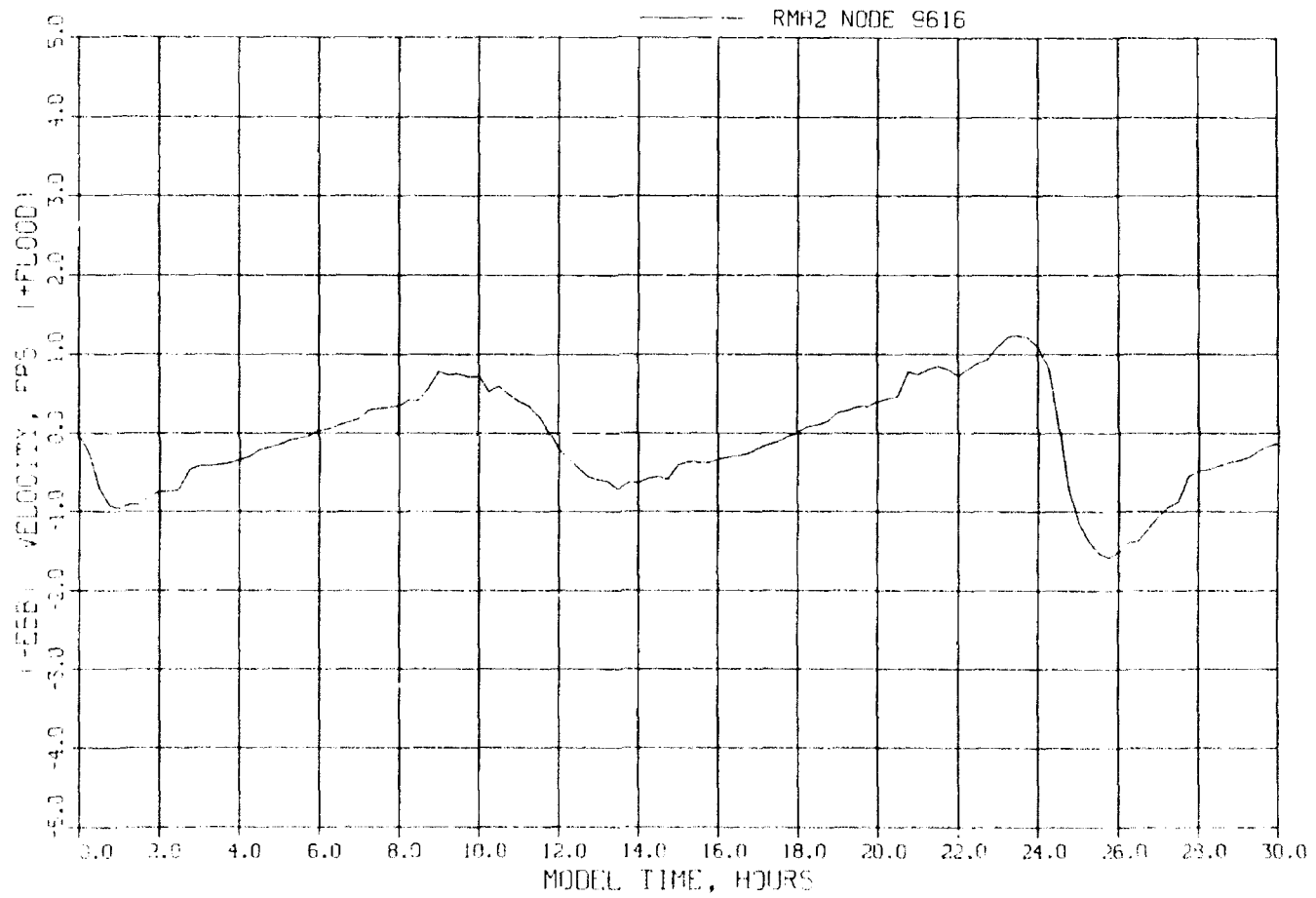


**VELOCITY TIME-HISTORY**
**BASE**
**EAST BRANCH OF PINES RIVER**
**BRIDGE OPENING = 90 FT**

PLATE 25

PLATE 26

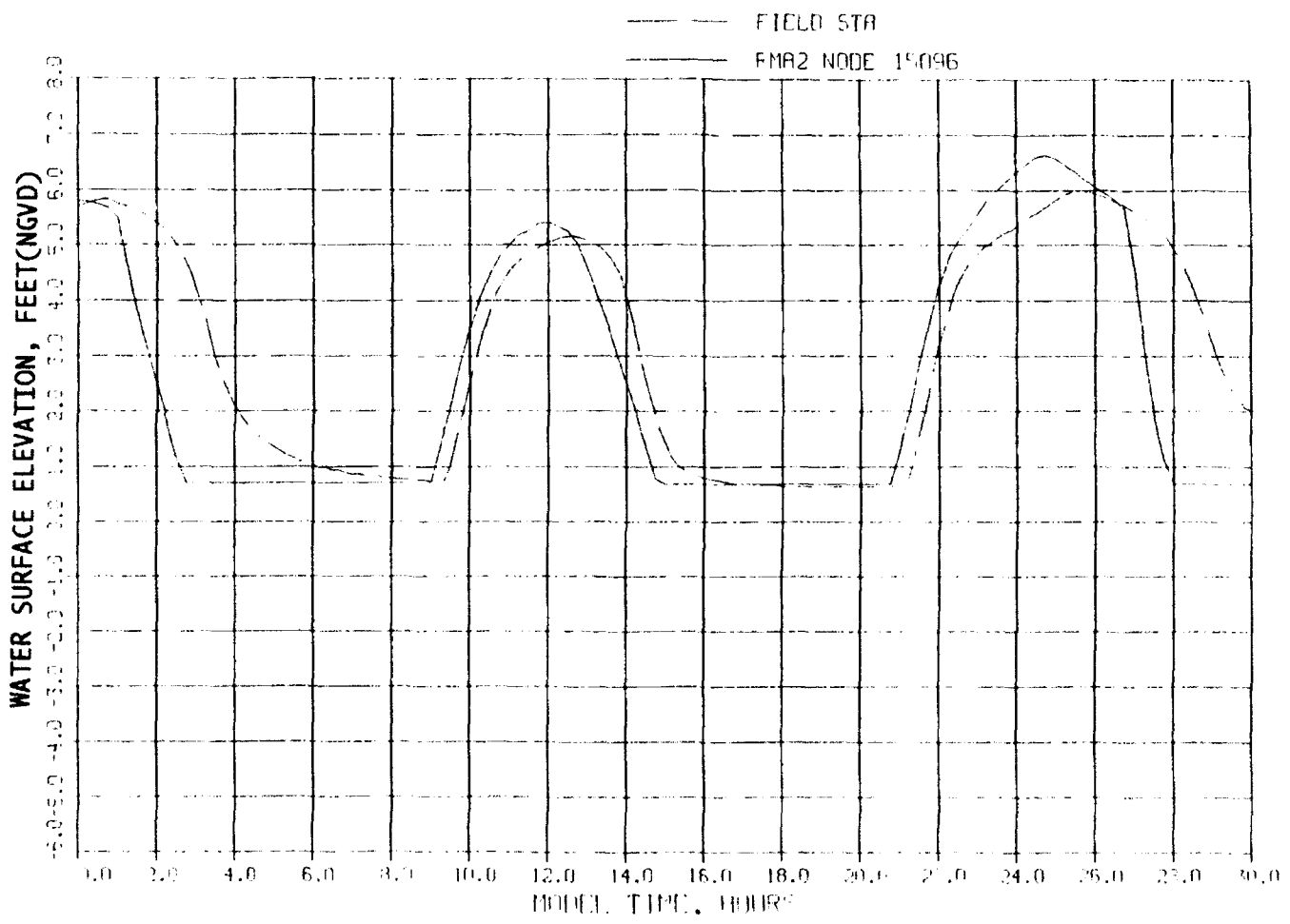


**WATER SURFACE ELEVATION TIME-HISTORY**
**FIELD DATA VERSUS BASE, EXISTING BRIDGE WIDTH**
**STA S9.3**

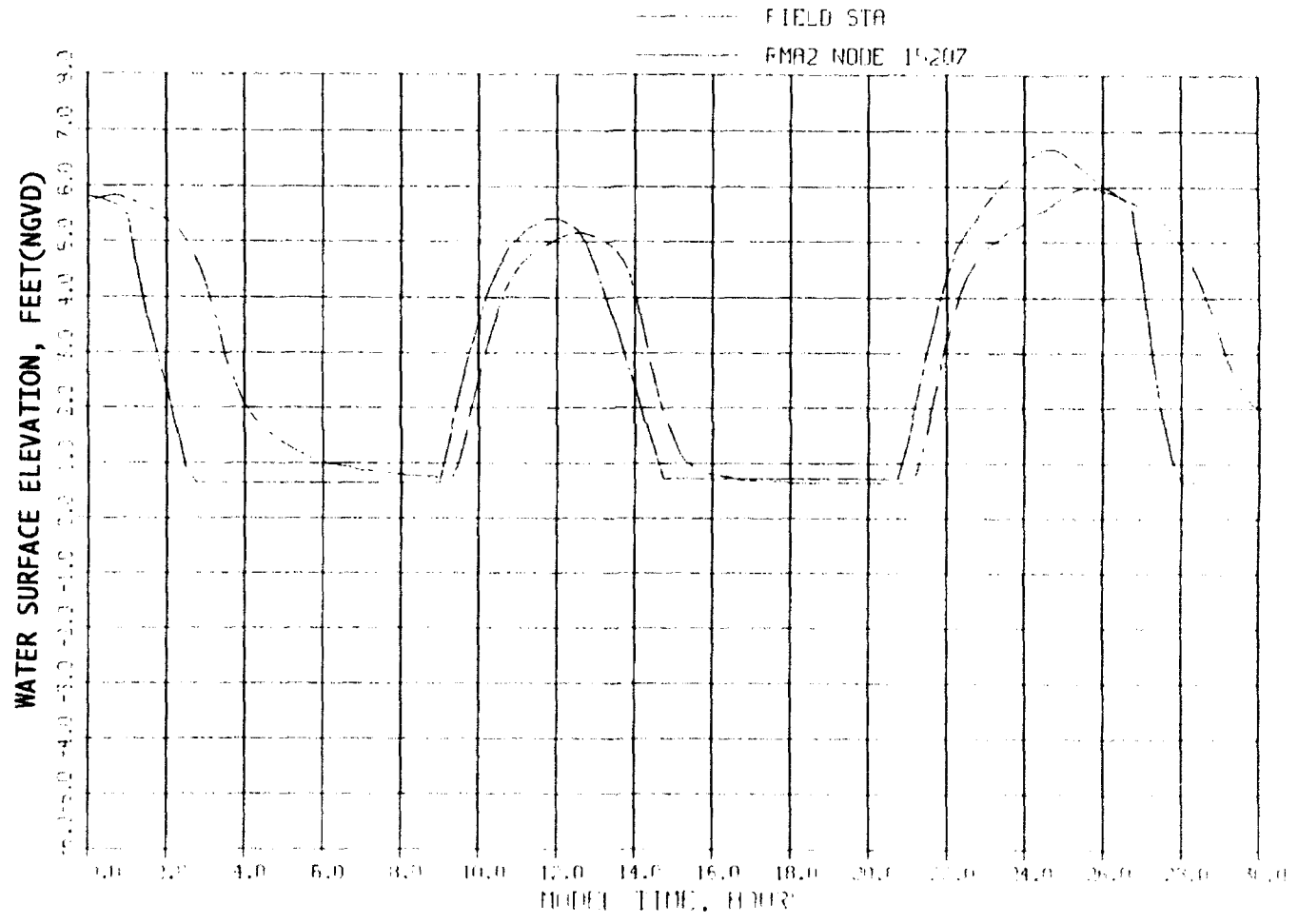


**WATER SURFACE ELEVATION TIME-HISTORY**
**FIELD DATA VERSUS BASE, BRIDGE WIDTH = 40 FT**
**STA S9.3**

PLATE 27

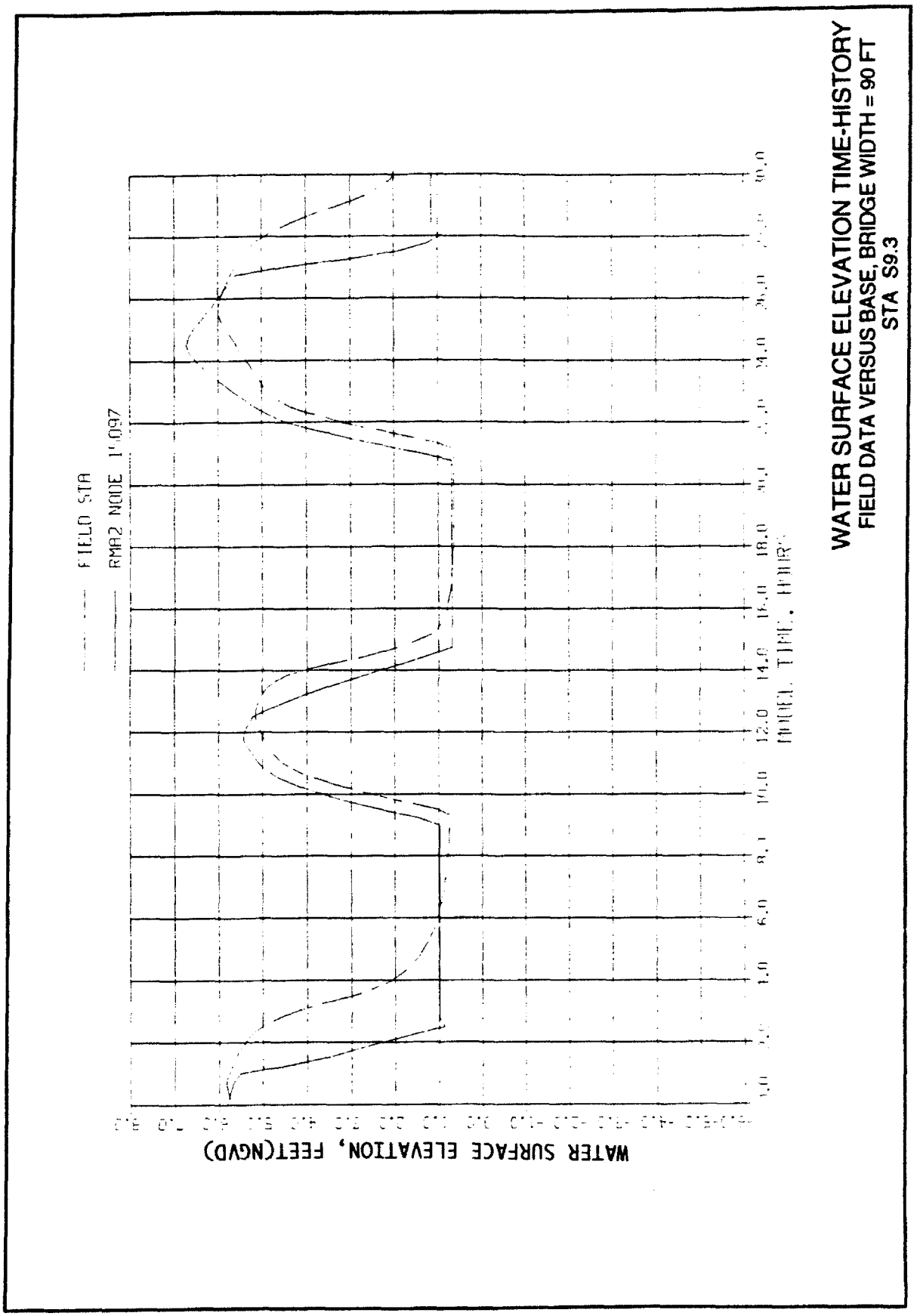
WATER SURFACE ELEVATION TIME-HISTORY
FIELD DATA VERSUS BASE, BRIDGE WIDTH = 90 FT
STA S9.3
FIELD STA
RMA2 NODE 1'097
WATER SURFACE ELEVATION, FEET(NGVD)
MODEL TIME, HOURS

PLATE 28

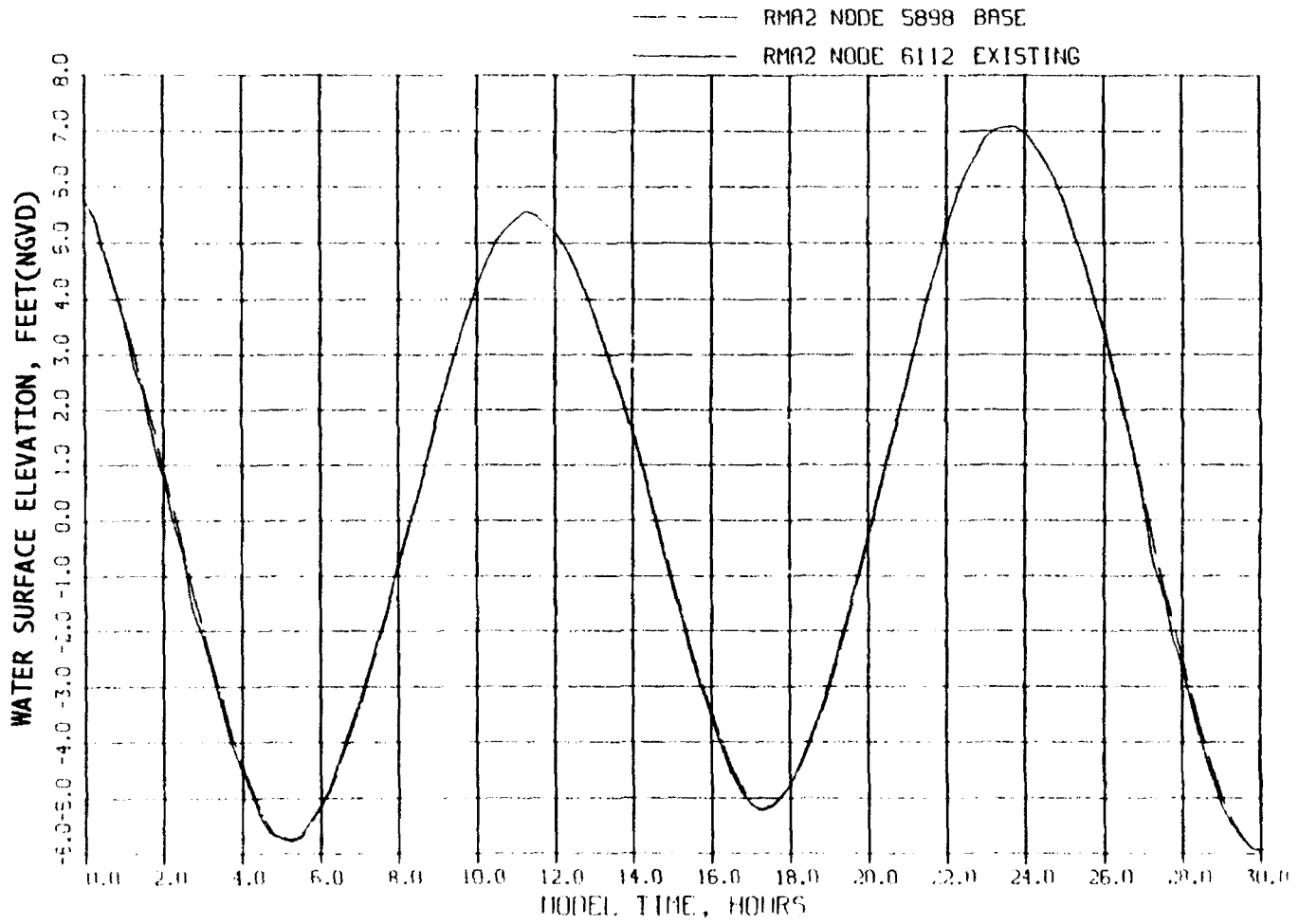


**WATER SURFACE ELEVATION TIME-HISTORY**
**EXISTING VERSUS BASE**
**STA S1.5**

PLATE 29

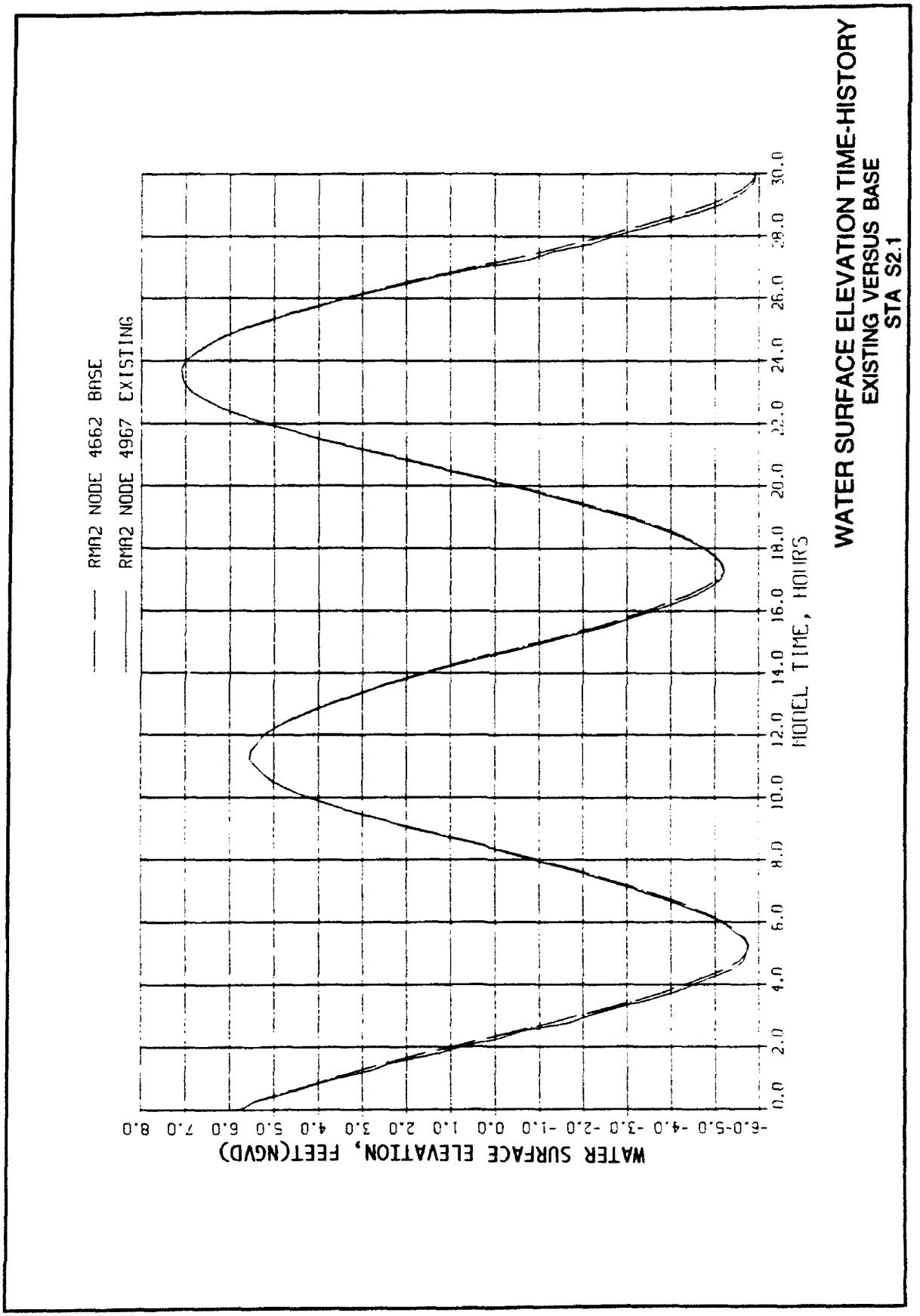
WATER SURFACE ELEVATION TIME-HISTORY
EXISTING VERSUS BASE
STA S2.1
RMA2 NODE 4662 BASE
RMA2 NODE 4967 EXISTING
WATER SURFACE ELEVATION, FEET(NGVD)
MODEL TIME, HOURS
8.0
7.0
6.0
5.0
4.0
3.0
2.0
1.0
0.0
-1.0
-2.0
-3.0
-4.0
-5.0
-6.0
0.0
2.0
4.0
6.0
8.0
10.0
12.0
14.0
16.0
18.0
20.0
22.0
24.0
26.0
28.0
30.0

PLATE 30

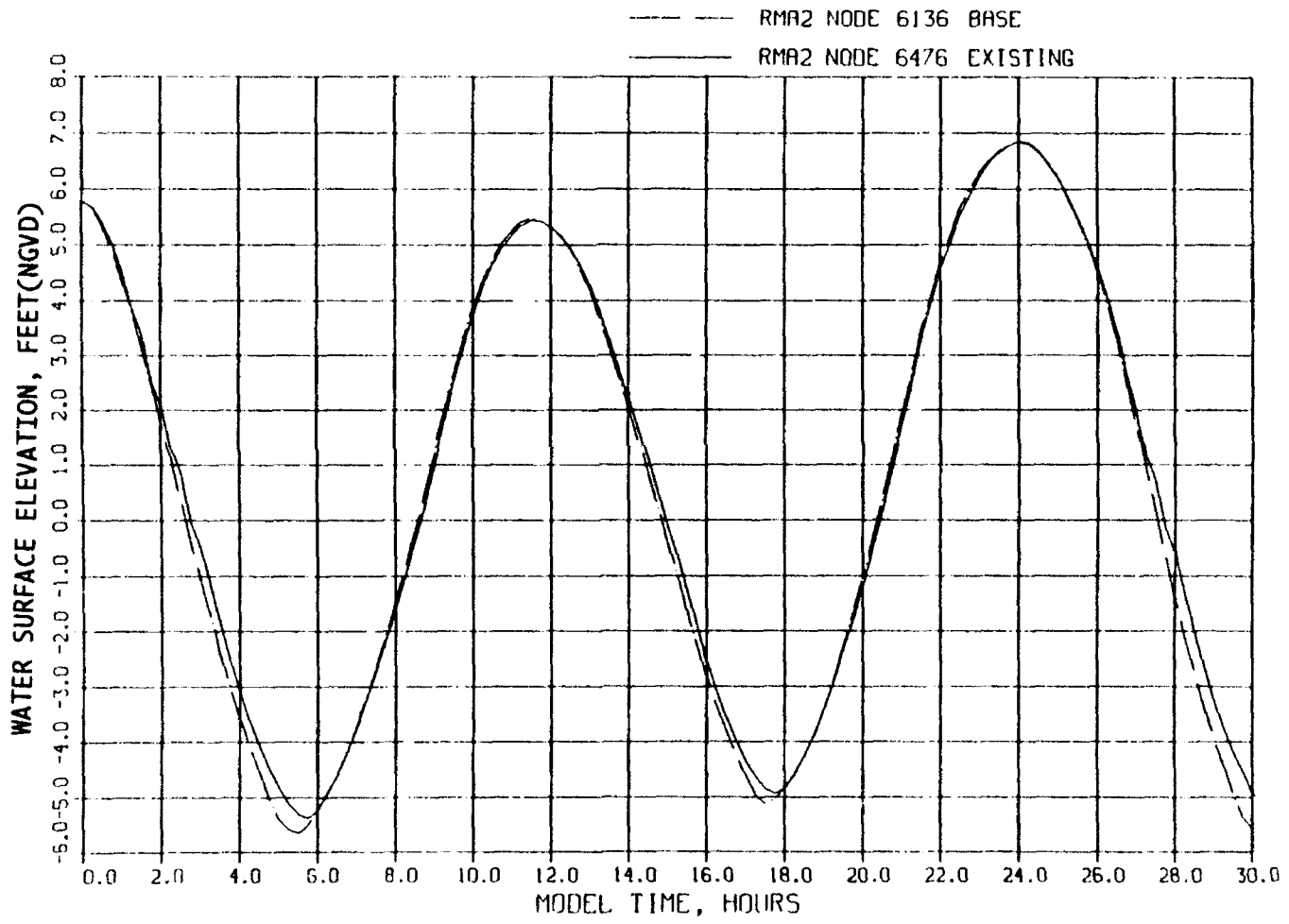


**WATER SURFACE ELEVATION TIME-HISTORY**
**EXISTING VERSUS BASE**
**STA S4.2**

PLATE 31

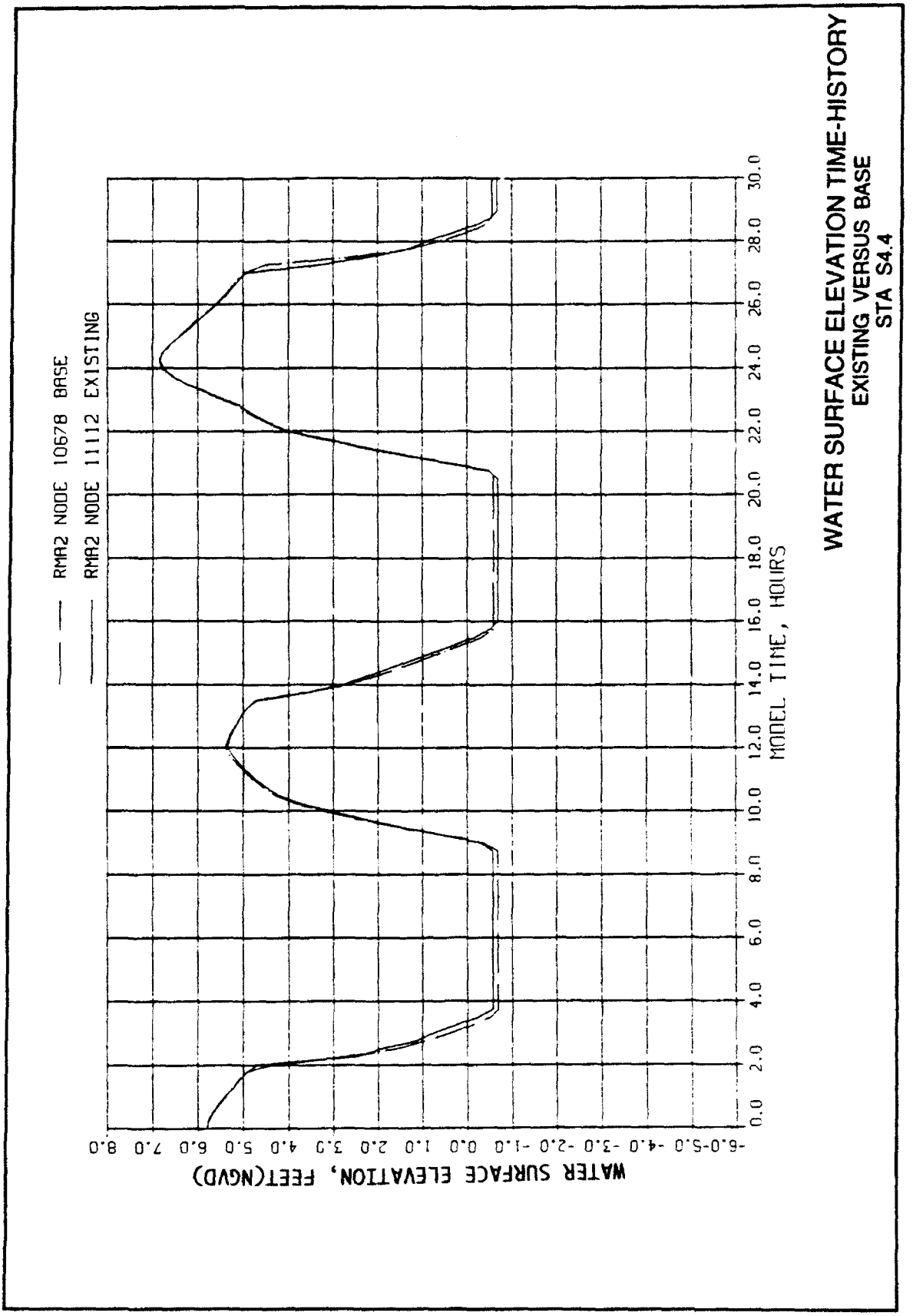
WATER SURFACE ELEVATION TIME-HISTORY
EXISTING VERSUS BASE
STA S4.4
RMA2 NODE 10678 BASE
RMA2 NODE 11112 EXISTING
WATER SURFACE ELEVATION, FEET(NGVD)
MODEL TIME, HOURS
8.0
7.0
6.0
5.0
4.0
3.0
2.0
1.0
0.0
-1.0
-2.0
-3.0
-4.0
-5.0
-6.0
0.0
2.0
4.0
6.0
8.0
10.0
12.0
14.0
16.0
18.0
20.0
22.0
24.0
26.0
28.0
30.0

PLATE 32

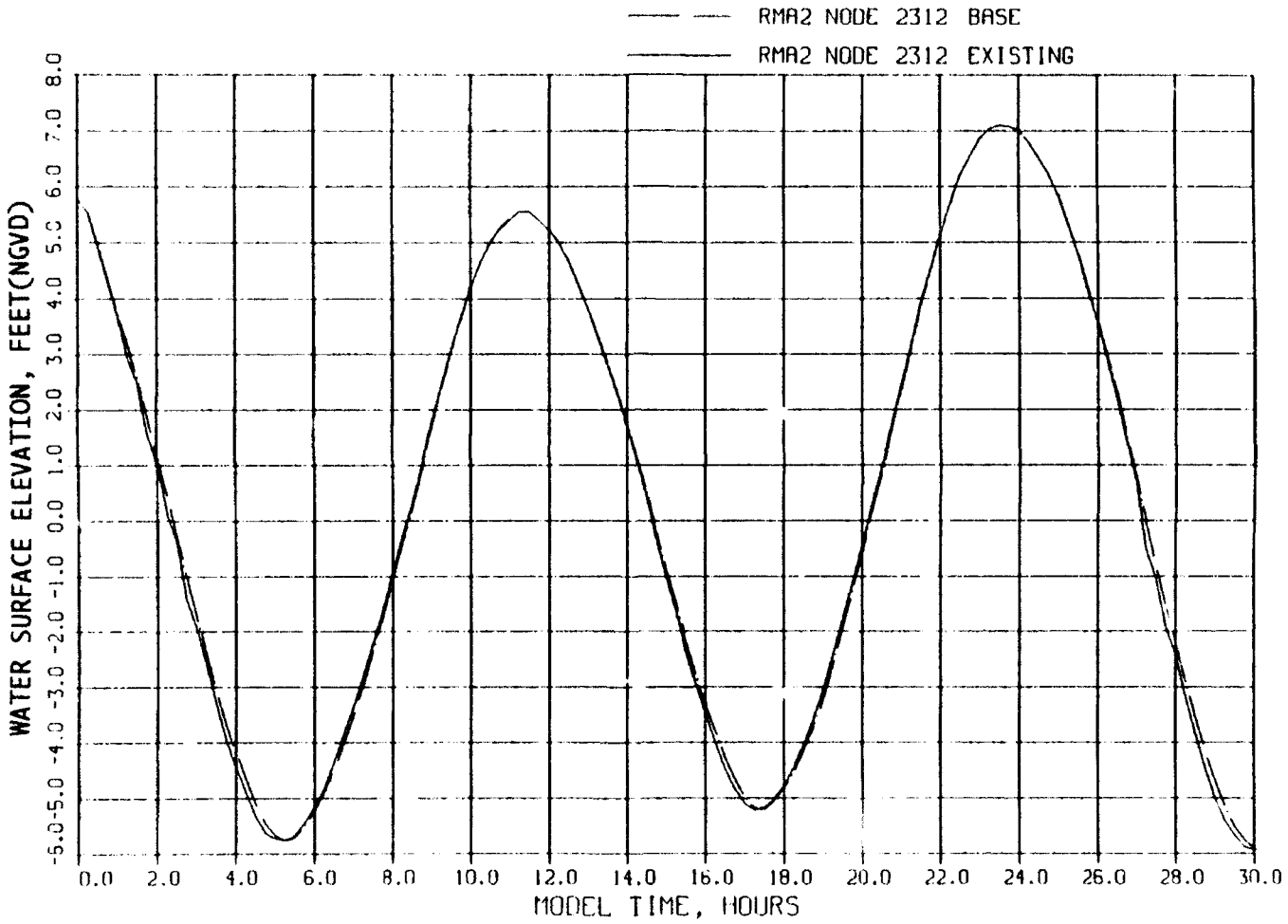


**WATER SURFACE ELEVATION TIME-HISTORY**
**EXISTING VERSUS BASE**
**STA S7.4**

PLATE 33

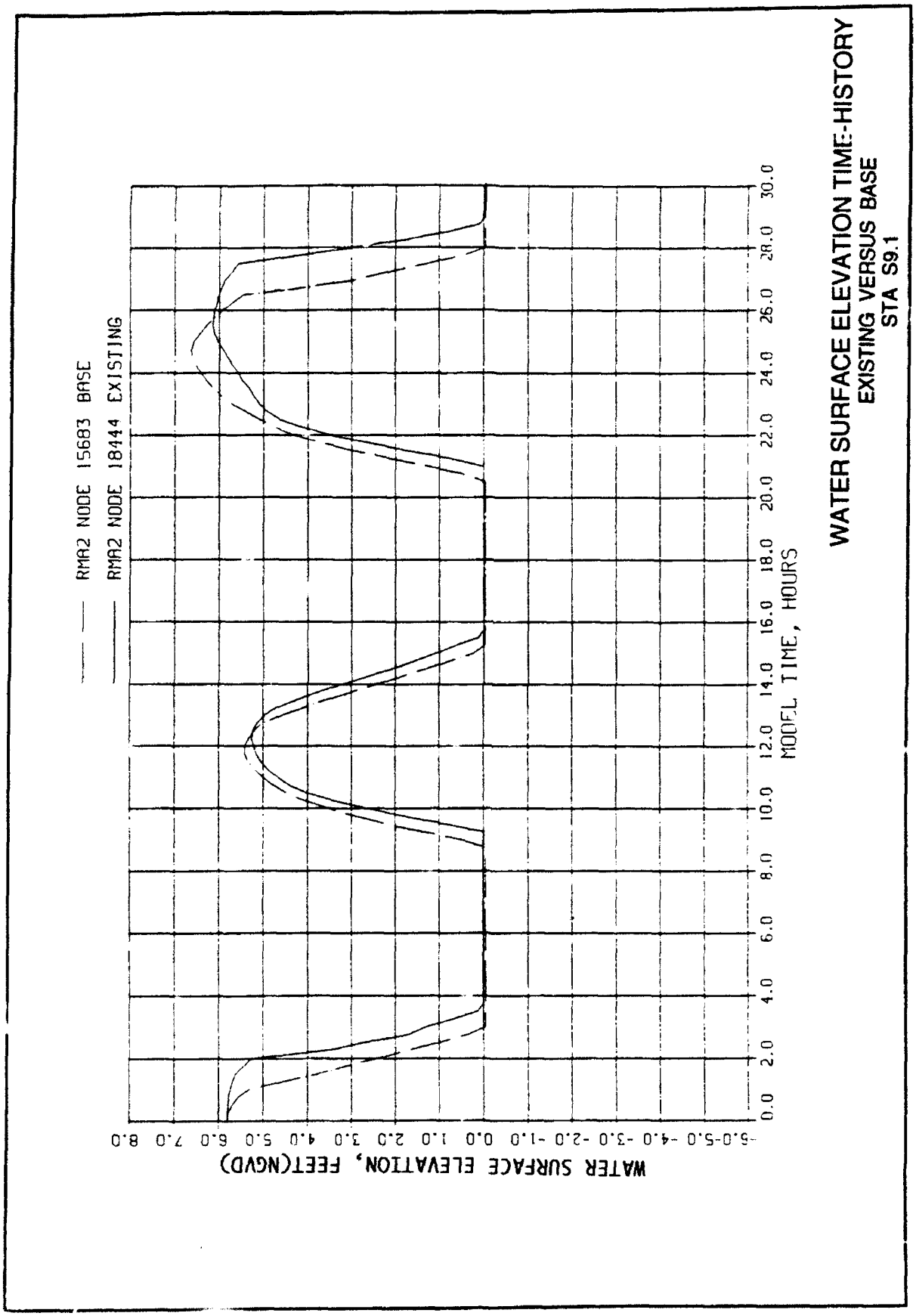
WATER SURFACE ELEVATION TIME-HISTORY
EXISTING VERSUS BASE
STA S9.1
RMA2 NODE 15683 BASE
RMA2 NODE 18444 EXISTING
WATER SURFACE ELEVATION, FEET(NGVD)
MODEL TIME, HOURS
8.0 7.0 6.0 5.0 4.0 3.0 2.0 1.0 0.0 -1.0 -2.0 -3.0 -4.0 -5.0
0.0 2.0 4.0 6.0 8.0 10.0 12.0 14.0 16.0 18.0 20.0 22.0 24.0 26.0 28.0 30.0

PLATE 34

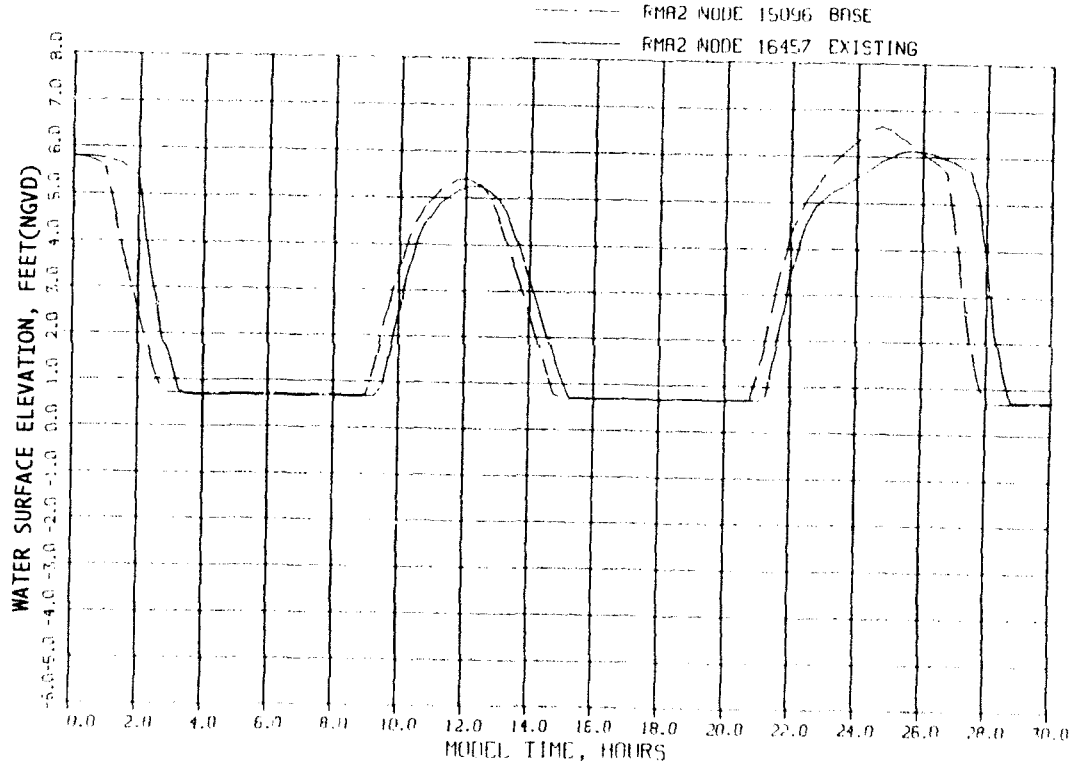


PLATE 35

**WATER SURFACE ELEVATION TIME-HISTORY**
**EXISTING VERSUS BASE**
**STA S9.3**

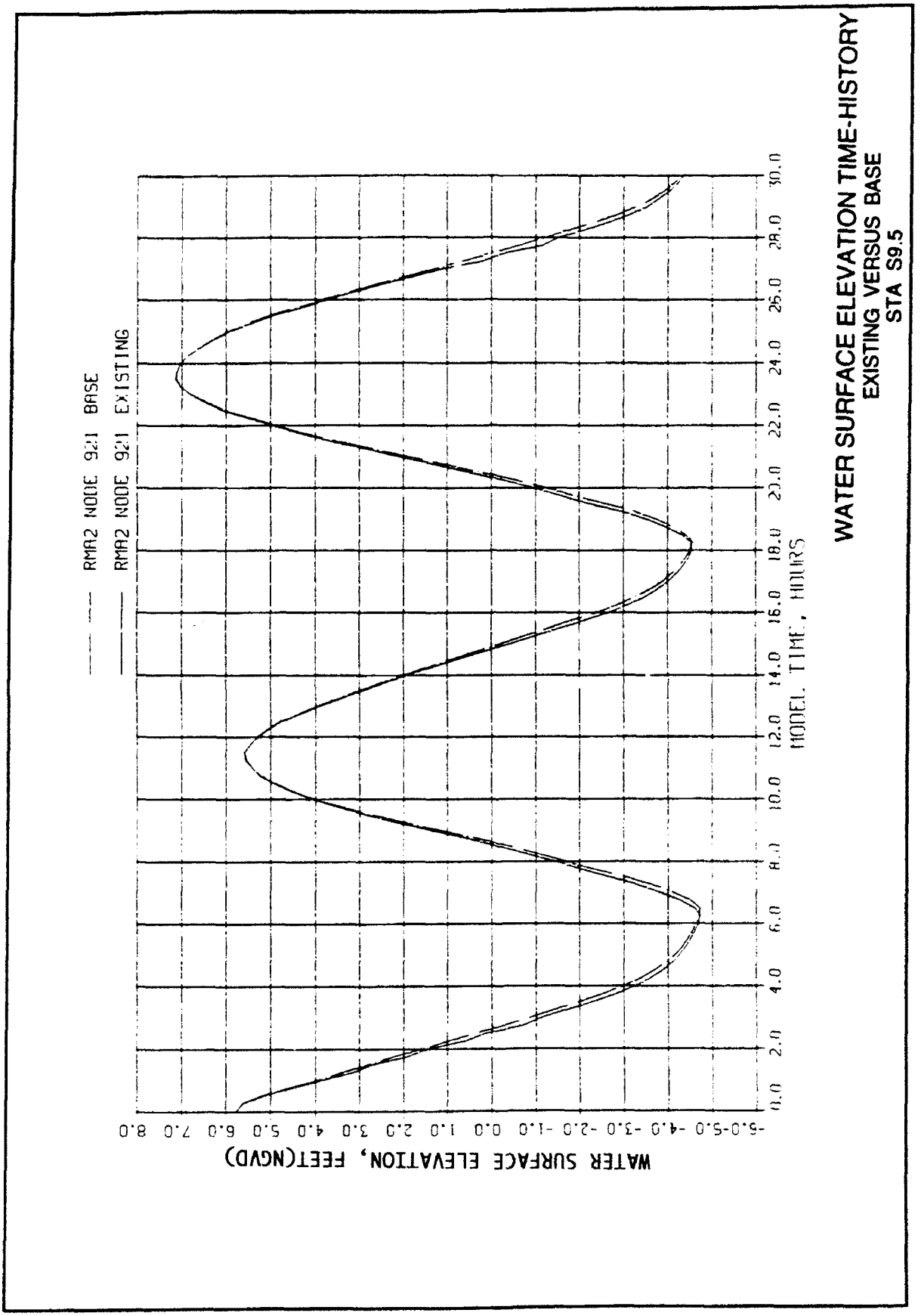
WATER SURFACE ELEVATION TIME-HISTORY
EXISTING VERSUS BASE
STA S9.5
RMA2 NODE 921 BASE
RMA2 NODE 921 EXISTING
WATER SURFACE ELEVATION, FEET(NGVD)
MODEL TIME, HOURS

PLATE 36

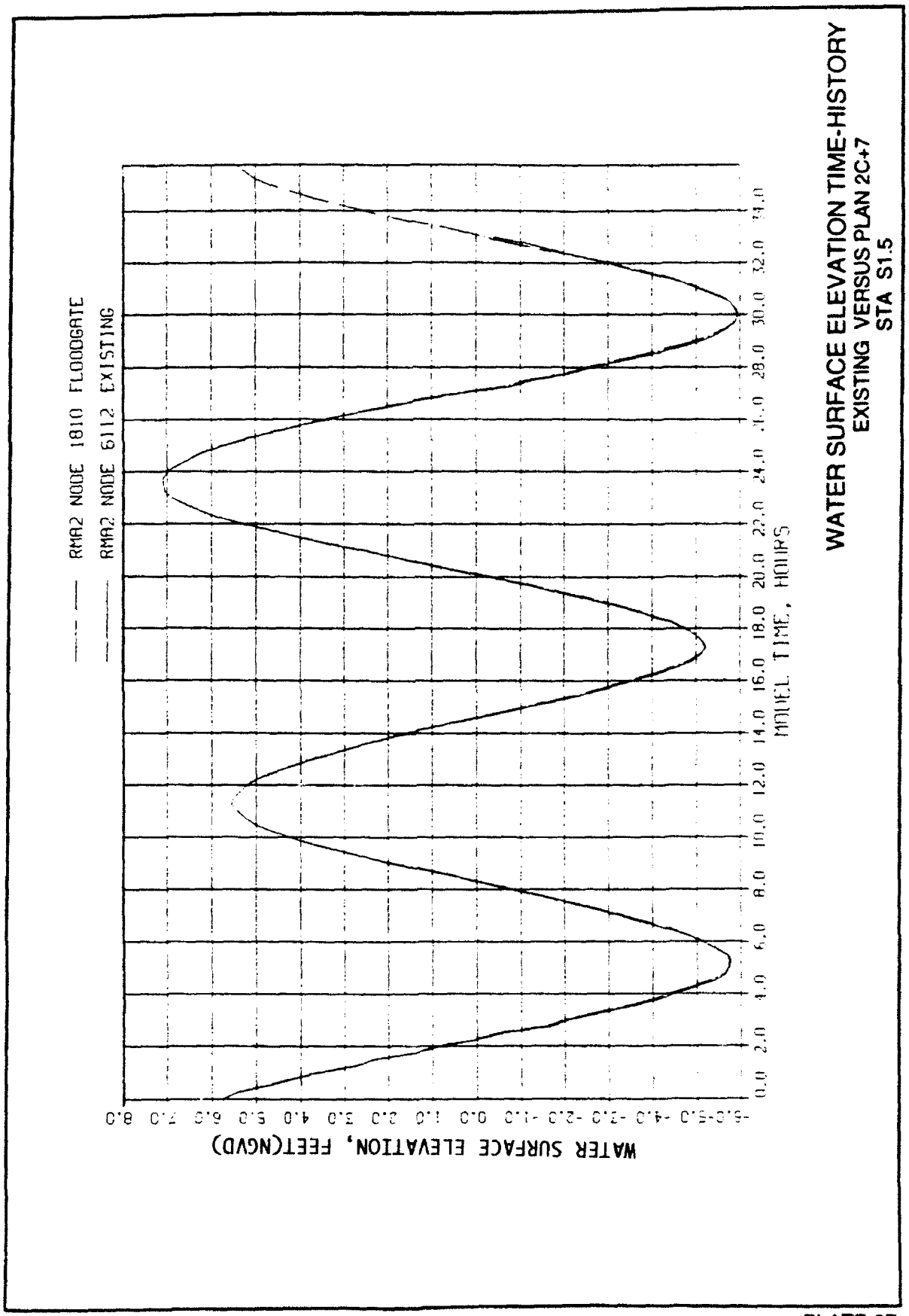
WATER SURFACE ELEVATION TIME-HISTORY
EXISTING VERSUS PLAN 2C+7
STA S1.5
RMA2 NODE 1810 FLOODGATE
RMA2 NODE 6112 EXISTING
WATER SURFACE ELEVATION, FEET(NGVD)
MODEL TIME, HOURS

PLATE 37

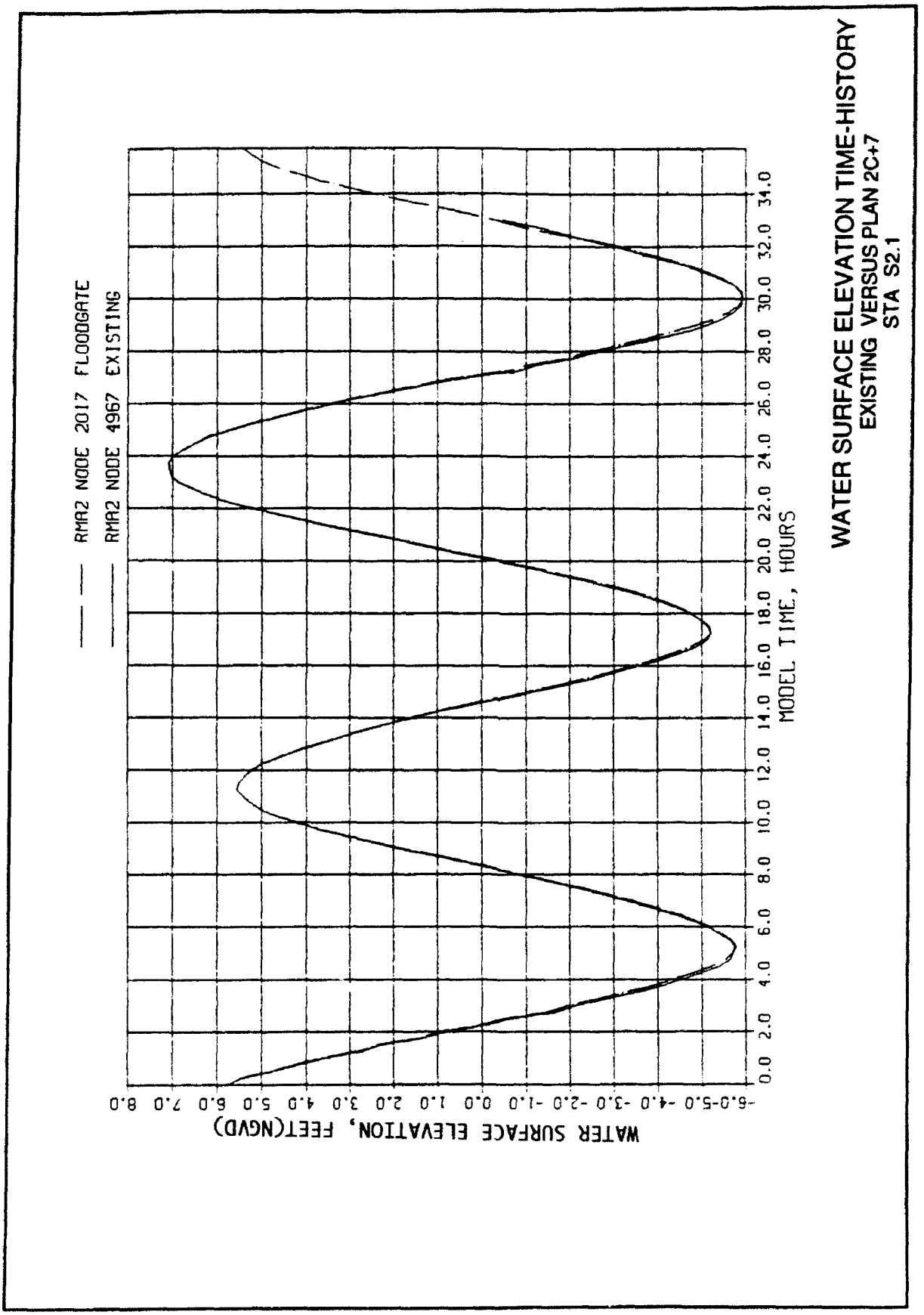
WATER SURFACE ELEVATION TIME-HISTORY
EXISTING VERSUS PLAN 2C+7
STA S2.1
RMA2 NODE 2017 FLOODGATE
RMA2 NODE 4967 EXISTING
WATER SURFACE ELEVATION, FEET(NGVD)
8.0 7.0 6.0 5.0 4.0 3.0 2.0 1.0 0.0 -1.0 -2.0 -3.0 -4.0 -5.0-6.0
MODEL TIME, HOURS
0.0 2.0 4.0 6.0 8.0 10.0 12.0 14.0 16.0 18.0 20.0 22.0 24.0 26.0 28.0 30.0 32.0 34.0

PLATE 38

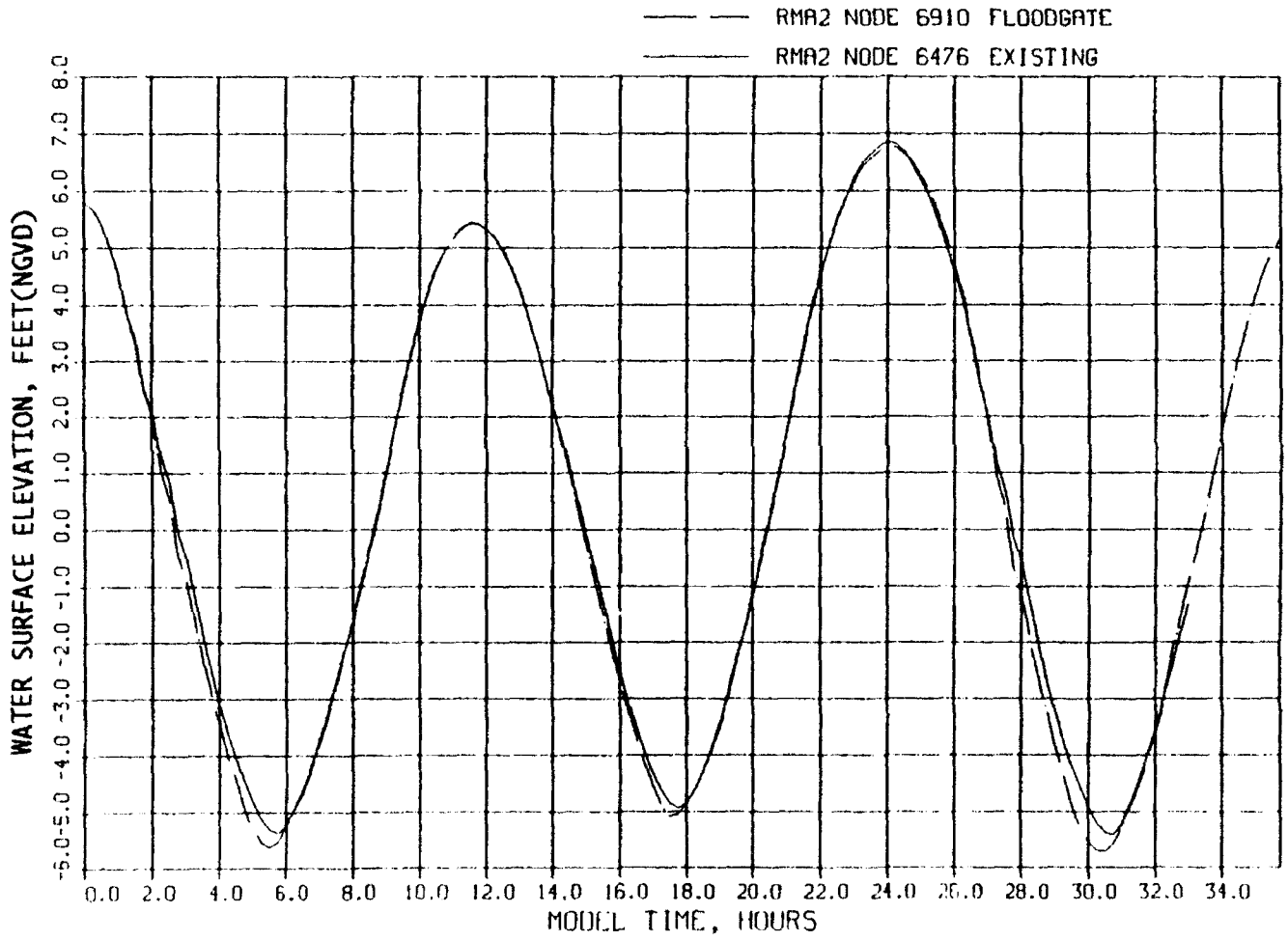


**WATER SURFACE ELEVATION TIME-HISTORY**
**EXISTING VERSUS PLAN 2C+7**
**STA S4.2**

PLATE 39

PLATE 40

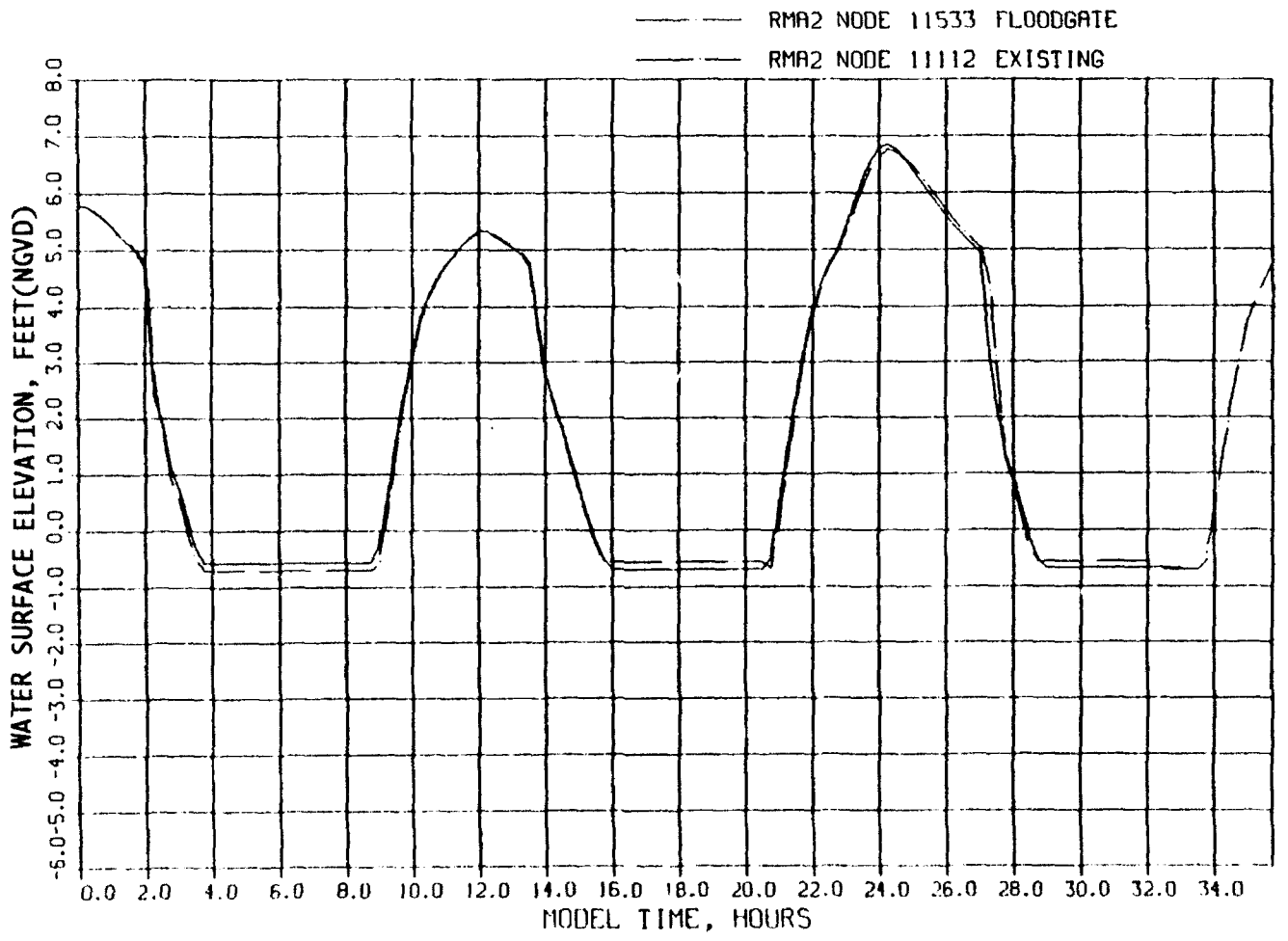


**WATER SURFACE ELEVATION TIME-HISTORY**
**EXISTING VERSUS PLAN 2C+7**
**STA S4.4**

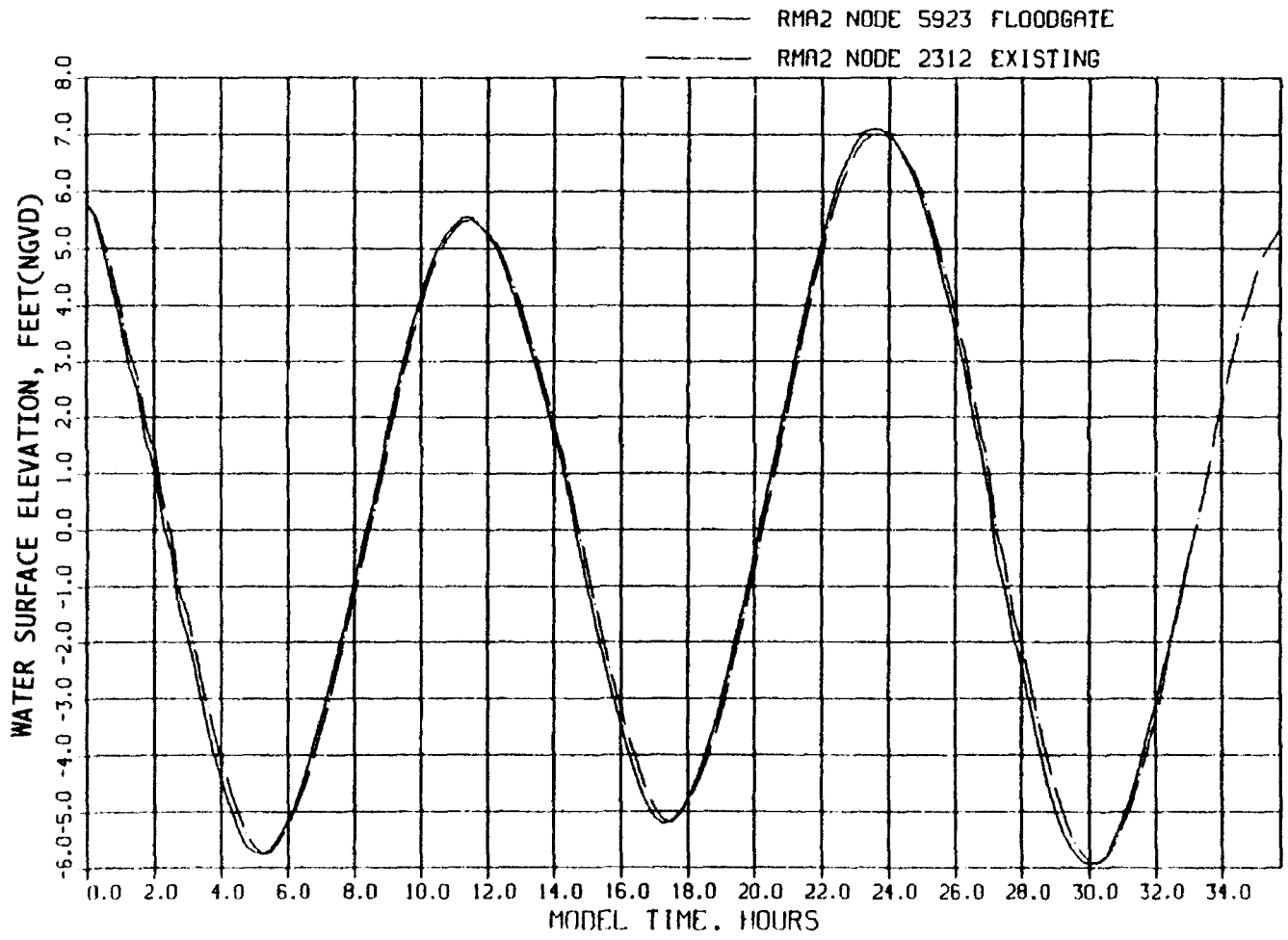


**WATER SURFACE ELEVATION TIME-HISTORY**
**EXISTING VERSUS PLAN 2C+7**
**STA S7.4**

PLATE 41

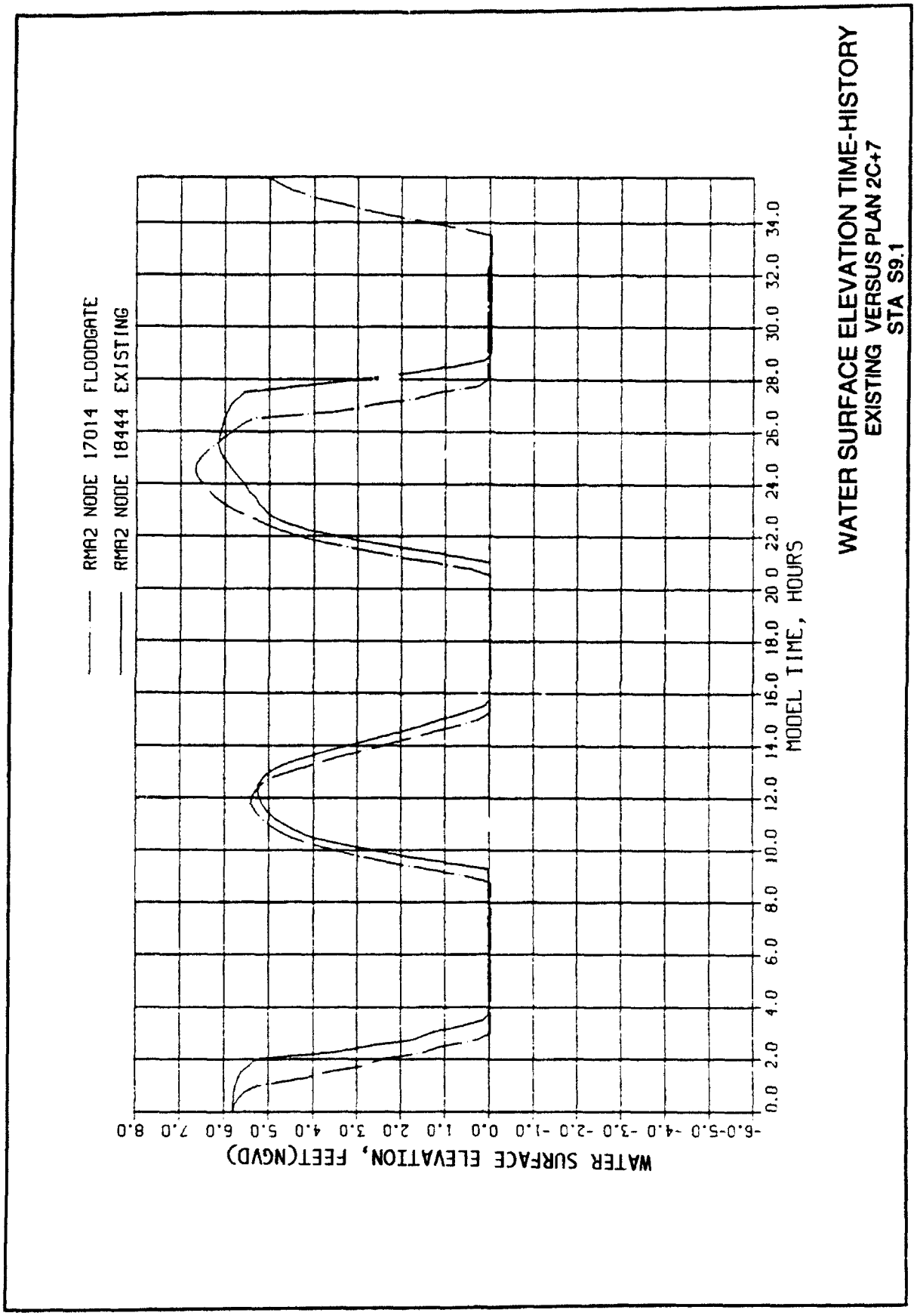
WATER SURFACE ELEVATION TIME-HISTORY
EXISTING VERSUS PLAN 2C+7
STA S9.1
RMA2 NODE 17014 FLOODGATE
RMA2 NODE 18444 EXISTING
WATER SURFACE ELEVATION, FEET(NGVD)
MODEL TIME, HOURS
8.0 7.0 6.0 5.0 4.0 3.0 2.0 1.0 0.0 -1.0 -2.0 -3.0 -4.0 -5.0-6.0
0.0 2.0 4.0 6.0 8.0 10.0 12.0 14.0 16.0 18.0 20.0 22.0 24.0 26.0 28.0 30.0 32.0 34.0

PLATE 42

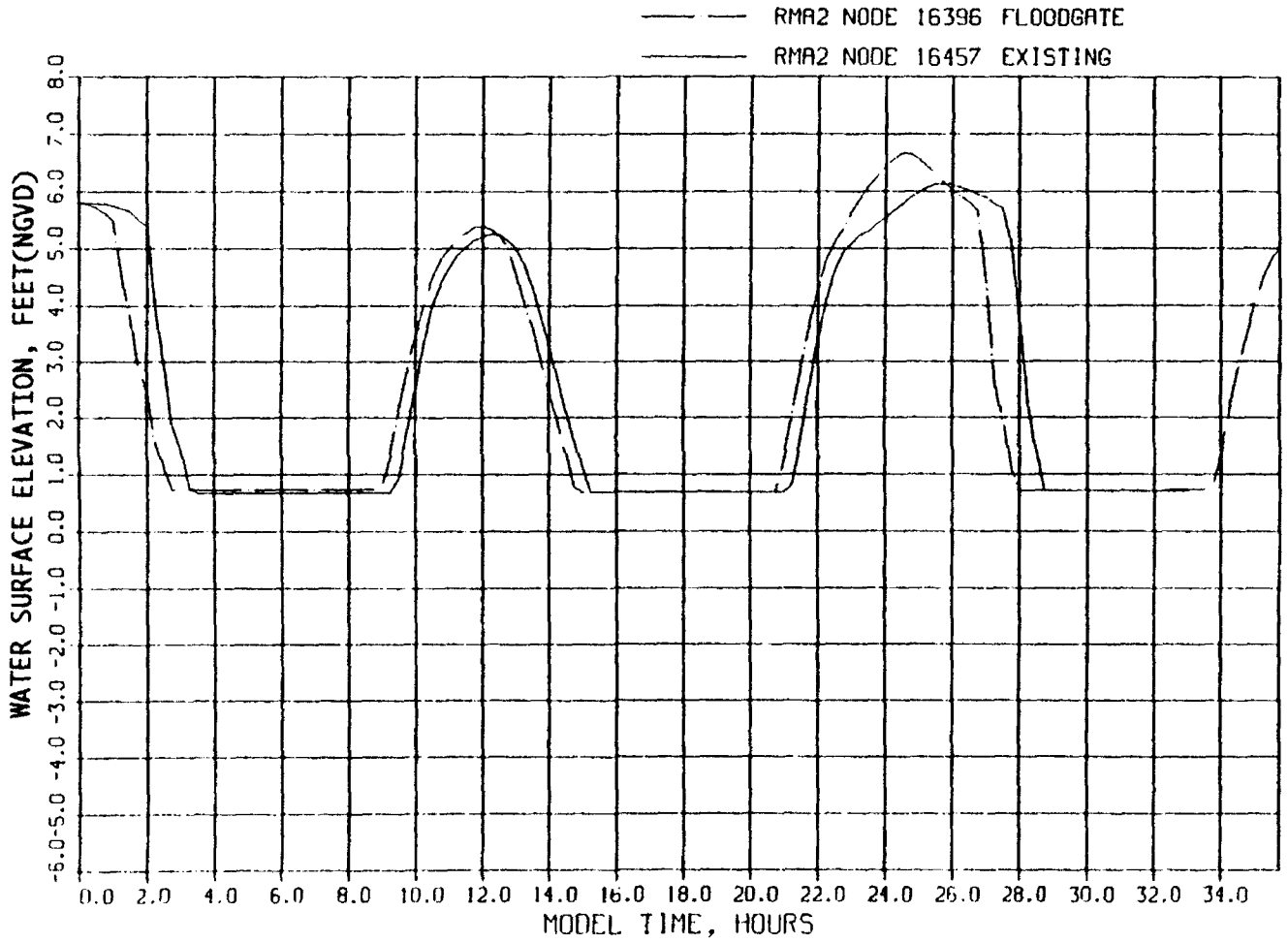


**WATER SURFACE ELEVATION TIME-HISTORY**
**EXISTING VERSUS PLAN 2C+7**
**STA S9.3**

PLATE 43

PLATE 44

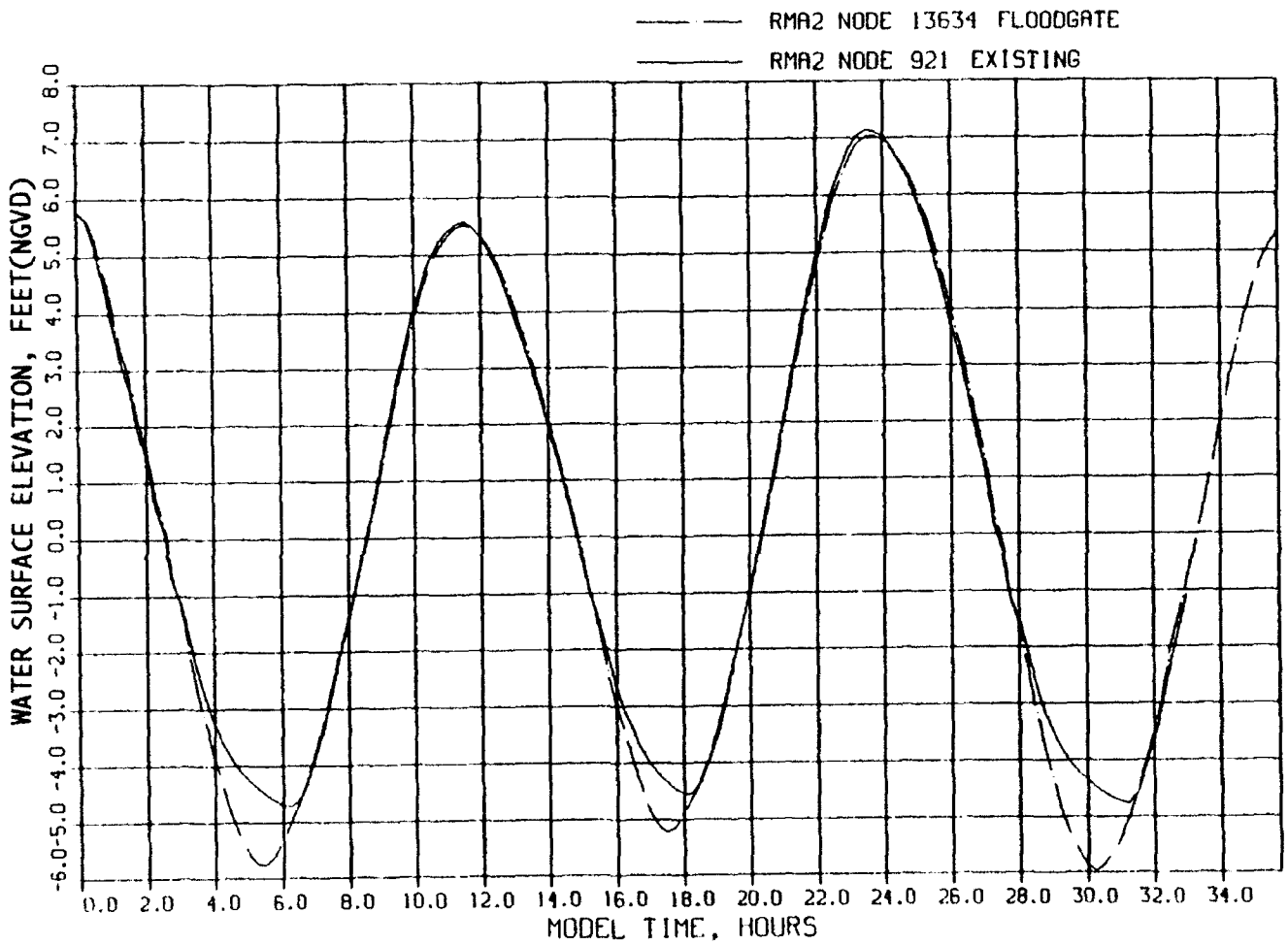


**WATER SURFACE ELEVATION TIME-HISTORY**
**EXISTING VERSUS PLAN 2C+7**
**STA S9.5**

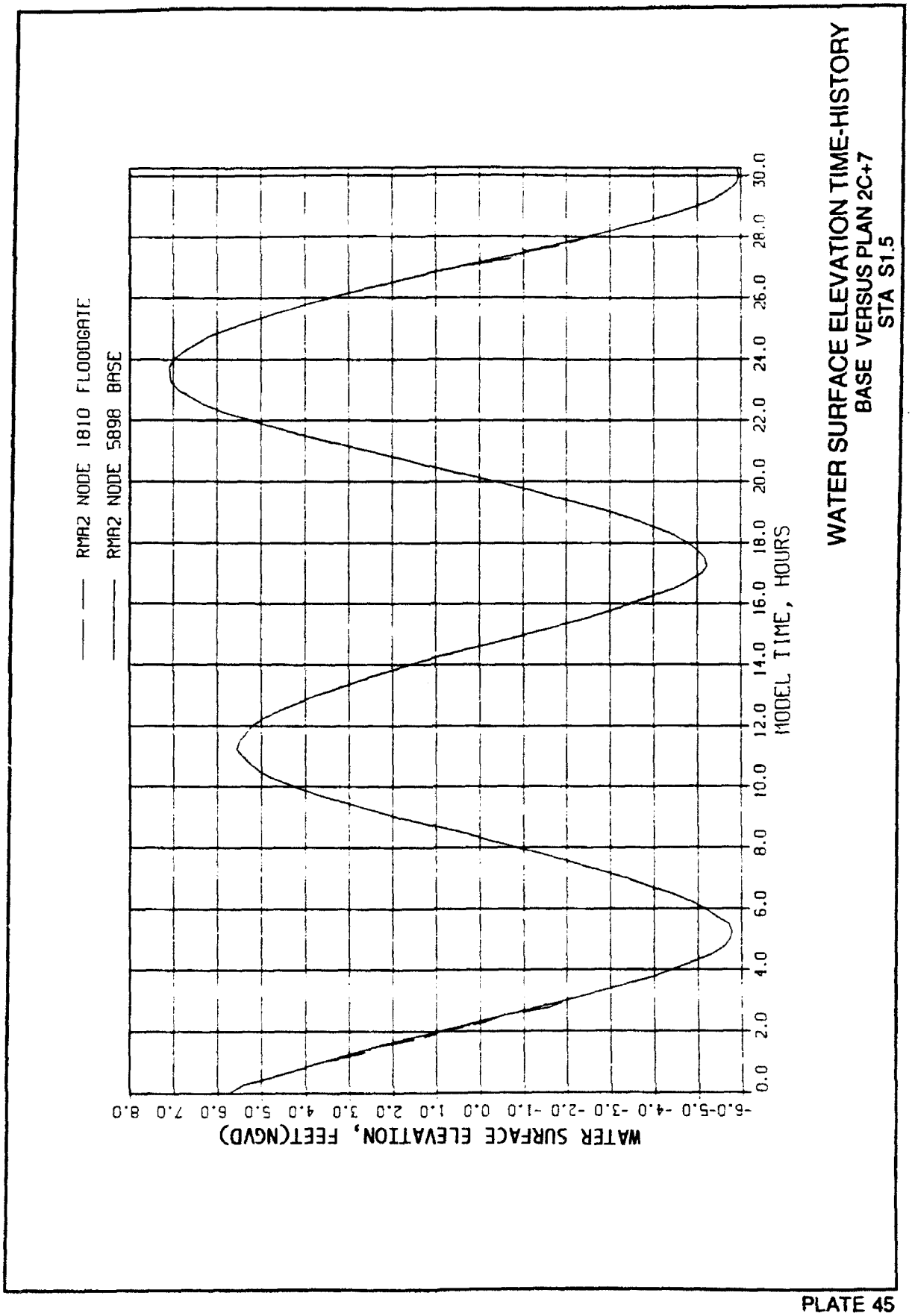
WATER SURFACE ELEVATION TIME-HISTORY
BASE VERSUS PLAN 2C+7
STA S1.5
RMA2 NODE 1810 FLOODGATE
RMA2 NODE 5898 BASE
WATER SURFACE ELEVATION, FEET(NGVD)
8.0 7.0 6.0 5.0 4.0 3.0 2.0 1.0 0.0 -1.0 -2.0 -3.0 -4.0 -5.0-6.0
MODEL TIME, HOURS
0.0 2.0 4.0 6.0 8.0 10.0 12.0 14.0 16.0 18.0 20.0 22.0 24.0 26.0 28.0 30.0

PLATE 45

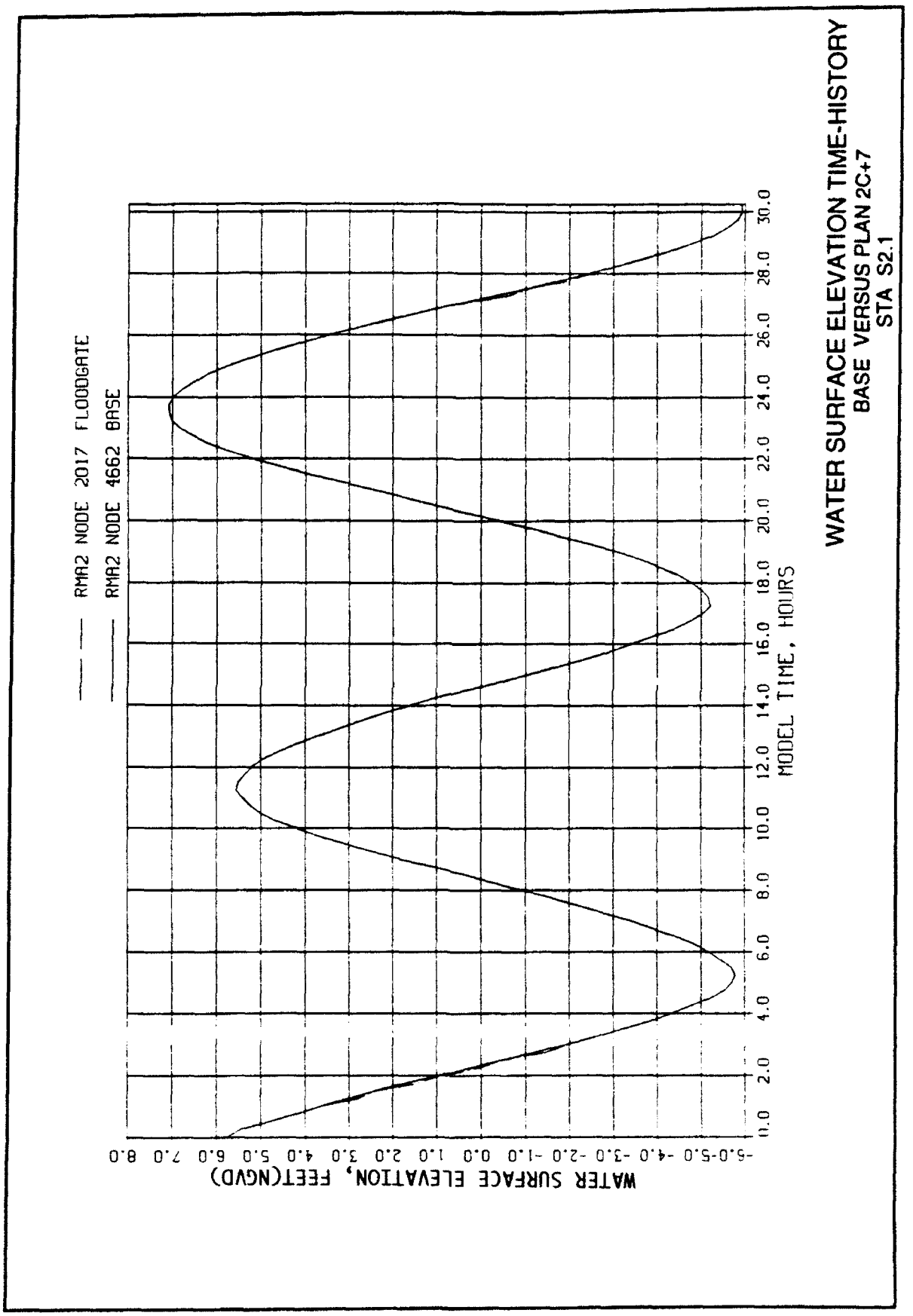
WATER SURFACE ELEVATION TIME-HISTORY
BASE VERSUS PLAN 2C+7
STA S2.1
RMA2 NODE 2017 FLOODGATE
RMA2 NODE 4662 BASE
WATER SURFACE ELEVATION, FEET(NGVD)
MODEL TIME, HOURS
-5.0 -4.0 -3.0 -2.0 -1.0 0.0 1.0 2.0 3.0 4.0 5.0 6.0 7.0 8.0
0.0 2.0 4.0 6.0 8.0 10.0 12.0 14.0 16.0 18.0 20.0 22.0 24.0 26.0 28.0 30.0

PLATE 46

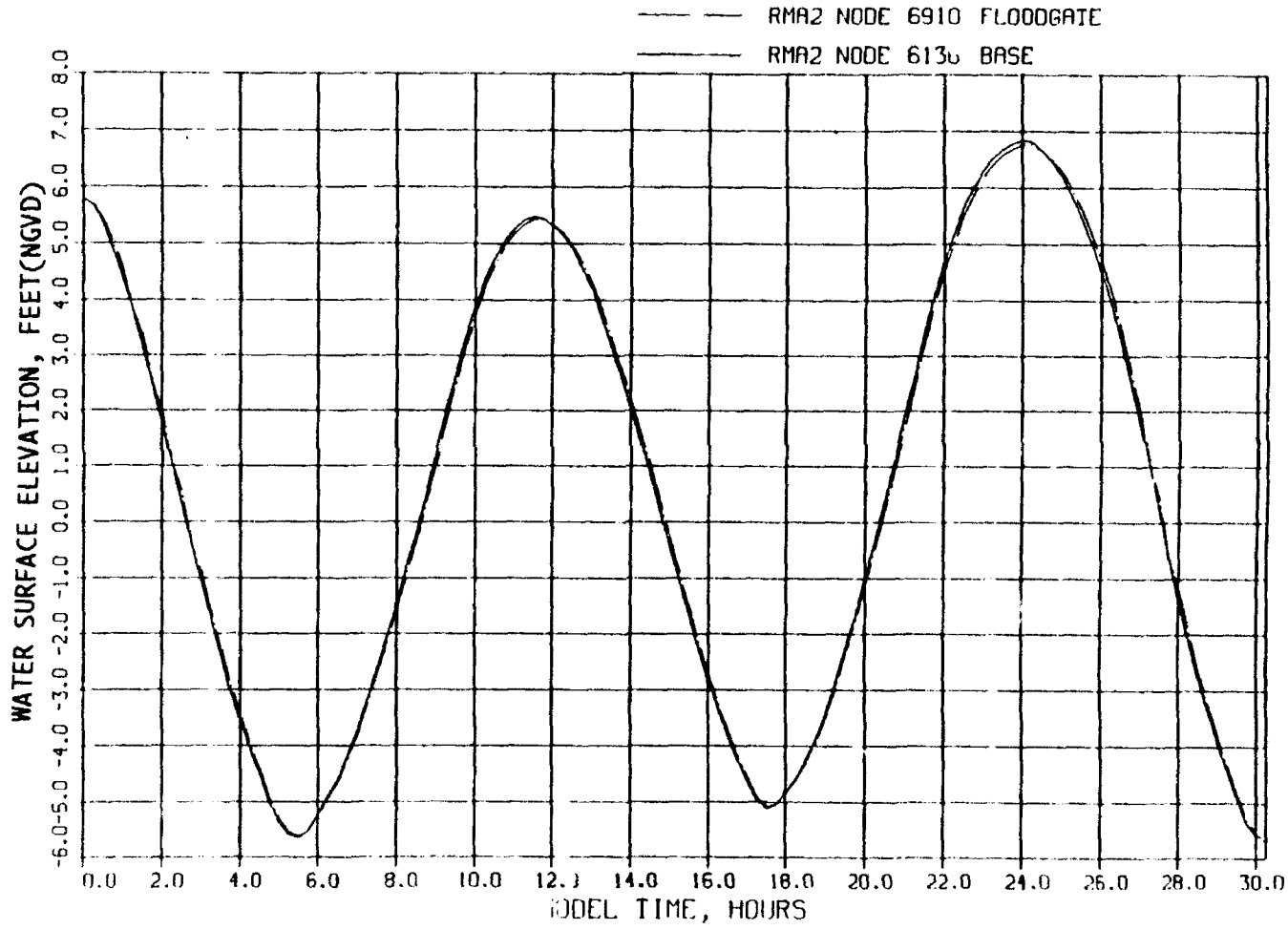


**WATER SURFACE ELEVATION TIME-HISTORY**
**BASE VERSUS PLAN 2C+7**
**STA S4.2**

PLATE 47

PLATE 48

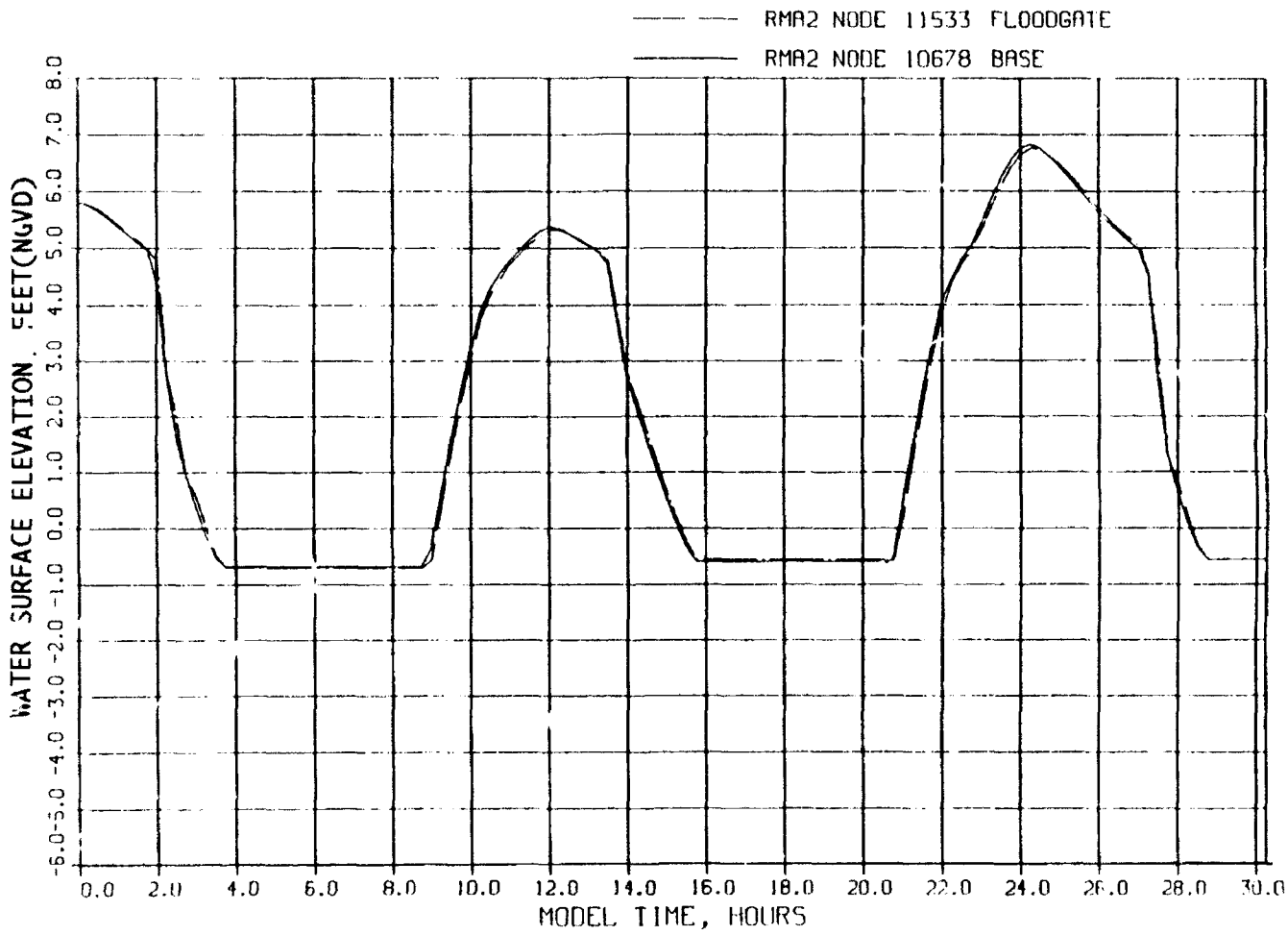


**WATER SURFACE ELEVATION TIME-HISTORY**
**BASE VERSUS PLAN 2C+7**
**STA S4.4**

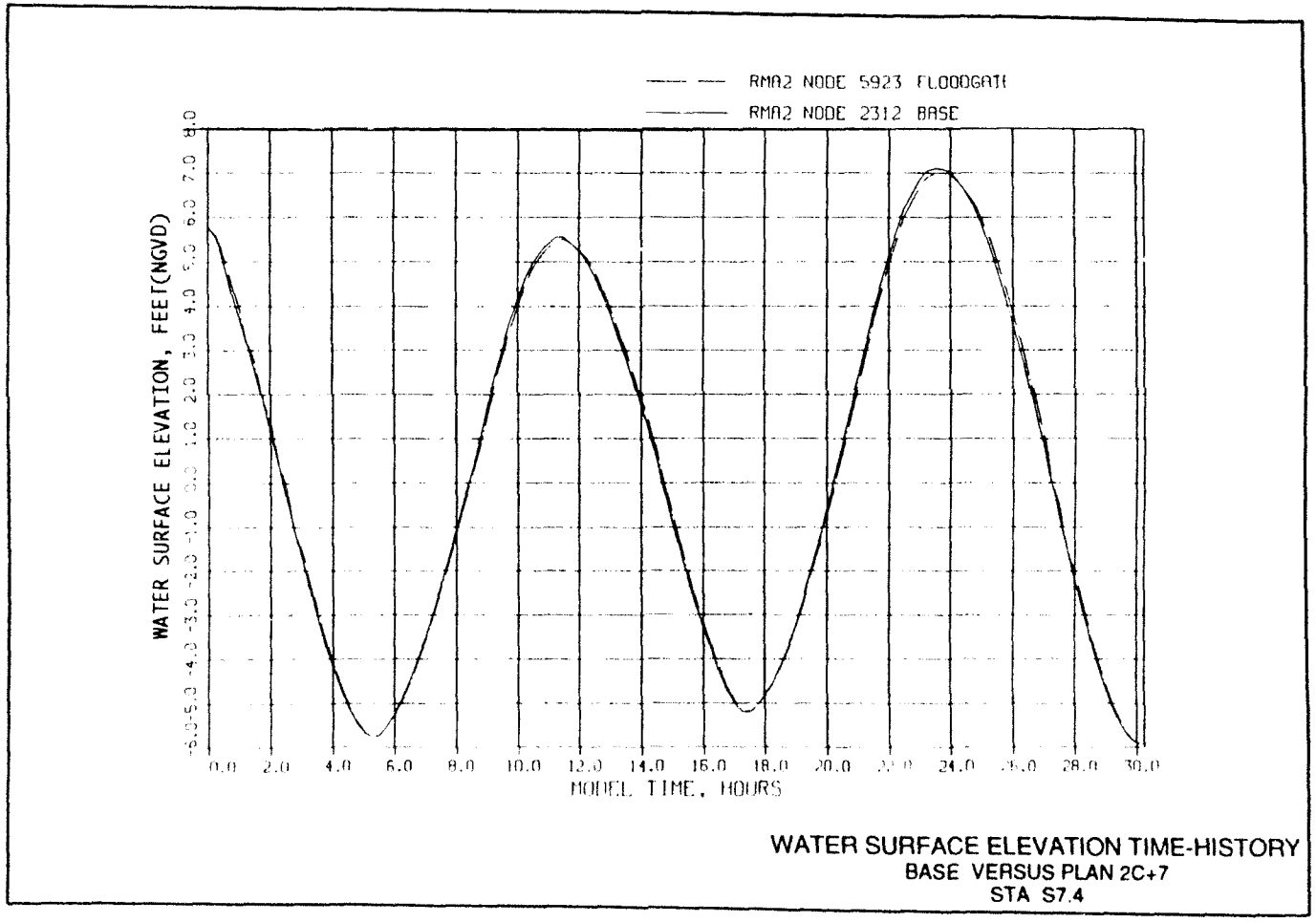


WATER SURFACE ELEVATION TIME-HISTORY
BASE VERSUS PLAN 2C+7
STA S7.4

PLATE 49

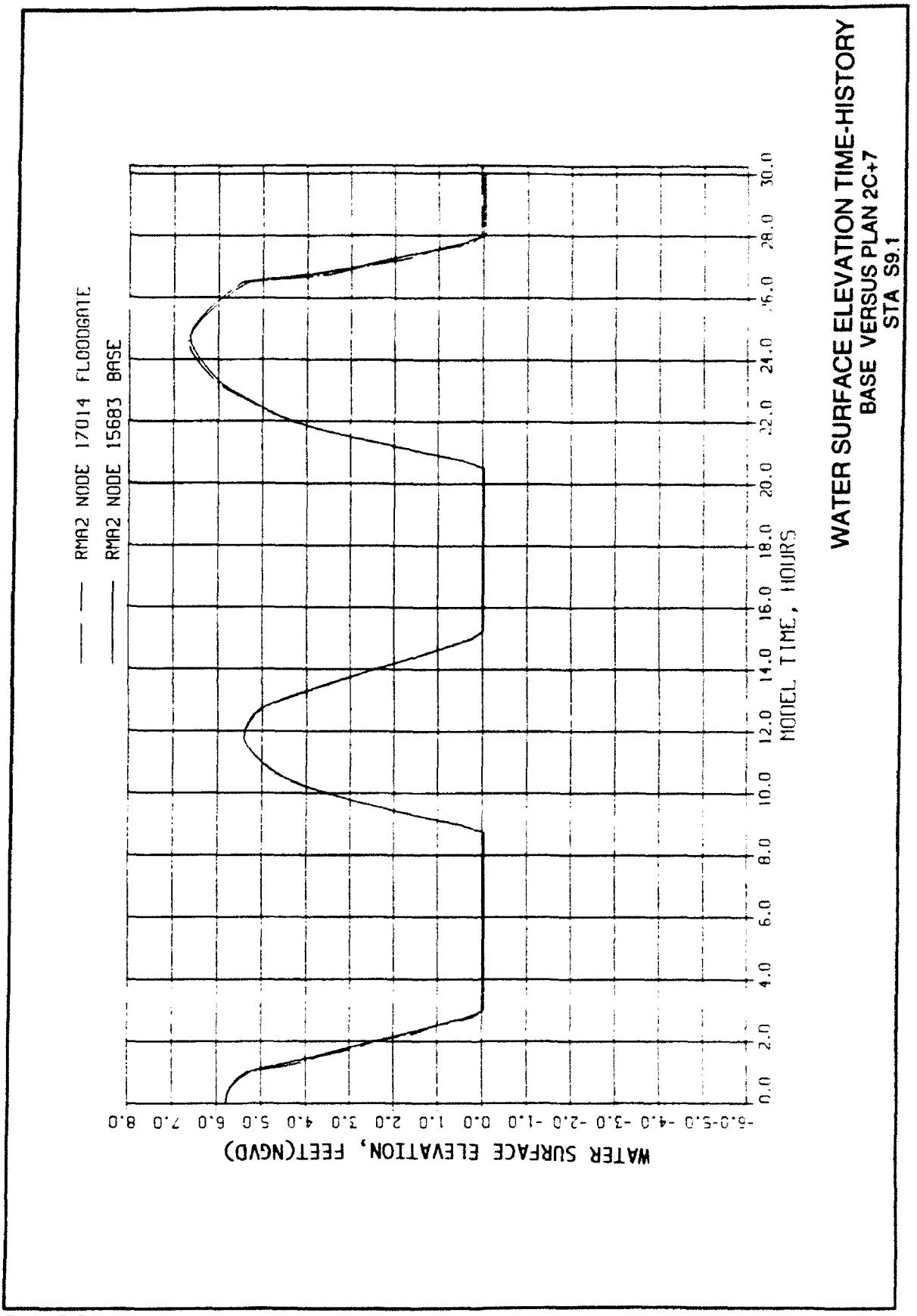
WATER SURFACE ELEVATION TIME-HISTORY
BASE VERSUS PLAN 2C+7
STA S9.1
RMA2 NODE 17014 FLOODGATE
RMA2 NODE 15683 BASE
WATER SURFACE ELEVATION, FEET(NGVD)
MODEL TIME, HOURS
8.0 7.0 6.0 5.0 4.0 3.0 2.0 1.0 0.0 -1.0 -2.0 -3.0 -4.0 -5.0-6.0
0.0 2.0 4.0 6.0 8.0 10.0 12.0 14.0 16.0 18.0 20.0 22.0 24.0 26.0 28.0 30.0

PLATE 50

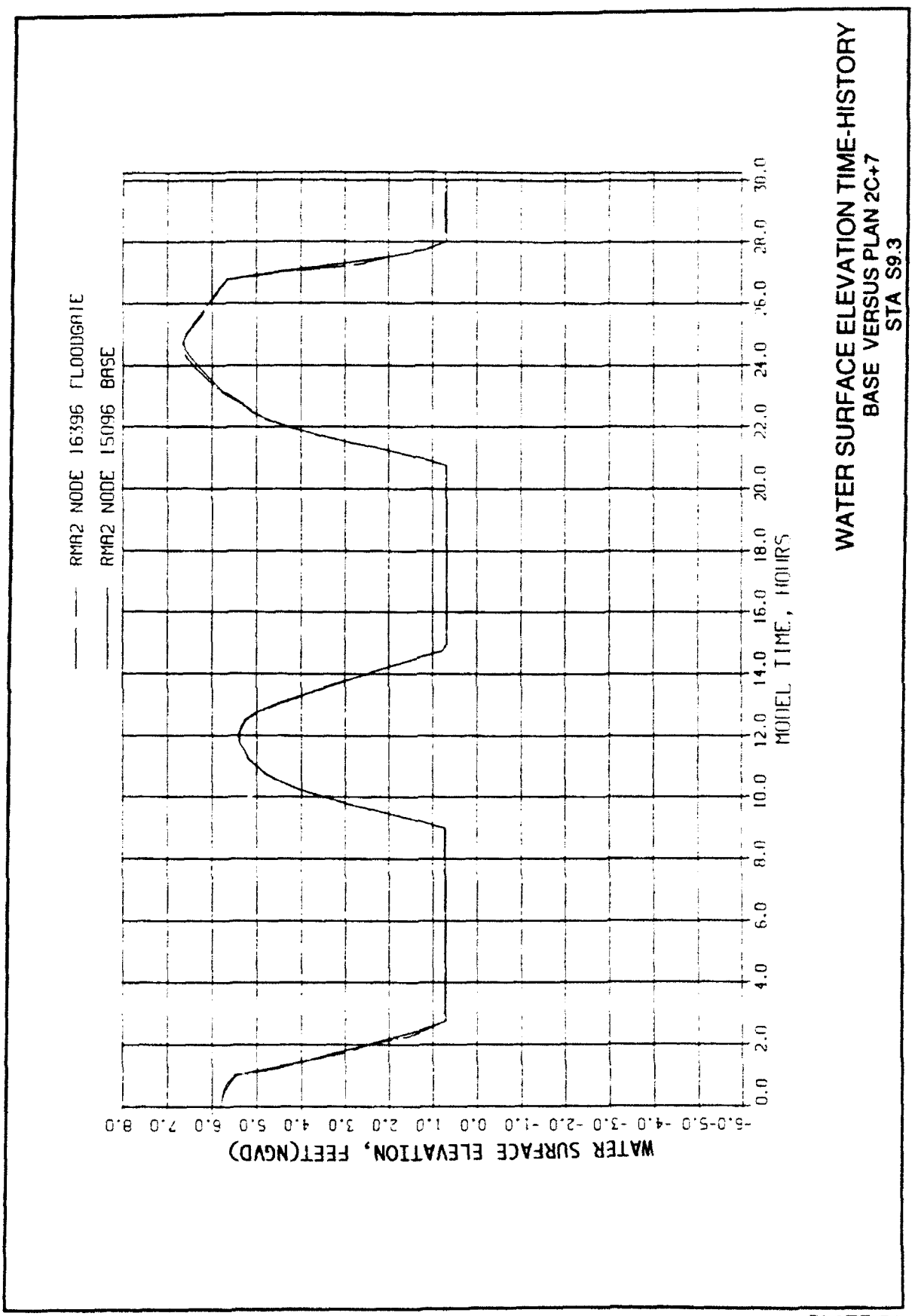
WATER SURFACE ELEVATION TIME-HISTORY
BASE VERSUS PLAN 2C+7
STA S9.3
RMA2 NODE 16396 FLOODGATE
RMA2 NODE 15096 BASE
WATER SURFACE ELEVATION, FEET(NGVD)
MODEL TIME, HOURS
8.0 7.0 6.0 5.0 4.0 3.0 2.0 1.0 0.0 -1.0 -2.0 -3.0 -4.0 -5.0
0.0 2.0 4.0 6.0 8.0 10.0 12.0 14.0 16.0 18.0 20.0 22.0 24.0 26.0 28.0 30.0

PLATE 51

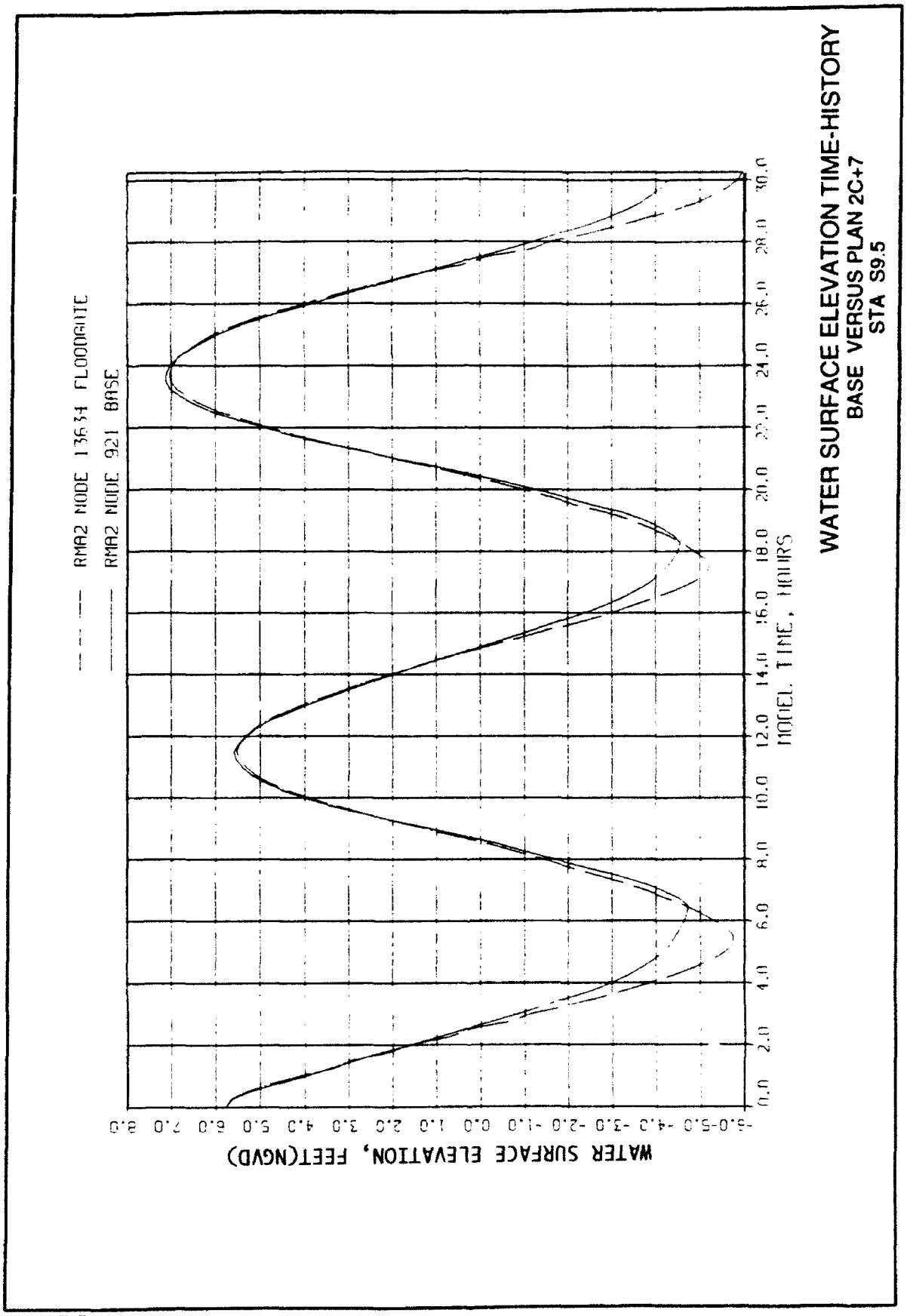
WATER SURFACE ELEVATION TIME-HISTORY
BASE VERSUS PLAN 2C+7
STA S9.5
RMA2 NODE 13634 FLOODGATE
RMA2 NODE 921 BASE
MODEL TIME, HOURS
WATER SURFACE ELEVATION, FEET(NGVD)

PLATE 52

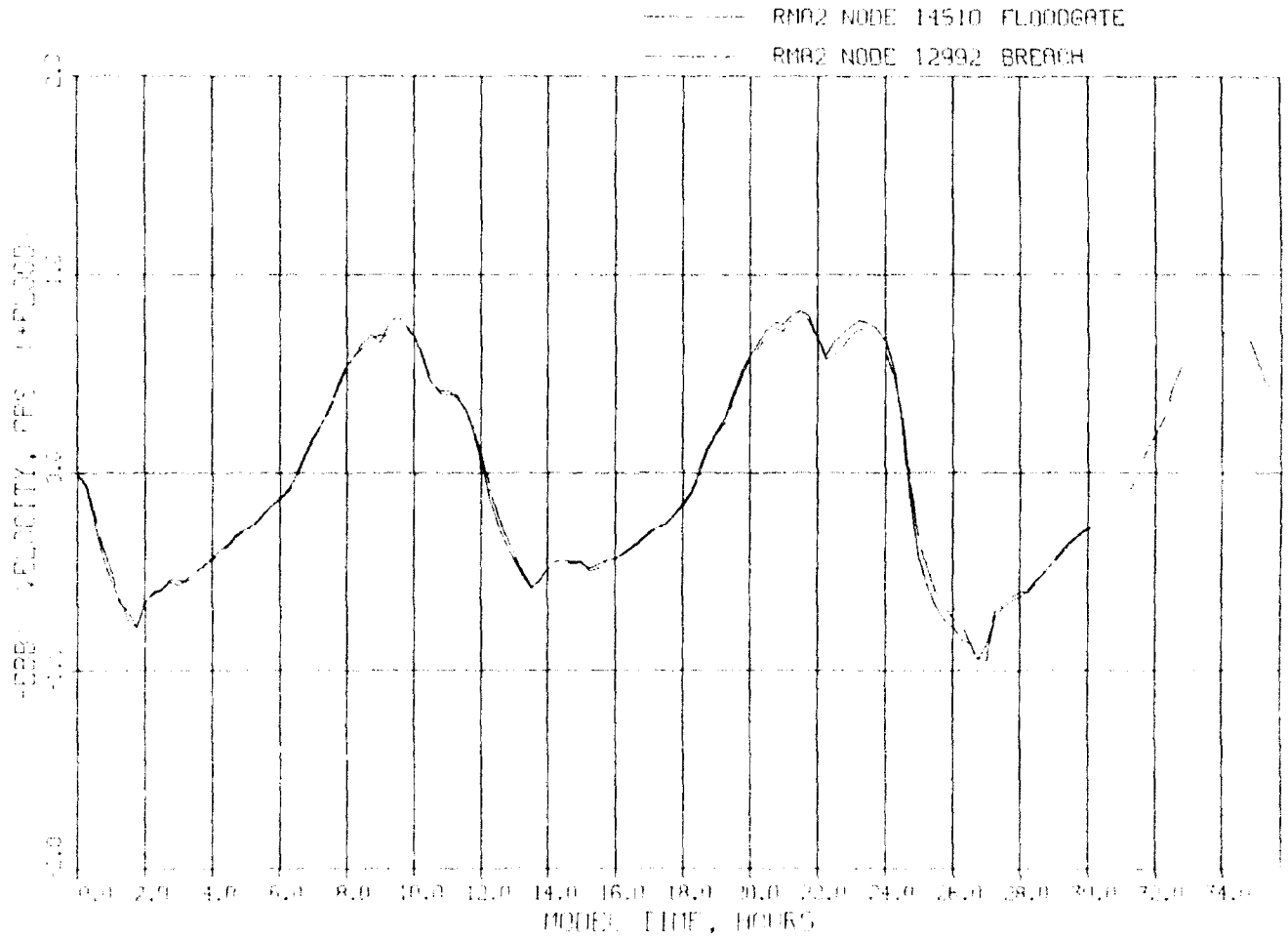


PLATE 53

**VELOCITY TIME-HISTORY**
**BASE VERSUS PLAN 2C+7**
**ENLARGED OPENING**

PLATE 54

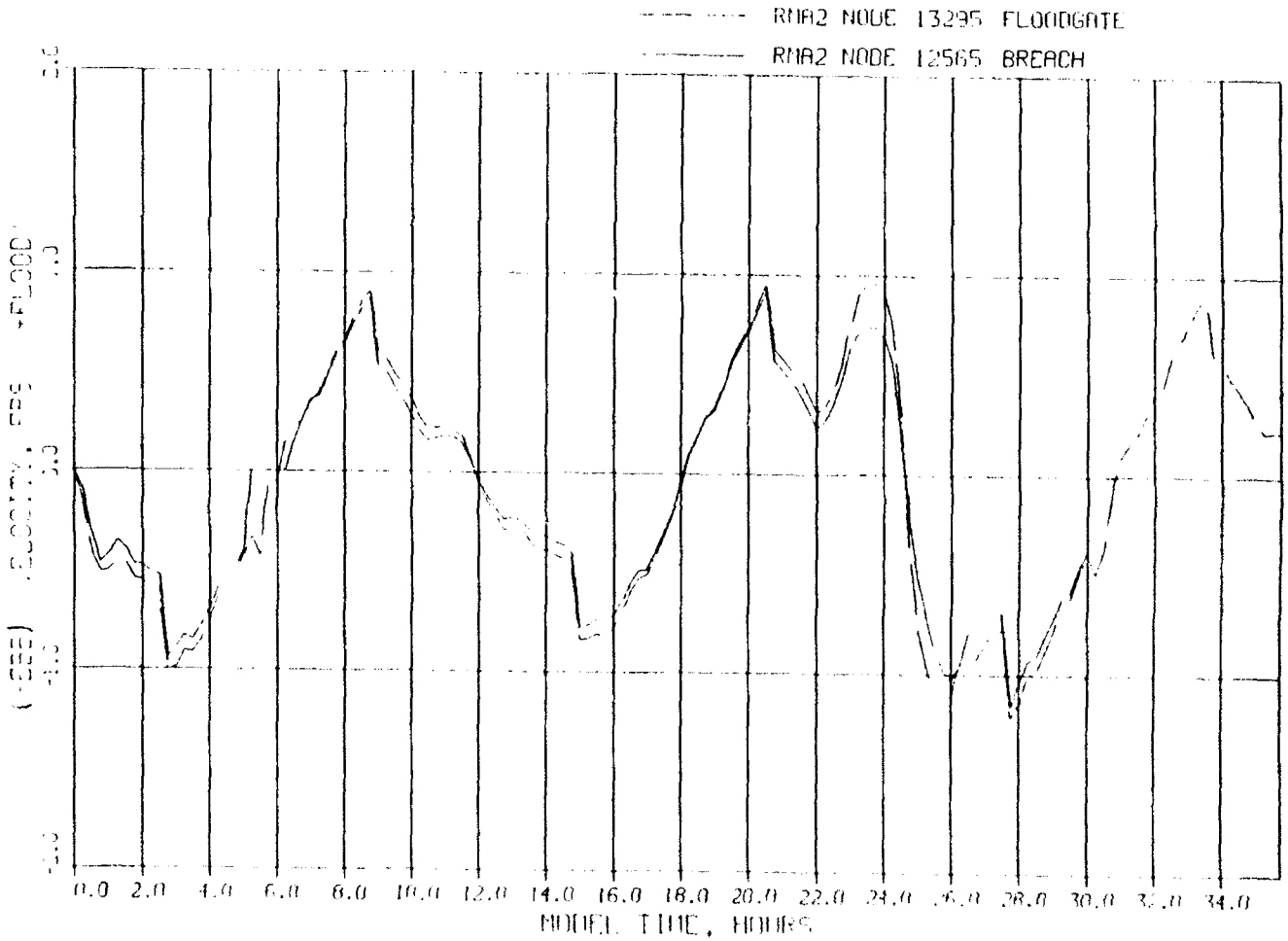


**VELOCITY TIME-HISTORY**
**BASE VERSUS PLAN 2C+7**
**BREACH CROSS SECTION**

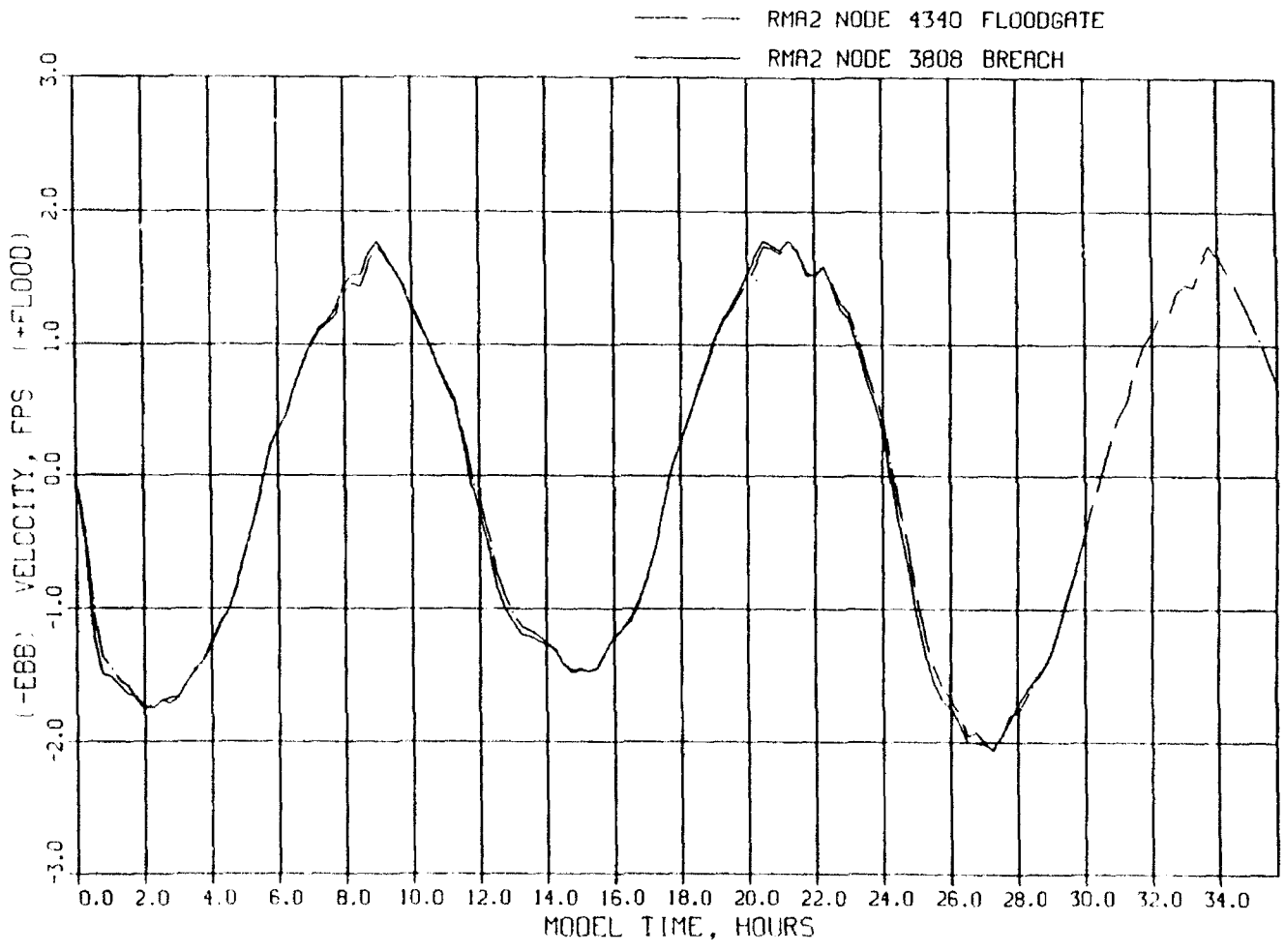


**VELOCITY TIME-HISTORY**
**BASE VERSUS PLAN 2C+7**
**UPSTREAM OF GENERAL EDWARDS BRIDGE**

PLATE 55

PLATE 56

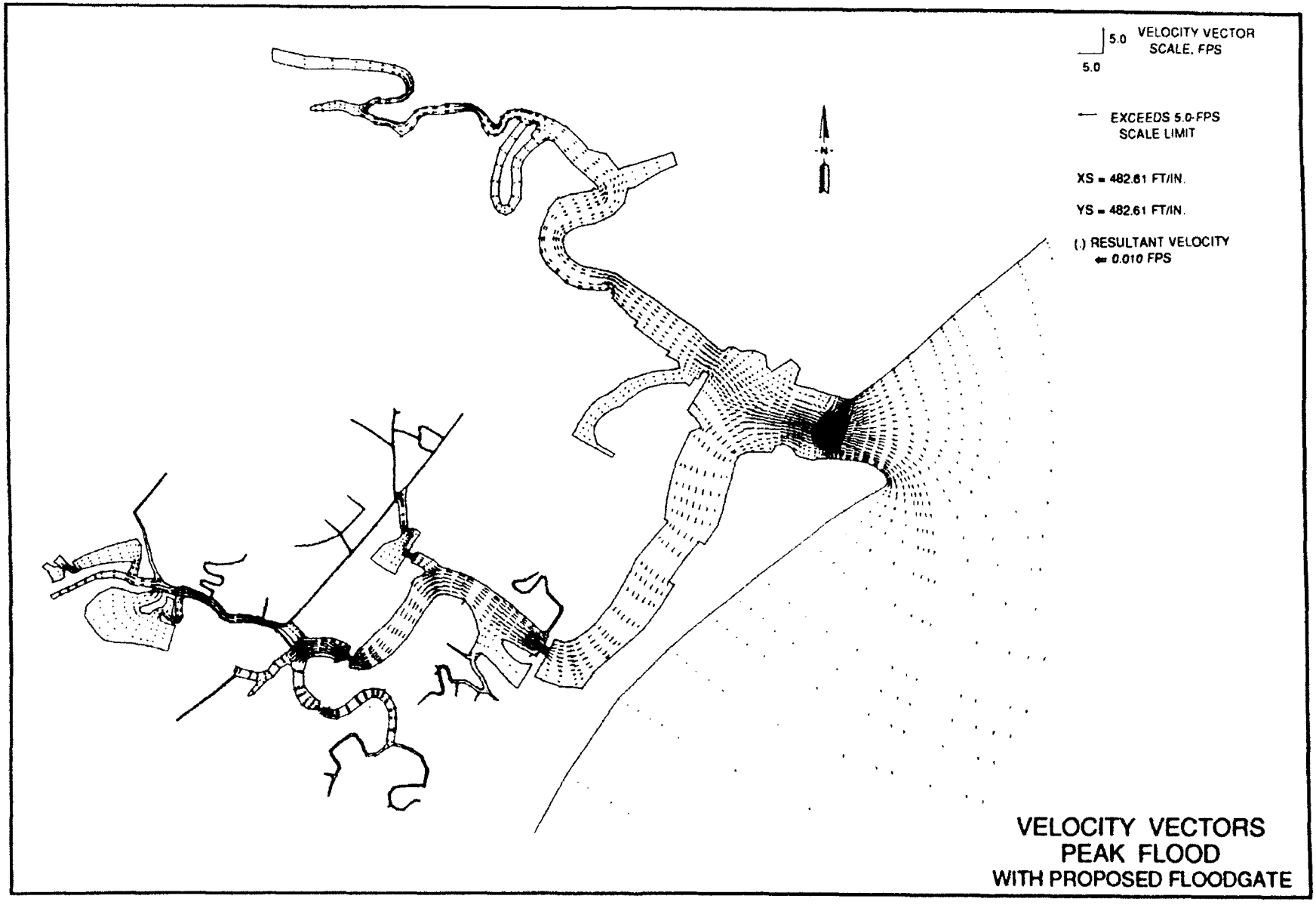


VELOCITY VECTORS
PEAK FLOOD
WITH PROPOSED FLOODGATE

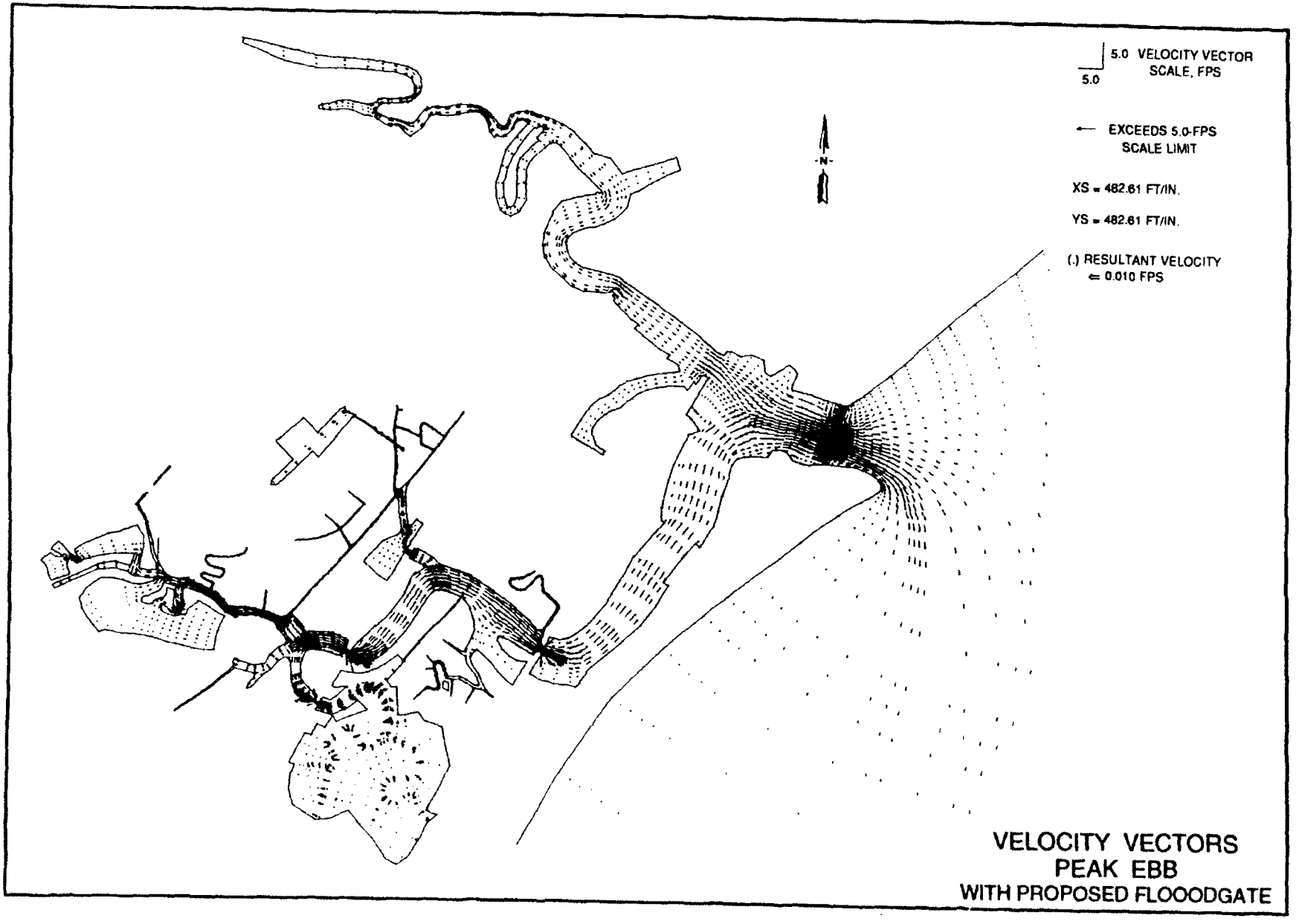
5.0 VELOCITY VECTOR SCALE, FPS
5.0
EXCEEDS 5.0-FPS SCALE LIMIT
N
XS = 482.61 FT/IN.
YS = 482.61 FT/IN.
(.) RESULTANT VELOCITY ≤ 0.010 FPS
VELOCITY VECTORS
PEAK EBB
WITH PROPOSED FLOOODGATE

PLATE 57

PLATE 58

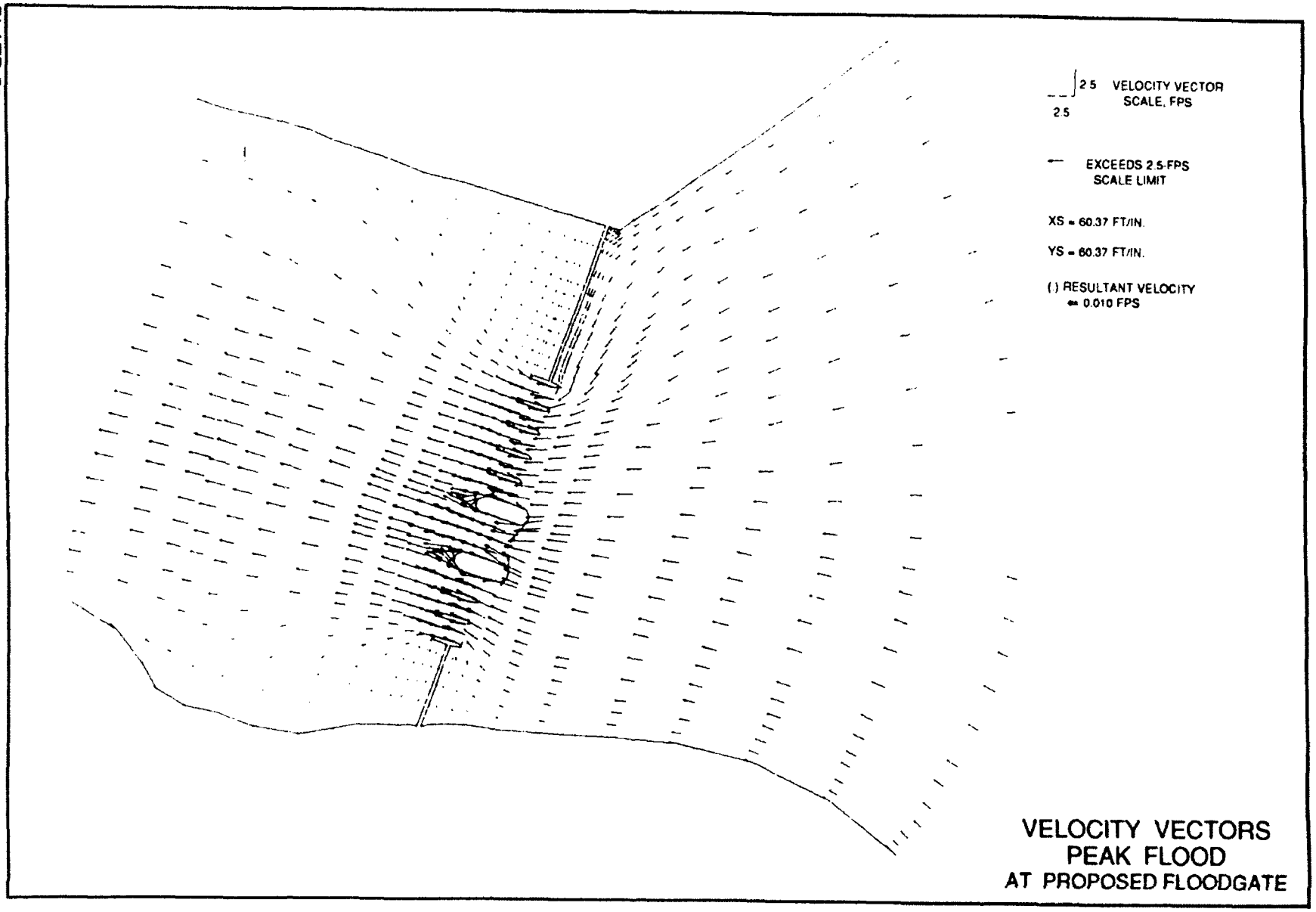


VELOCITY VECTORS
PEAK FLOOD
AT PROPOSED FLOODGATE

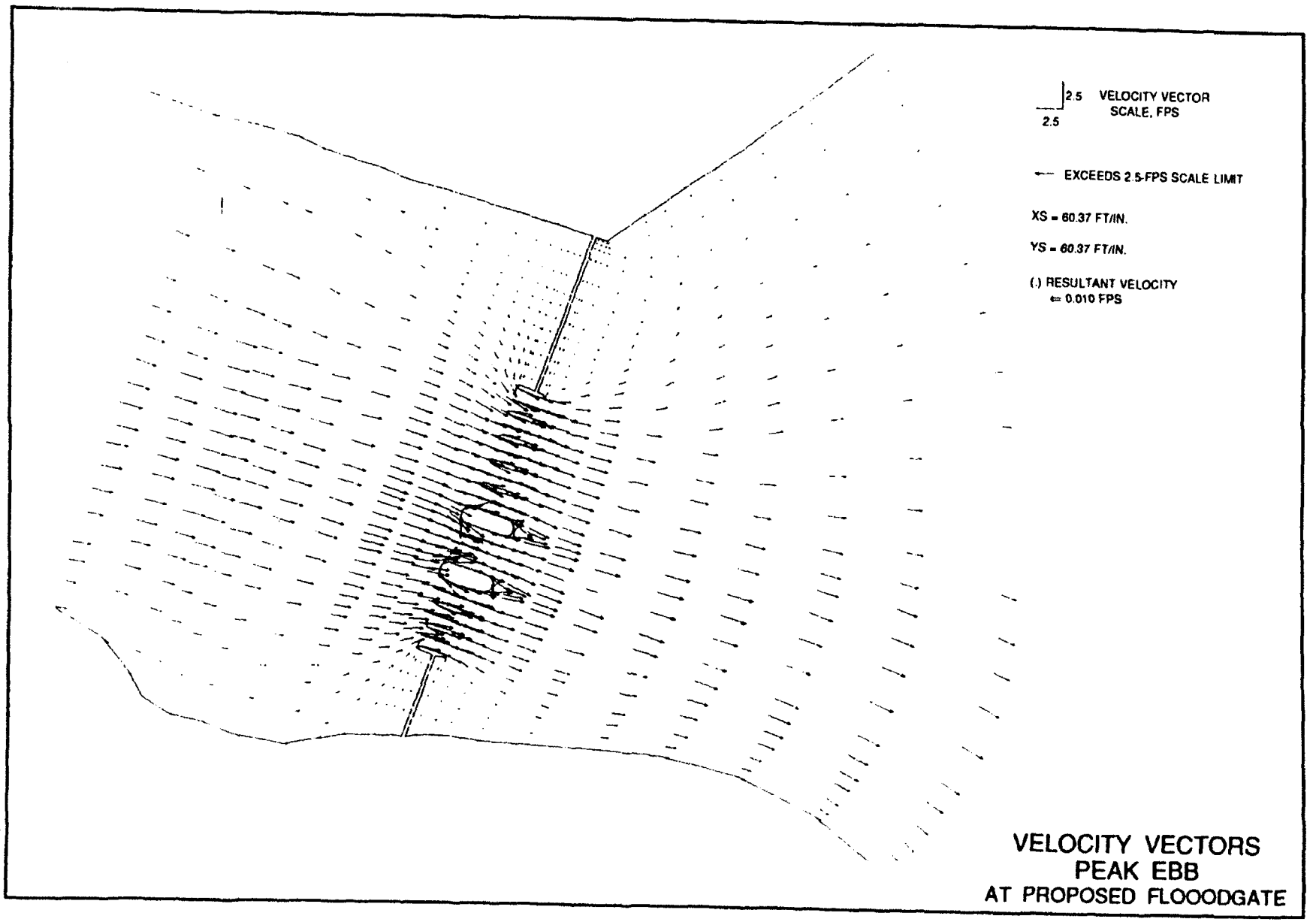


PLATE 59

# VELOCITY VECTORS PEAK EBB AT PROPOSED FLOOODGATE

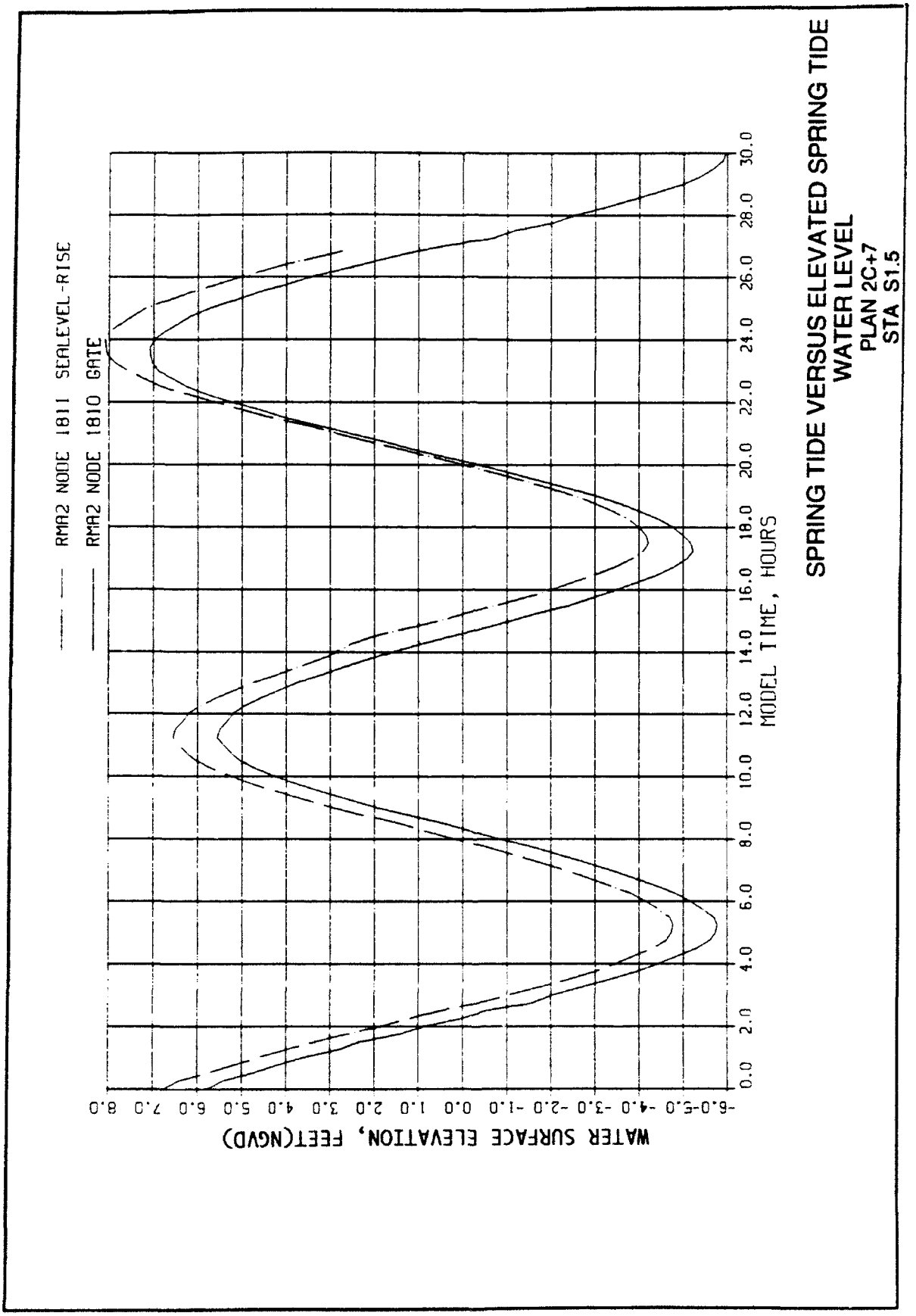
SPRING TIDE VERSUS ELEVATED SPRING TIDE
WATER LEVEL
PLAN 2C+7
STA S1.5
RMA2 NODE 1811 SEALEVEL-RISE
RMA2 NODE 1810 GATE
WATER SURFACE ELEVATION, FEET(NGVD)
MODEL TIME, HOURS
-6.0 -5.0 -4.0 -3.0 -2.0 -1.0 0.0 1.0 2.0 3.0 4.0 5.0 6.0 7.0 8.0
0.0 2.0 4.0 6.0 8.0 10.0 12.0 14.0 16.0 18.0 20.0 22.0 24.0 26.0 28.0 30.0

PLATE 60

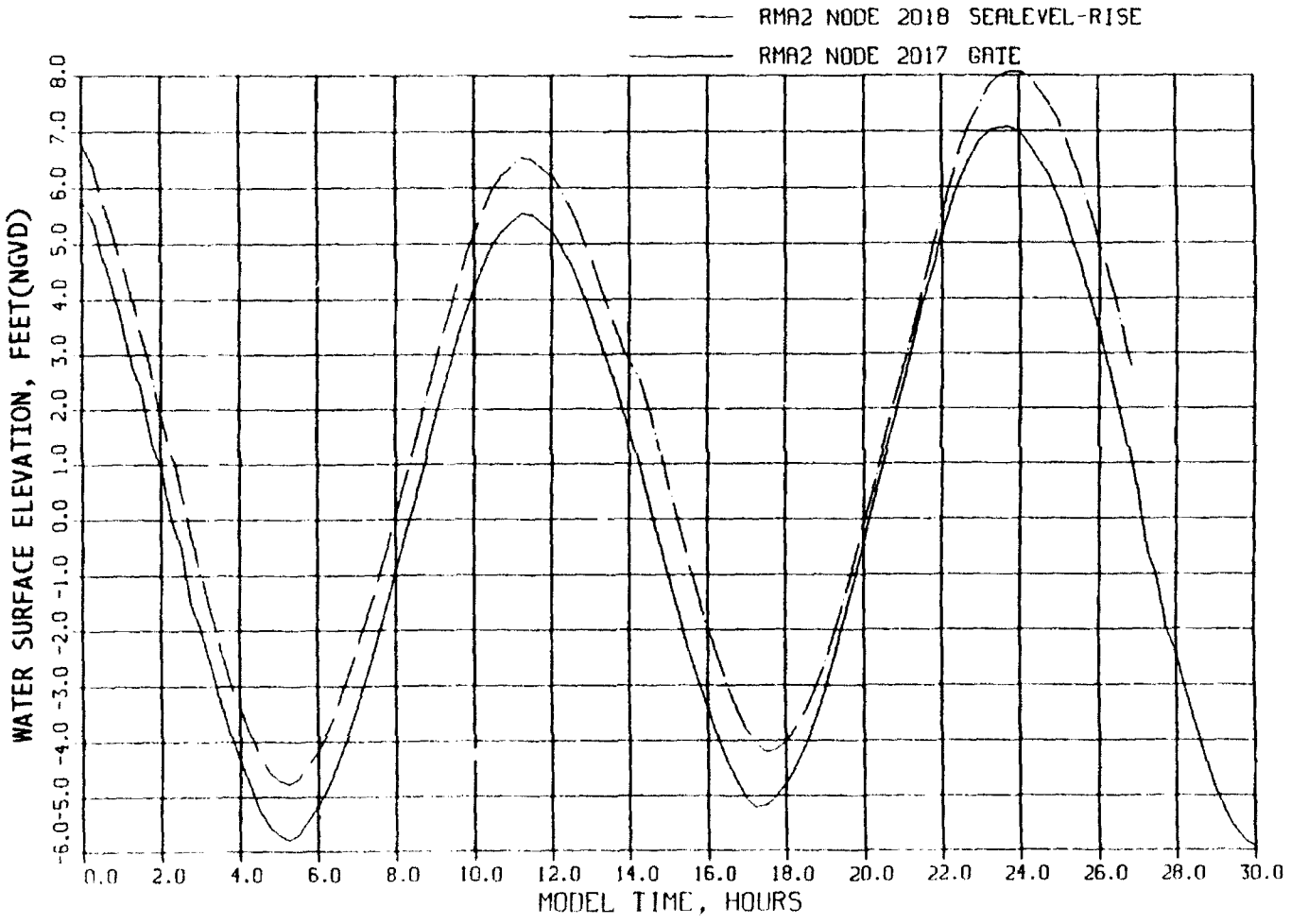


**SPRING TIDE VERSUS ELEVATED SPRING TIDE WATER LEVEL**
**PLAN 2C+7**
**STA S2.1**

PLATE 61

PLATE 62

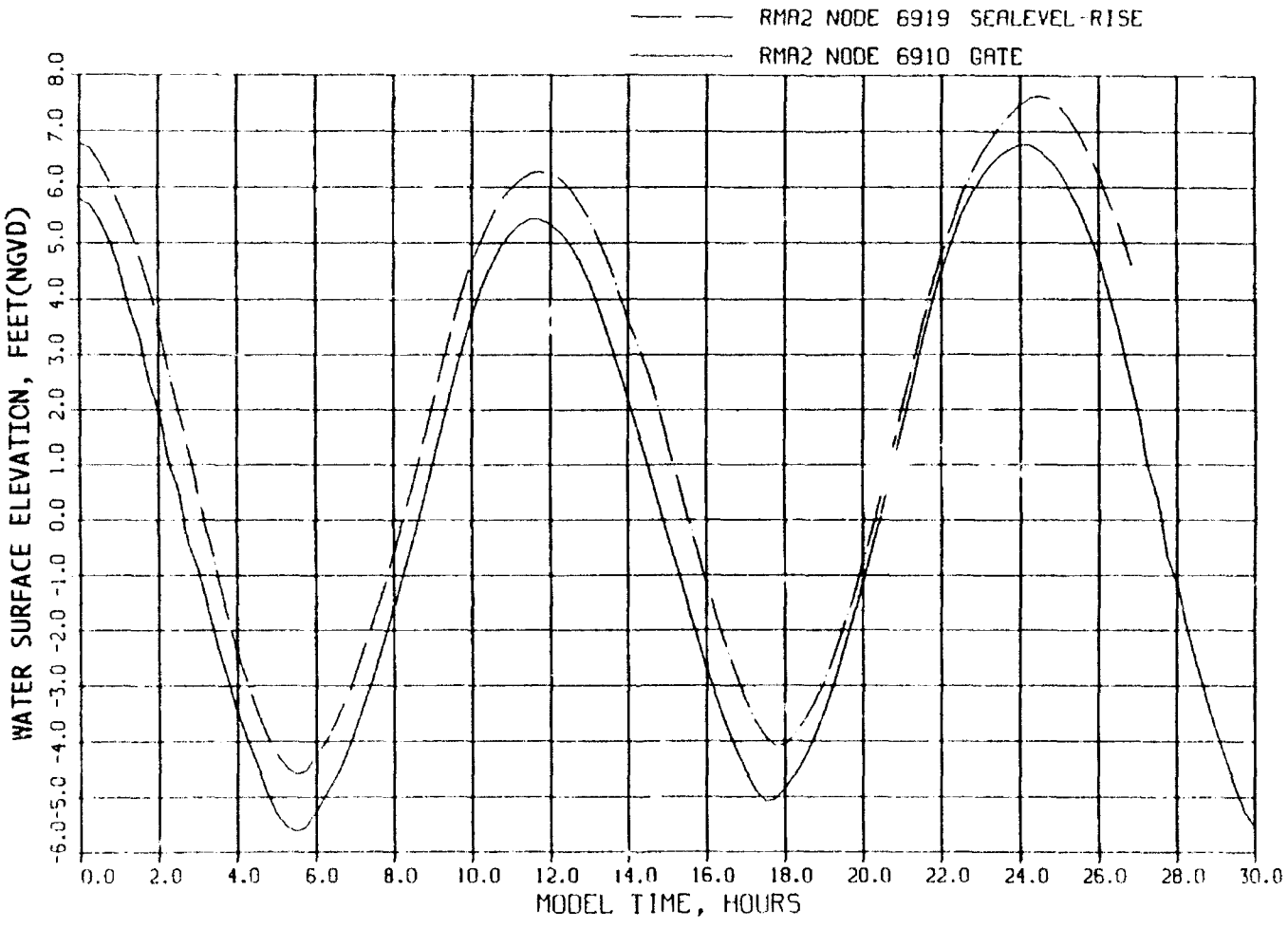


**SPRING TIDE VERSUS ELEVATED SPRING TIDE WATER LEVEL**
**PLAN 2C+7**
**STA S4.2**

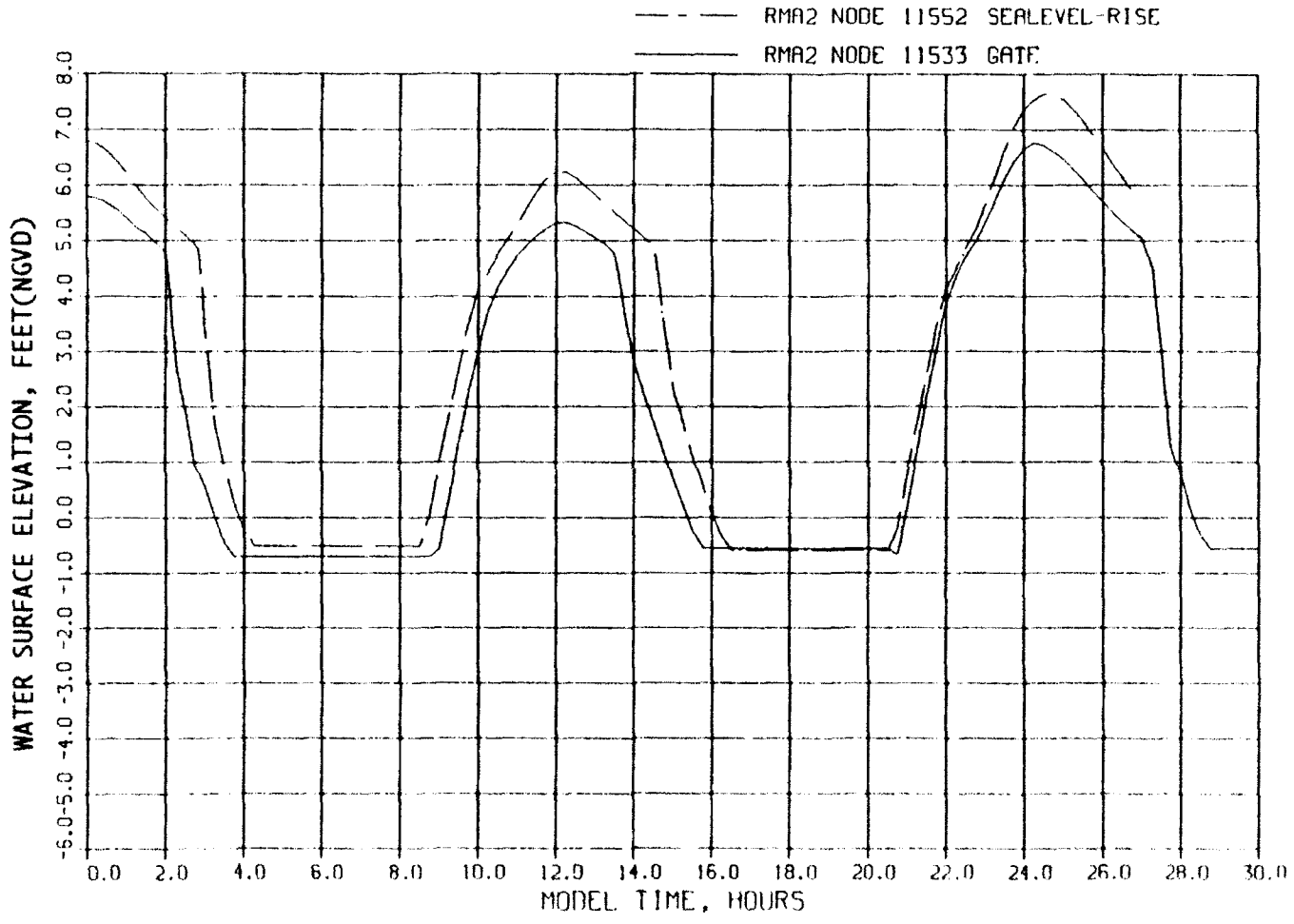


**SPRING TIDE VERSUS ELEVATED SPRING TIDE WATER LEVEL**
**PLAN 2C+7**
**STA S4.4**

PLATE 63

PLATE 64

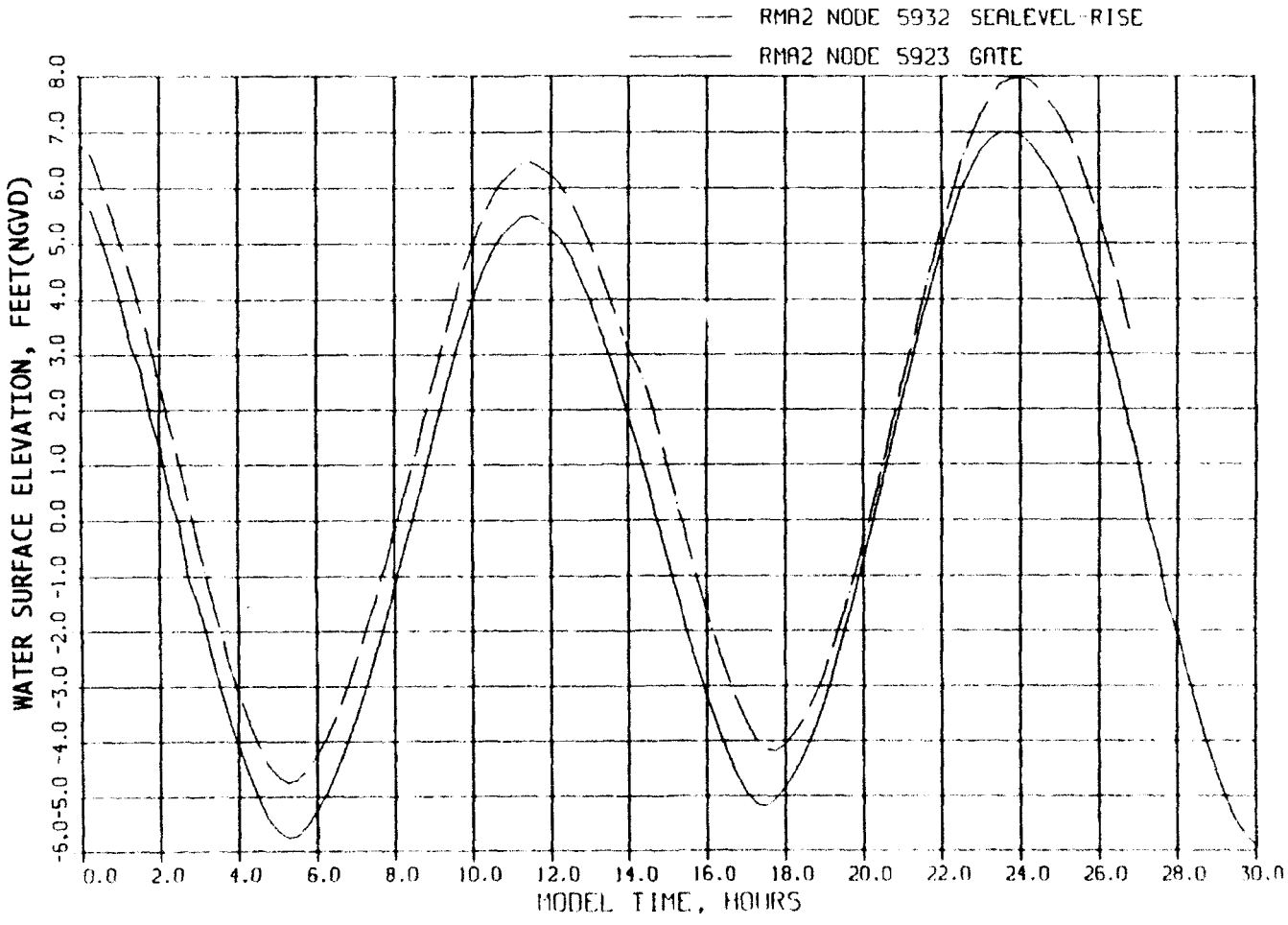


**SPRING TIDE VERSUS ELEVATED SPRING TIDE WATER LEVEL**
**PLAN 2C+7**
**STA S7.4**

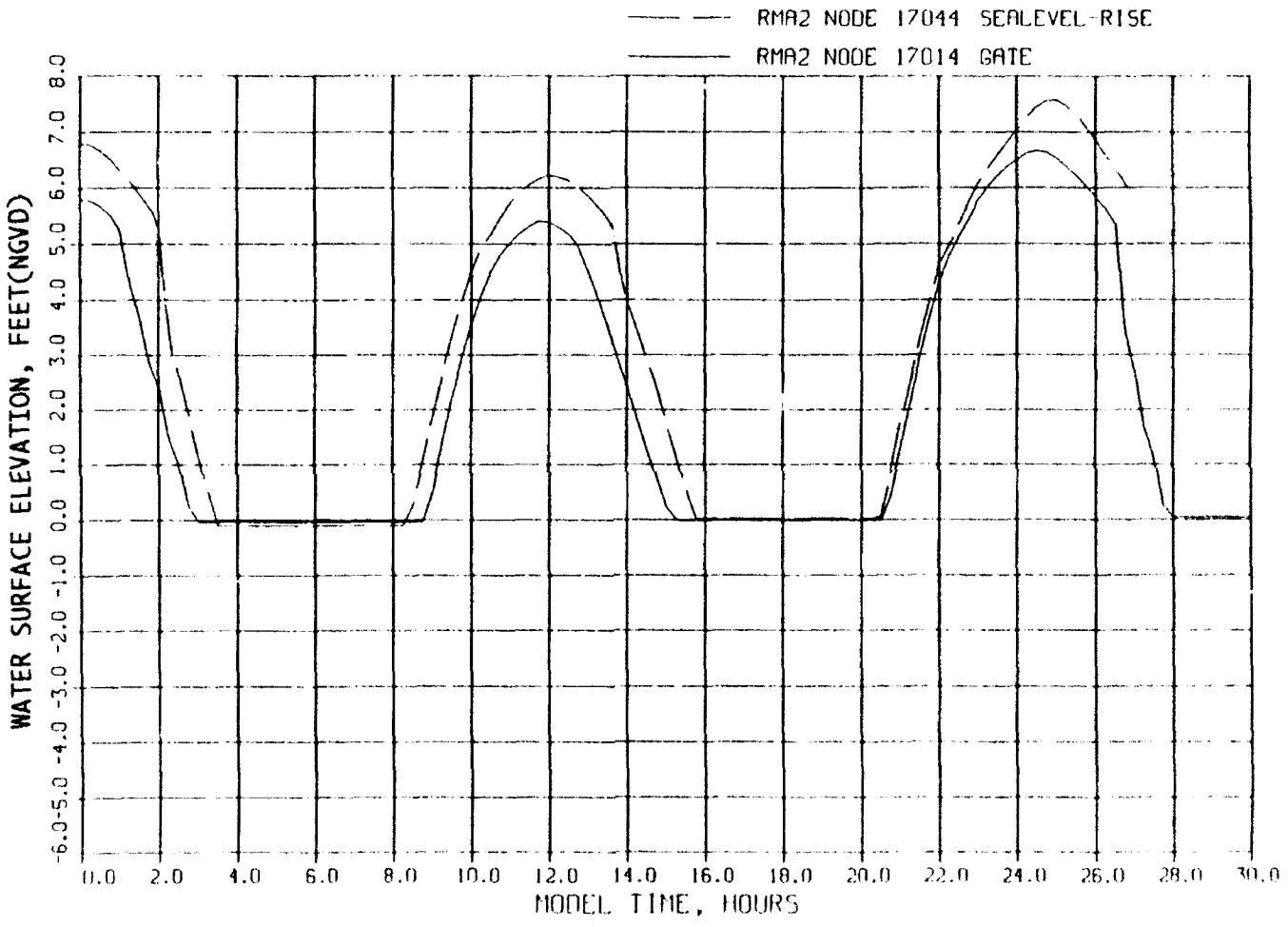


**SPRING TIDE VERSUS ELEVATED SPRING TIDE WATER LEVEL**
**PLAN 2C+7**
**STA S9.1**

PLATE 65

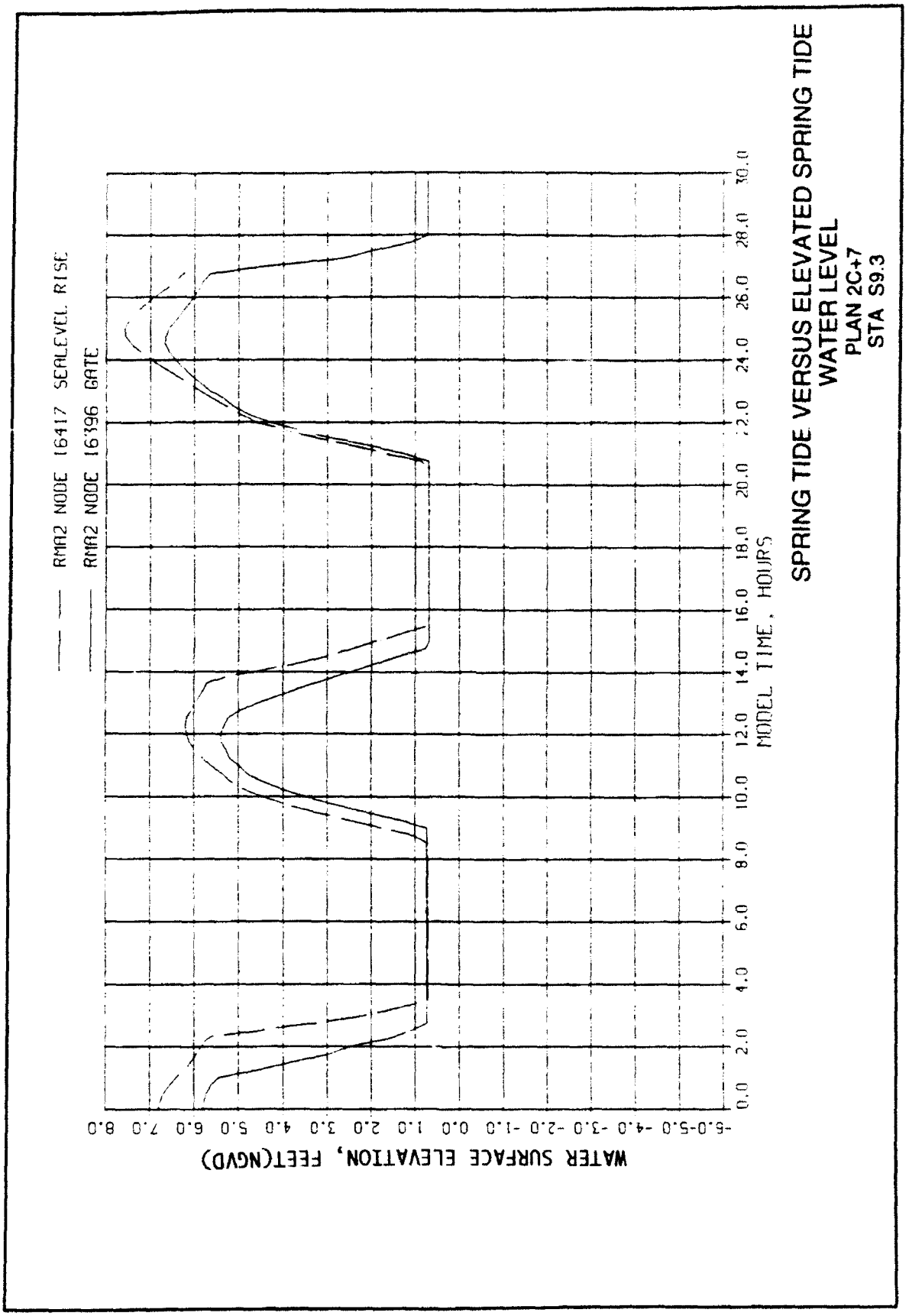
SPRING TIDE VERSUS ELEVATED SPRING TIDE
WATER LEVEL
PLAN 2C+7
STA S9.3
RMA2 NODE 16417 SEALEVEL RISE
RMA2 NODE 16396 GATE
WATER SURFACE ELEVATION, FEET(NGVD)
8.0 7.0 6.0 5.0 4.0 3.0 2.0 1.0 0.0 -1.0 -2.0 -3.0 -4.0 -5.0
MODEL TIME, HOURS
0.0 2.0 4.0 6.0 8.0 10.0 12.0 14.0 16.0 18.0 20.0 22.0 24.0 26.0 28.0 30.0

PLATE 66

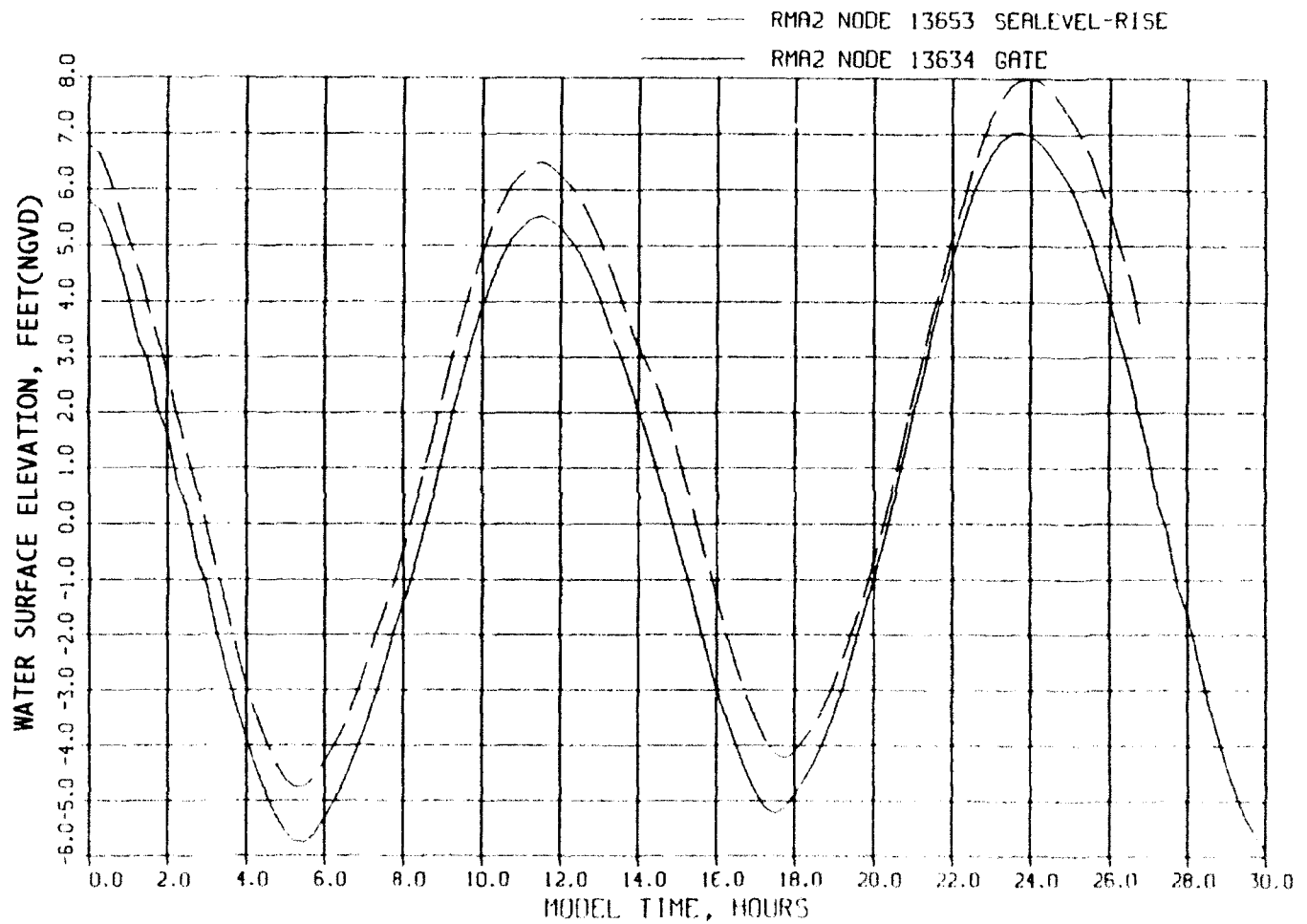


PLATE 67

**SPRING TIDE VERSUS ELEVATED SPRING TIDE WATER LEVEL**

PLAN 2C+7

STA S9.5

PLATE 68

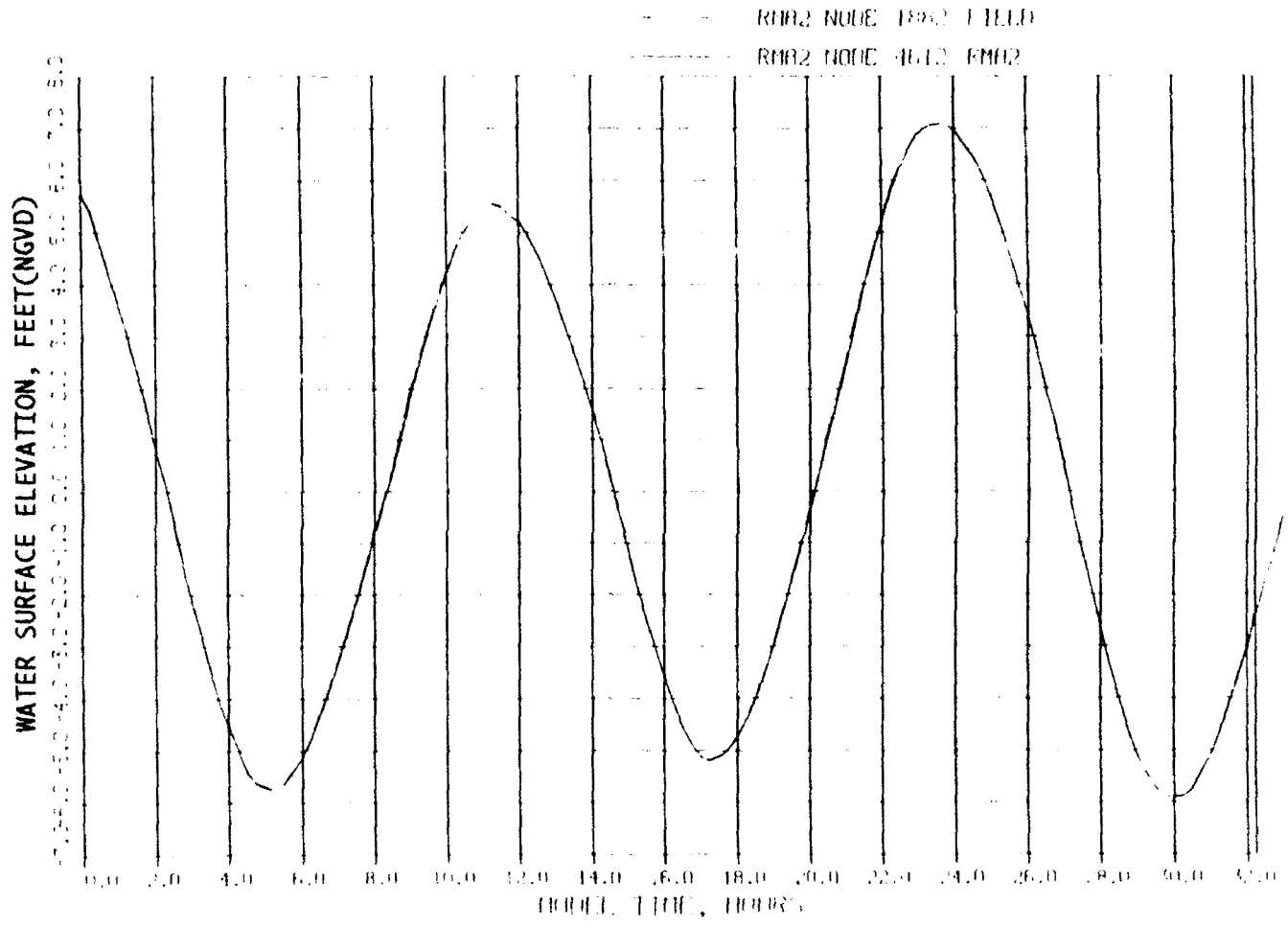


EXISTING VERSUS FLOODGATE CLOSED
WATER LEVEL
AT OCEAN SIDE FLOODGATE

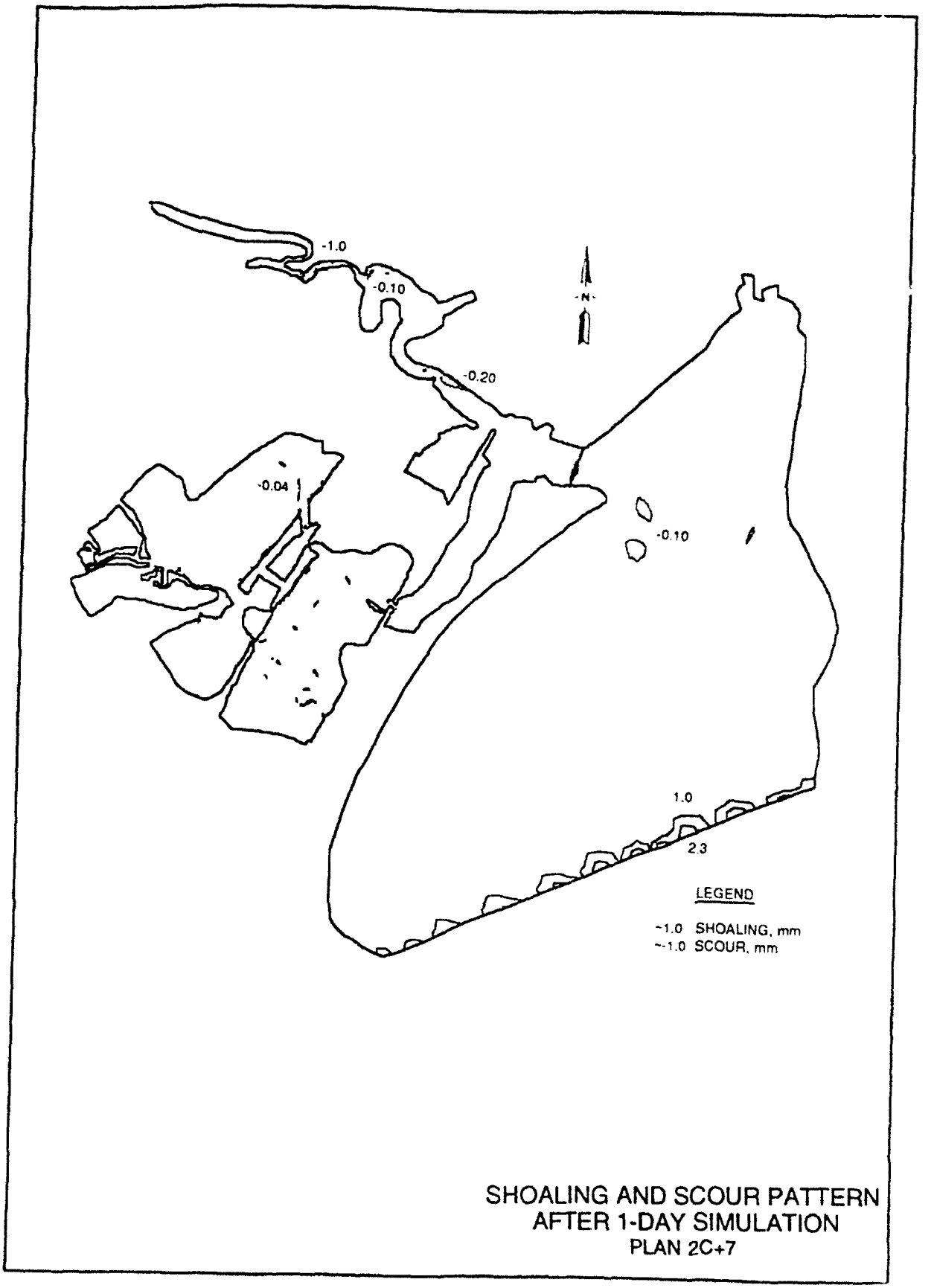


SHOALING AND SCOUR PATTERN
AFTER 1-DAY SIMULATION
PLAN 2C+7

PLATE 69

# Appendix A
# The TABS-MD System

TABS-MD is a collection of generalized computer programs and utility codes integrated into a numerical modeling system for studying two-dimensional hydrodynamics, sedimentation, and transport problems in rivers, reservoirs, bays, and estuaries. A schematic representation of the system is shown in Figure A1. It can be used either as a stand-alone solution technique or as a step in the hybrid modeling approach. The basic concept is to calculate water-surface elevations, current patterns, sediment erosion, transport and deposition, the resulting bed surface elevations, and the feedback to hydraulics. Existing and proposed geometry can be analyzed to determine the impact on sedimentation of project designs and to determine the impact of project designs on salinity and on the stream system. The system is described in detail by Thomas and McAnally (1985).

The three basic components of the system are as follows:

*a.* "A Two-Dimensional Model for Free Surface Flows," RMA-2V.

*b.* "Sediment Transport in Unsteady 2-Dimensional Flows, Horizontal Plane," STUDH.

*c.* "Two-Dimensional Finite Element Program for Water Quality," RMA-4.

RMA-2V is a finite element solution of the Reynolds form of the Navier-Stokes equations for turbulent flows. Friction is calculated with Manning's equation and eddy viscosity coefficients are used to define the turbulent losses. A velocity form of the basic equation is used with side boundaries treated as either slip or static. The model automatically recognizes dry elements and corrects the mesh accordingly. Boundary conditions may be water-surface elevations, velocities, or discharges and may occur inside the mesh as well as along the edges.

The sedimentation model, STUDH, solves the convection-diffusion equation with bed source terms. These terms are structured for either sand or cohesive sediments. The Ackers-White (1973) procedure is used to calculate a sediment transport potential for the sands from which the actual transport is calculated

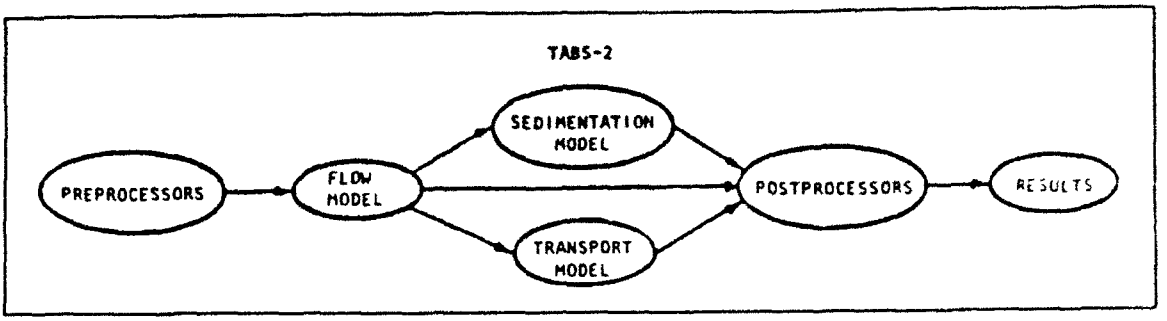


Figure A1. TABS-2 schematic

based on availability. Clay erosion is based on work by Partheniades (1962) and Ariathurai and the deposition of clay utilizes Krone's equations (Ariathurai, MacArthur, and Krone 1977). Deposited material forms layers, as shown in Figure A2, and bookkeeping allows up to 10 layers at each node for maintaining separate material types, deposit thickness, and age. The code uses the same mesh as RMA-2V.

Salinity calculations, RMA-4, are made with a form of the convective-diffusion equation which has general source-sink terms. Up to seven conservative substances or substances requiring a decay term can be routed. The code uses the same mesh as RMA-2V.

Each of these generalized computer codes can be used as a stand-alone program, but to facilitate the preparation of input data and to aid in analyzing results, a family of utility programs was developed for the following purposes:

*a.* Digitizing

*b.* Mesh generation

*c.* Spatial data management

*d.* Graphical output

*e.* Output analysis

*f.* File management

*g.* Interfaces

*h.* Job control language

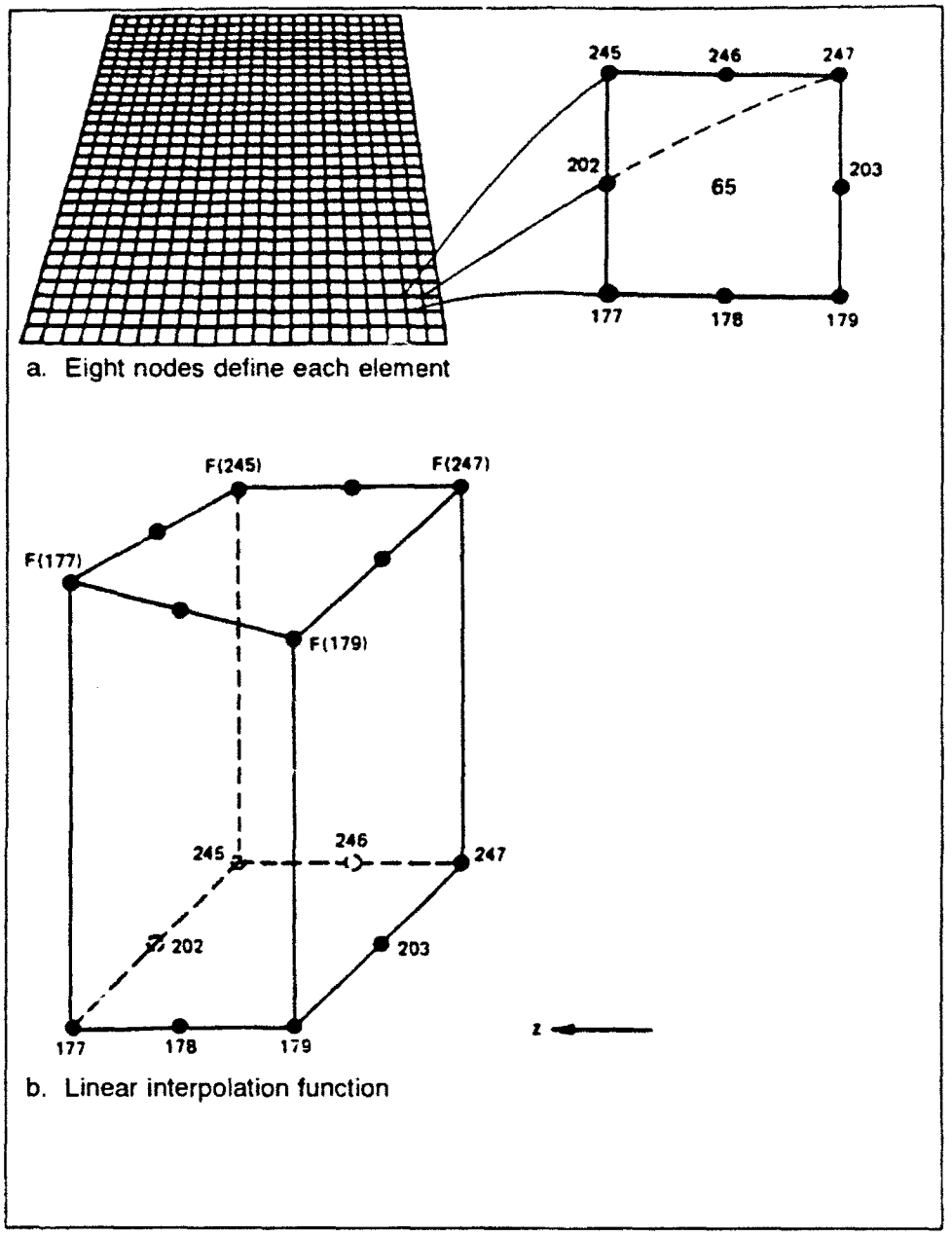


Figure A2. Two-dimensional finite element mesh

## Finite Element Modeling

The TABS-2 numerical models used in this effort employ the finite element method to solve the governing equations. To help those who are unfamiliar with the method to better understand this report, a brief description of the method is given here.

The finite element method approximates a solution to equations by dividing the area of interest into smaller subareas, which are called elements. The dependent variables (e.g., water-surface elevations and sediment concentrations) are approximated over each element by continuous functions which interpolate in terms of unknown point (node) values of the variables. An error, defined as the deviation of the approximation solution from the correct solution, is minimized. Then, when boundary conditions are imposed, a set of solvable simultaneous equations is created. The solution is continuous over the area of interest.

In one-dimensional problems, elements are line segments. In twodimensional problems, the elements are polygons, usually either triangles or quadrilaterals. Nodes are located on the edges of elements and occasionally inside the elements. The interpolating functions may be linear or higher order polynomials. Figure A2 illustrates a quadrilateral element with eight nodes and a linear solution surface where $F$ is the interpolating function.

Most water resource applications of the finite element method use the Galerkin method of weighted residuals to minimize error. In this method the residual, the total error between the approximate and correct solutions, is weighted by a function that is identical with the interpolating function and then minimized. Minimization results in a set of simultaneous equations in terms of nodal values of the dependent variable (e.g. water-surface elevations or sediment concentration). The time portion of time-dependent problems can be solved by the finite element method, but it is generally more efficient to express derivatives with respect to time in finite difference form.

## The Hydrodynamic Model, RMA-2V

### Applications

This program is designed for far-field problems in which vertical accelerations are negligible and the velocity vectors at a node generally point in the same directions over the entire depth of the water column at any instant of time. It expects a homogeneous fluid with a free surface. Both steady and unsteady state problems can be analyzed. A surface wind stress can be imposed.

The program has been applied to calculate flow distribution around islands; flow at bridges having one or more relief openings, in contracting and expanding reaches, into and out of off-channel hydropower plants, at river junctions, and into and out of pumping plant channels; and general flow patterns in rivers, reservoirs, and estuaries.

## Limitations

This program is not designed for near-field problems where flowstructure interactions (such as vortices, vibrations, or vertical accelerations) are of interest. Areas of vertically stratified flow are beyond this program's capability unless it is used in a hybrid modeling approach. It is two-dimensional in the horizontal plane, and zones where the bottom current is in a different direction from the surface current must be analyzed with considerable subjective judgment regarding long-term energy considerations. It is a free-surface calculation for subcritical flow problems.

## Governing equations

The generalized computer program RMA-2V solves the depth-integrated equations of fluid mass and momentum conservation in two horizontal directions. The form of the solved equations is

$$h\frac{\partial u}{\partial t} + hu\frac{\partial u}{\partial x} + hv\frac{\partial u}{\partial y} - \frac{h}{\rho}\left(\varepsilon_{xx}\frac{\partial^2 u}{\partial x^2} + \varepsilon_{xy}\frac{\partial^2 u}{\partial y^2}\right) + gh\left(\frac{\partial a}{\partial x} + \frac{\partial h}{\partial x}\right) + \frac{gun^2}{\left(1.486h^{1/6}\right)^2}\left(u^2 + v^2\right)^{1/2} - \zeta V_a^2 \cos\psi - 2h\omega v \sin\phi = 0 \qquad \text{(A1)}$$

$$h\frac{\partial v}{\partial t} + hu\frac{\partial v}{\partial x} + hv\frac{\partial v}{\partial y} - \frac{h}{\rho}\left(\varepsilon_{yx}\frac{\partial^2 v}{\partial x^2} + \varepsilon_{yy}\frac{\partial^2 v}{\partial y^2}\right) + gh\left(\frac{\partial a}{\partial y} + \frac{\partial h}{\partial y}\right) + \frac{gvn^2}{\left(1.486h^{1/6}\right)^2}\left(u^2 + v^2\right)^{1/2} - \zeta V_a^2 \cos\psi - 2\omega hu \sin\phi = 0 \qquad \text{(A2)}$$

$$\frac{\partial h}{\partial t} + h\left(\frac{\partial u}{\partial x} + \frac{\partial v}{\partial y}\right) + u\frac{\partial h}{\partial x} + v\frac{\partial h}{\partial y} = 0 \qquad \text{(A3)}$$

where

$h$ = depth
$u,v$ = velocities in the Cartesian directions
$x,y,t$ = Cartesian coordinates and time
$\rho$ = density

$\varepsilon$ = eddy viscosity coefficient, for $xx$ = normal direction on x-axis surface; $yy$ = normal direction on y-axis surface; $xy$ and $yx$ = shear direction on each surface
$g$ = acceleration due to gravity
$a$ = elevation of bottom
$n$ = Manning's n value
1.486 = conversion from SI to non-SI units
$\zeta$ = empirical wind shear coefficient
$V_a$ = wind speed
$\psi$ = wind direction
$\omega$ = rate of earth's angular rotation
$\phi$ = local latitude

Equations A1, A2, and A3 are solved by the finite element method using Galerkin weighted residuals. The elements may be either quadrilaterals or triangles and may have curved (parabolic) sides. The shape functions are quadratic for flow and linear for depth. Integration in space is performed by Gaussian integration. Derivatives in time are replaced by a nonlinear finite difference approximation. Variables are assumed to vary over each time interval in the form

$$f(t) = f(0) + at + bt^c \qquad t_0 \le t < t \tag{A4}$$

which is differentiated with respect to time, and cast in finite difference form. Letters $a$, $b$, and $c$ are constants. It has been found by experiment that the best value for $c$ is 1.5 (Norton and King 1977).

The solution is fully implicit and the set of simultaneous equations is solved by Newton-Raphson iteration. The computer code executes the solution by means of a front-type solver that assembles a portion of the matrix and solves it before assembling the next portion of the matrix. The front solver's efficiency is largely independent of bandwidth and thus does not require as much care in formation of the computational mesh as do traditional solvers.

The code RMA-2V is based on the earlier version RMA-2 (Norton and King 1977) but differs from it in several ways. It is formulated in terms of velocity ($v$) instead of unit discharge ($vh$), which improves some aspects of the code's behavior; it permits drying and wetting of areas within the grid; and it permits specification of turbulent exchange coefficients in directions other than along the $x$- and $z$-axes. For a more complete description, see Appendix F of Thomas and McAnally (1985).

# The Sediment Transport Model, STUDH

## Applications

STUDH can be applied to clay and/or sand bed sediments where flow velocities c n be considered two-dimensional (i.e., the speed and direction can be satisfactorily represented as a depth-averaged velocity). It is useful for both deposition and erosion studies and, to a limited extent, for stream width studies. The program treats two categories of sediment: noncohesive, which is referred to as sand here, and cohesive, which is referred to as clay.

## Limitations

Both clay and sand may be analyzed, but the model considers a single, effective grain size for each and treats each separately. Fall velocity must be prescribed along with the water-surface elevations, x-velocity, y-velocity, diffusion coefficients, bed density, critical shear stresses for erosion, erosion rate constants, and critical shear stress for deposition.

Many applications cannot use long simulation periods because of their computation cost. Study areas should be made as small as possible to avoid an excessive number of elements when dynamic runs are contemplated yet must be large enough to permit proper posing of boundary conditions. The same computation time interval must be satisfactory for both the transverse and longitudinal flow directions.

The program does not compute water-surface elevations or velocities; therefore these data must be provided. For complicated geometries, the numerical model for hydrodynamic computations, RMA-2V, is used.

## Governing equations

The generalized computer program STUDH solves the depth-integrated convection-dispersion equation in two horizontal dimensions for a single sediment constituent. For a more complete description, see Appendix G of Thomas and McAnally (1985). The form of the solved equation is

$$\frac{\partial C}{\partial t} + u\frac{\partial C}{\partial x} + v\frac{\partial C}{\partial y} = \frac{\partial}{\partial x}\left(D_x\frac{\partial C}{\partial x}\right) + \frac{\partial}{\partial y}\left(D_y\frac{\partial C}{\partial y}\right) + \alpha_1 C_2 + \alpha = 0 \qquad \text{(A5)}$$

where

$C$ = concentration of sediment

$u$ = depth-integrated velocity in x-direction

$v$ = depth-integrated velocity in y-direction
$D_x$ = dispersion coefficient in x-direction
$D_y$ = dispersion coefficient in y-direction
$\alpha_1$ = coefficient of concentration-dependent source/sink term
$\alpha_2$ = coefficient of source/sink term

The source/sink terms in Equation B5 are computed in routines that treat the interaction of the flow and the bed. Separate sections of the code handle computations for clay bed and sand bed problems.

## Sand transport

The source/sink terms are evaluated by first computing a potential sand transport capacity for the specified flow conditions, comparing that capacity with amount of sand actually being transported, and then eroding from or depositing to the bed at a rate that would approach the equilibrium value after sufficient elapsed time.

The potential sand transport capacity in the model is computed by the method of Ackers and White (1973), which uses a transport power (work rate) approach. It has been shown to provide superior results for transport under steady-flow conditions (White, Milli, and Crabbe 1975) and for combined waves and currents (Swart 1976). Flume tests at the U.S. Army Engineer Waterways Experiment Station have shown that the concept is valid for transport by estuarine currents.

The total load transport function of Ackers and White is based upon a dimensionless grain size

$$D_{gr} = D\left[\frac{g(s-1)}{\nu^2}\right]^{1/3} \tag{A6}$$

where
$D$ = sediment particle diameter
$s$ = specific gravity of the sediment
$\nu$ = kinematic viscosity of the fluid

and a sediment mobility parameter

$$F_{gr} = \left[\frac{\tau^{n'}\tau'^{(1-n')}}{\rho g D(s-1)}\right]^{1/2} \tag{A7}$$

where

$\tau$ = total boundary shear stress

$n'$ = a coefficient expressing the relative importance of bed-load and suspended-load transport, given in Equation A9

$\tau'$ = boundary surface shear stress

The surface shear stress is that part of the total shear stress which is due to the rough surface of the bed only, i.e., not including that part due to bed forms and geometry. It therefore corresponds to that shear stress that the flow would exert on a plane bed.

The total sediment transport is expressed as an effective concentration

$$G_p = C \left[ \frac{F_{gr}}{A} - 1 \right]^m \frac{sD}{h} \left[ \sqrt{\frac{\rho}{\tau}} U \right]^{n'} \tag{A8}$$

where $U$ is the average flow speed, and for $1 < D_{gr} \leq 60$

$$n' = 1.00 - 0.56 \log D_{gr} \tag{A9}$$

$$A = \frac{0.23}{\sqrt{D_{gr}}} + 0.14 \tag{A10}$$

$$\log C = 2.86 \log D_{gr} - (\log D_{gr})^2 - 3.53 \tag{A11}$$

$$m = \frac{9.66}{D_{gr}} + 1.34 \tag{A12}$$

For $D_{gr} < 60$

$$n' = 0.00 \tag{A13}$$

$$A = 0.17 \tag{A14}$$

$$C = 0.025 \tag{A15}$$

$$m = 1.5 \tag{A16}$$

Equations A6-A16 result in a potential sediment concentration $G_p$. This value is the depth-averaged concentration of sediment that will occur if an equilibrium transport rate is reached with a nonlimited supply of sediment. The rate of sediment deposition (or erosion) is then computed as

$$R = \frac{G_p - C}{t_c} \tag{A17}$$

where

$C$ = present sediment concentration
$t_c$ = time constant

For deposition, the time constant is

$$t_c = \text{larger of} \begin{cases} \Delta t \\ \text{or} \\ \dfrac{C_d h}{V_s} \end{cases} \tag{A18}$$

and for erosion it is

$$t_c = \text{larger of} \begin{cases} \Delta t \\ \text{or} \\ \dfrac{C_e h}{U} \end{cases} \tag{A19}$$

where

$\Delta t$ = computational time-step
$C_d$ = response time coefficient for deposition
$V_s$ = sediment settling velocity
$C_e$ = response time coefficient for erosion

The sand bed has a specified initial thickness which limits the amount of erosion to that thickness.

## Cohesive sediments transport

Cohesive sediments (usually clays and some silts) are considered to be depositional if the bed shear stress exerted by the flow is less than a critical value $\tau_d$. When that value occurs, the deposition rate is given by Krone's (1962) equation

$$S = \begin{cases} -\frac{2V_s}{h} C \left(1 - \frac{\tau}{\tau_d}\right) \text{ for } C < C_c & \text{(A20)} \\ -\frac{2V_s}{hC_c^{4/3}} C^{5/3} \left(1 - \frac{\tau}{\tau_d}\right) \text{ for } C > C_c & \text{(A21)} \end{cases}$$

where

$S$ = source term
$V_s$ = fall velocity of a sediment particle
$h$ = flow depth
$C$ = sediment concentration in water column
$\tau$ = bed shear stress
$\tau_d$ = critical shear stress for deposition
$C_c$ = critical concentration = 300 mg/$\ell$

If the bed shear stress is greater than the critical value for particle erosion $\tau_e$, material is removed from the bed. The source term is then computed by Ariathurai's (Ariathurai, MacArthur, and Krone 1977) adaptation of Partheniades' (1962) findings:

$$S = \frac{P}{h}\left(\frac{\tau}{\tau_e} - 1\right) \text{ for } \tau > \tau_e \qquad \text{(A22)}$$

where $P$ is the erosion rate constant, unless the shear stress is also greater than the critical value for mass erosion. When this value is exceeded, mass failure of a sediment layer occurs and

$$S = \frac{T_L P_L}{h\Delta T} \text{ for } \tau > \tau_s \qquad \text{(A23)}$$

where

$T_L$ = thickness of the failed layer

$P_L$ = density of the failed layer
$\Delta t$ = time interval over which failure occurs
$\tau_s$ = bulk shear strength of the layer

The cohesive sediment bed consists of 1 to 10 layers, each with a distinct density and erosion resistance. The layers consolidate with overburden and time.

## Bed shear stress

Bed shear stresses are calculated from the flow speed according to one of four optional equations: the smooth-wall log velocity profile or Manning equation for flows alone; and a smooth bed or rippled bed equation for combined currents and wind waves. Shear stresses are calculated using the shear velocity concept where

$$\tau_b = \rho u_*^2 \tag{A24}$$

where
$\tau_b$ = bed shear stress
$u_*$ = shear velocity

and the shear velocity is calculated by one of four methods:

*a*. Smooth-wall log velocity profiles

$$\frac{\bar{u}}{u_*} = 5.75 \log\left(3.32 \frac{u_* h}{\nu}\right) \tag{A25}$$

which is applicable to the lower 15 percent of the boundary layer when

$$\frac{u_* h}{\nu} > 30$$

where $u$ is the mean flow velocity (resultant of $u$ and $v$ components)

*b*. The Manning shear stress equation

$$u_* = \frac{(\bar{u}n)\sqrt{g}}{CME\ (h)^{1/6}} \tag{A26}$$

where $CME$ is a coefficient of 1 for SI (metric) units and 1.486 for non-SI units of measurement.

*c.* A Jonsson-type equation for surface shear stress (plane beds) caused by waves and currents

$$u_* = \sqrt{\frac{1}{2}\left(\frac{f_w u_{om} + f_c \bar{u}}{u_{om} + \bar{u}}\right)\left(\bar{u} + u_{om}\right)^2} \tag{A27}$$

where

$f_w$ = shear stress coefficient for waves
$u_{om}$ = maximum orbital velocity of waves
$f_c$ = shear stress coefficient for currents

*d.* A Bijker-type equation for total shear stress caused by waves and current

$$u_* = \sqrt{\frac{1}{2} f_c \bar{u}^2 + \frac{1}{4} f_w u_{om}^2} \tag{A28}$$

## Solution method

Equation A5 is solved by the finite element method using Galerkin weighted residuals. Like RMA-2V, which uses the same general solution technique, elements are quadrilateral and may have parabolic sides. Shape functions are quadratic. Integration in space is Gaussian. Time-stepping is performed by a Crank-Nicholson approach with a weighting factor ($\theta$) of 0.66. A front-type solver similar to that in RMA-2V is used to solve the simultaneous equations.

# References


Ackers, P., and White, W. R. 1973. (Nov). "Sediment Transport: New Approach and Analysis," *Journal, Hydraulics Division, American Society of Civil Engineers*, Vol 99, No. HY-11, pp 2041-2060.

Ariathurai, R., MacArthur, R. D., and Krone, R. C. 1977 (Oct). "Mathematical Model of Estuarial Sediment Transport," Technical Report D-77-12, U.S. Army Engineer Waterways Experiment Station, Vicksburg, MS.

Krone, R. B. 1962. "Flume Studies of Transport of Sediment in Estuarial Shoaling Processes," Final Report, Hydraulics Engineering Research Laboratory, University of California, Berkeley, CA.

Norton, W. R., and King, I. P. 1977 (Feb). "Operating Instructions for the Computer Program RMA-2V," Resource Management Associates, Lafayette, CA.

Partheniades, E. 1962. "A Study of Erosion and Deposition of Cohesive Soils in Salt Water," Ph.D. Dissertation, University of California, Berkeley, CA.

Swart, D. H. 1976 (Sep). "Coastal Sediment Transport, Computation of Longshore Transport," R968, Part 1, Delft Hydraulics Laboratory, The Netherlands.

Thomas, W. A., and McAnally, W. H., Jr. 1985 (Aug). "User's Manual for the Generalized Computer Program System; Open-Channel Flow and Sedimentation, TABS-2, Main Text and Appendices A through O," Instruction Report HL-85-1, U.S. Army Engineer Waterways Experiment Station, Vicksburg, MS.

White, W. R., Milli, H., and Crabbe, A. D. 1975. "Sediment Transport Theories: An Appraisal of Available Methods," Report Int 119, Vols 1 and 2, Hydraulics Research Station, Wallingford, England.

# REPORT DOCUMENTATION PAGE

Form Approved
OMB No 0704-0188



| 1. AGENCY USE ONLY (Leave blank) | 2. REPORT DATE | 3. REPORT TYPE AND DATES COVERED |
|---|---|---|
| | May 1993 | Final report |

**4. TITLE AND SUBTITLE**
Numerical Model Investigation of Saugus River and Tributaries, Massachusetts, Flood Damage Reduction Project

**5. FUNDING NUMBERS**

**6. AUTHOR(S)**
Hsin-Chi J. Lin
David R. Richards

**7. PERFORMING ORGANIZATION NAME(S) AND ADDRESS(ES)**
U.S. Army Engineer Waterways Experiment Station
Hydraulics Laboratory
3909 Halls Ferry Road, Vicksburg, MS 39180-6199

**8. PERFORMING ORGANIZATION REPORT NUMBER**
Technical Report
HL-93-5

**9. SPONSORING/MONITORING AGENCY NAME(S) AND ADDRESS(ES)**
U.S. Army Engineer Division, New England
424 Trapelo Road, Waltham, MA 02254-9149

**10. SPONSORING/MONITORING AGENCY REPORT NUMBER**

**11. SUPPLEMENTARY NOTES**
Available from National Technical Information Service, 5285 Port Royal Road, Springfield, VA 22161.

**12a. DISTRIBUTION/AVAILABILITY STATEMENT**
Approved for public release; distribution is unlimited.

**12b. DISTRIBUTION CODE**

**13. ABSTRACT** *(Maximum 200 words)*

The Saugus and Pines Rivers estuary is located along the Atlantic coast approximately 10 miles north of Boston, MA. Because of the topography and hydraulics of the Saugus and Pines river basins, a big storm event creates a significant flooding in the areas along the Saugus and Pines Rivers.

A plan was developed by the U.S. Army Engineer Division, New England, to provide flood damage reduction against the Standard Project Northeaster event. The principal component of this plan is construction of tidal floodgates at the mouth of the Saugus River.

The objectives of this study were to use the TABS-MD numerical modeling system to (a) provide upstream and downstream boundary conditions for testing the proposed floodgate plan in a physical model study; (b) determine the impacts caused by breaching of the I-95 embankment at the east branch of Pines River and widened Pines River openings in the I-95 embankment; and (c) evaluate the impacts of floodgate structure on basin tide levels, circulation patterns, and storm surges and sedimentation and the effect of sea level rise on these responses.

(Continued)

| 14. SUBJECT TERMS | | 15. NUMBER OF PAGES |
|---|---|---|
| Finite element method | Physical model | 117 |
| Floodgate | Saugus River Estuary | 16. PRICE CODE |
| Hydrodynamic model | Sediment model | |

| 17. SECURITY CLASSIFICATION OF REPORT | 18. SECURITY CLASSIFICATION OF THIS PAGE | 19. SECURITY CLASSIFICATION OF ABSTRACT | 20. LIMITATION OF ABSTRACT |
|---|---|---|---|
| UNCLASSIFIED | UNCLASSIFIED | | |

NSN 7540-01-280-5500

Standard Form 298 (Rev 2-89)
Prescribed by ANSI Std Z39-18
298-102

13. (Concluded).

Since the proposed floodgate area has not experienced sediment problems, the sediment study was focused on a sensitivity analysis of model parameters. A 24-hr simulation was used to indicate any significant change in sediment deposition and scour pattern in the study area.

The RMA-2V model was successfully verified to limited field measurements including a 3-day field survey of water levels at nine tide gages and a 14-hr survey of velocity measurements at nine current stations. The comparisons of the computed water levels and velocities to field measurements were good.

Breaching of the abandoned I-95 embankment and widening the Pines River opening on I-95 will increase tidal flow in marshy areas. The water levels in marshy areas will increase about 0.5 ft at the peak tide under a spring tide condition. The time lag of the peak water levels between the Broad Sound and upper marshy areas was reduced from 2 hr to 1 hr.

The proposed floodgate will not cause significant change of water levels in the Pines and Saugus Rivers under the normal tide conditions. It will protect the study areas from flooding during the storm events.

The water levels in the marshy areas under Plan 2C+7 will increase about 1.0 ft at the peak flood tide and ebb tide for the 1-ft rise in sea level.

The proposed floodgate will not alter the sediment deposition or scour pattern in the estuary under the normal tide condition, but local scour near the piers may occur.